AN INVESTIGATION INTO THE PERFORMANCE OF INTEGRATION METHODOLOGIES FOR REAL TIME MASS-SPRING CLOTH SIMULATIONS

by

CHRISTOPHER PHILLIPS
ID: 15022229

A dissertation submitted in partial fulfilment of the
requirements for the award of

MASTER OF SCIENCE IN COMPUTER GAMES PROGRAMMING

September 2016

Department of Computing
Staffordshire University
Stafford ST18 0AD

Supervised by: Christopher McCreadie

I declare that this dissertation is my own work and that the work of others is acknowledged and indicated by explicit references.

Christopher Phillips
September 2016

Abstract

There has been much research into teaching computers to play games effectively, resulting in programs which are capable of beating the best human players at chess and other board games. These programs typically make use of strongly defined rules to provide their intelligence. This project suggests a different technique; applying stochastic optimisation techniques to effectively learn the strategic rules for playing Connect 4.

Three popular algorithms, a genetic algorithm, evolution strategies and particle swarm optimisation, were implemented to play Connect 4 in The Arena, a Java based framework providing the implementation of the game. Following a training period to learn the rules of the game, the playing performance of these algorithms was tested. The test results showed limited success, with only one of the algorithms able to play relatively successfully. The time constraints for the development of this project may be the reason for the poor performance of the algorithms, therefore more research and testing should be considered.

Acknowledgements

With thanks to Dr James Heather, for his help during the development of this project, and Dr Johann A. Briffa, for no doubt saving the author countless arguments with word processing software whilst trying to format this dissertation.

Contents

List of Figures

List of Tables

Chapter 1

Introduction

The visual fidelity of video games has increased dramatically in recent years largely due to developments in discrete graphics hardware, or graphics processing units (GPUs). As a result, there is a need for realistic cloth in order to sell the appearance of video game characters and scenes. It is essential that the cloth should react to dynamic behaviour, such as a character moving or the wind blowing, and it must be animated in real time, i.e. at a minimum of 30 frames per second (FPS). These requirements render many cloth simulation techniques inappropriate, as they are too computationally expensive to be run in real time. The Mass-Spring model is one technique that is appropriate for use in video games, and is the most popular method for handling cloth for games. Whilst not necessarily providing 100% accuracy, Mass-Spring models result in visually pleasing animations, good enough for games, at, most importantly, real time frame rates.

Mass-Spring models use forces, calculated using Newtonian mechanics, to animate the cloth. This results in a series of differential equations that must be approximated by a numerical integrator at discrete time intervals. There are many different integrators that can be used and the choice of integrator can directly affect the performance of the simulation. Some integrators must necessarily use small time intervals in order to maintain the stability of the cloth, and this increases the frequency of the integration calculations thus reducing performance.

This project will investigate the effect different integration methods have on a real time cloth simulation using the Mass-Spring model.

1.1 Project Aims

The aim of this project is to investigate the performance effects of different integration methods on real time cloth simulation using the Mass-Spring model.

Based on this aim, the objectives of the project are as follows:

- To research cloth simulation and numerical integration techniques

- To implement the Mass-Spring model for cloth simulation and several integrators, including explicit Euler

- To investigate the performance effects of the implemented integration methods on the simulation

1.2 Hypotheses

Volino and Magnenat-Thalmann (2001) were the first to investigate the performance impact of different integrators on cloth simulation. Their results, however, are extremely outdated, due to the vast increase in CPU power since 2001; from a 200MHz workstation CPU to the 3GHz+ CPUs available in modern desktops and laptops. Later work by Wang, Hu, and Zhuang (2009) also investigated the impact of different integrators, and found that integrator choice still has an impact on simulation performance. However they make no reference to the hardware their experiments were run on.

As a result, two hypotheses are proposed for this project, a null and an alternative.

1.2.1 Null Hypothesis

The null hypothesis is that all integration methods result in a real time cloth simulation when running on modern hardware.

This was chosen because Wang, Hu, and Zhuang (ibid.) make no reference to the hardware used, and the simulation developed will be run on an Intel I7 4770K at 4.2GHz, so it may be the case that there are no performance concerns with this modern hardware.

1.2.2 Alternative Hypothesis

The alternate hypothesis is that some integration methods are prohibitively expensive for real time cloth simulation and other methods provide better performance.

Recently, some researchers, such as Zeller (2005) and Tang et al. (2013), have proposed GPU accelerated approaches to Mass-Spring models which suggests that performance is still a consideration. Third party physics engines, such as NVIDIA ® PhysX®, also use GPU accelerated models (Kim 2011) again suggesting performance of Mass-Spring models are still a concern.

1.3   Report Structure

This remainder of this report will be structured as follows:

- Chapter 2: literature review. An overview of cloth simulation techniques will be given and the Mass-Spring model and some numerical integrators described in detail

- Chapter 3: design and implementation. This chapter will describe the development methodology, design and some of the implementation details of the project

- Chapter 4: test plan. Details on how the hypotheses will be tested described

Chapter 2

Literature Review

2.1 Cloth Simulation

The simulation of cloth is a relatively old and well studied field with applications in many different areas, including, but not limited to:

- Virtual Garment Design

- Virtual Fitting Rooms

- Films

- Video Games

Different use cases require different things from the cloth simulation. For example, in virtual garment design, the physical accuracy of the simulation is paramount whereas cloth simulation for video games prioritises real-time simulation, sacrificing accuracy. Hence, many different models for cloth simulation have been proposed.

Since this project is concerned with the real-time simulation of cloth, only those models appropriate for real-time simulations have been studied in detail. However, a brief overview of other techniques will be provided. For a more detailed overview of cloth simulation techniques, see Ng and Grimsdale (1996).

2.1.1 Cloth Properties

Cloth has several properties that should be considered for modelling.
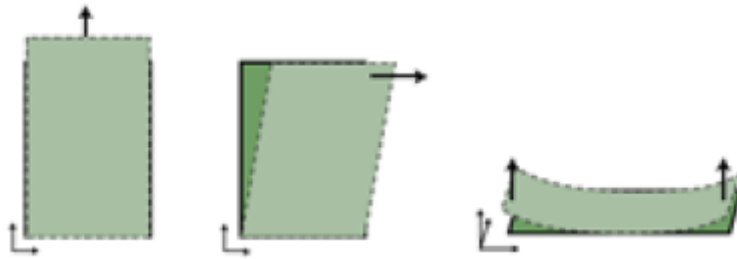
Figure 2.1: Mechanical properties of cloth (*Techniques for Animating Cloth*, p. 1)

2.1.1.1   Mechanical Properties

Cloth has three mechanical properties that control its behaviour; stretching, shearing and bending, Fig 2.1 shows how each property affects the cloth.

Stretching is the displacement of the cloth in either the horizontal or vertical direction. Most cloth has a high resistance to stretching and can typically only be stretched by 10% (*Techniques for Animating Cloth*, p. 1; Provot 1995, p. 4).

Shearing is the displacement of the cloth in a diagonal direction. Again, most cloths have high shearing resistance and this, coupled with high stretch resistance, makes cloth incompressible.

Finally, bending is the overall curvature of the cloth surface. Typically, cloth has low bending resistance and so is easily folded.

2.1.1.2   Visual Properties

The mechanical properties of cloth, discussed above, cause cloth to exhibit two visual properties. These properties arise from the fact that cloth is typically non-elastic, due to stretch and shear resistances, but highly flexible, due to low bend resistance.

Firstly, cloth will drape over objects and secondly the cloth will form many folds and wrinkles. Fig 2.2 demonstrates the visual properties of cloth.

2.1.2   Cloth Models

Techniques for modelling cloth are usually classified as either Geometric or Physically-based, and the choice of which modelling method to use depends on the use-case for the simulation.
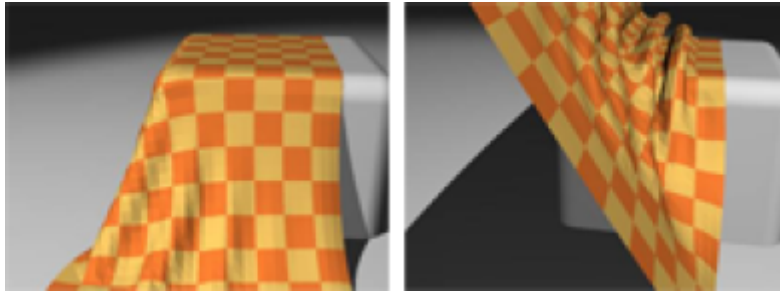
Figure 2.2: Visual properties of cloth (*Techniques for Animating Cloth*, p. 1)

2.1.2.1 Geometric Models

This family of techniques were the first models used to simulate cloth. They model the cloth using geometric equations and are especially good at modelling folds and wrinkles.

According to Ng and Grimsdale (1996), Weil was the first to propose a geometric model in 1986 and uses catenary curves to model the drape and folds of a hanging cloth. Following on from Weil, a number of other geometric models were proposed (see Ng and Grimsdale (ibid.) for more information).

All geometric techniques focus on simulating the appearance of cloth, rather than the physical properties. As such, geometric models are typically more computationally efficient than physically-based models, as there is no need to solve a series of complex equations. However, geometric techniques are unable to accurately simulate the motion of cloth, (Mongus et al. 2012, p. 1; Zhang and Yuen 2001, p. 2; Xinrong et al. 2009, pp. 1-2), and so are mostly useful for static cloth simulations.

As such, geometric models have not been considered for this project.

2.1.2.2 Physically-based Models

By contrast, physically-based models are concerned with the accurate modelling of the physical properties of the cloth and can therefore be used to produce realistic animations.

These models typically use a system of partial differential equations (PDE), or other differential equations, to model the cloth. These equations cannot be solved analytically and therefore the system requires discretisation to solve the equations at specific points in space and time. Following discretisation, a physically-based model typically involves the solving of an ordinary differential equation (ODE) of

the form (Baraff and Witkin 1998, p. 1):

$$\ddot{x} = M^{-1}\left(-\frac{\delta E}{\delta x} + F \right)$$

where:

x is a vector representing the geometric state of the system

M is a diagonal matrix representing the mass distribution of the system

(2.1)

E is a function of x which yields the internal cloth energy

F is a function of x and $\dot{x}$ which describes other forces

Physically-based models can be classified as either Continuum or Discrete.

2.1.2.2.1   Continuum Models

Continuum models were the first physical models to be proposed. Techniques in this family model cloth as a continuous surface and utilise continuum mechanics to calculate its behaviour; the Lagrange equations are most commonly used.

To discretise the continuous model, a numerical technique, such as a finite element method (FEM), is used. This is one of the advantages of continuum methods; they allow the use of a low resolution discretisation without sacrificing the accuracy of the simulation (Wacker, Thomaszewski, and Keckeisen 2005, pp. 4-5).

Another advantage of continuum models are that they are accurate; "they provide accurate models of the material derived directly from mechanical laws and models of material properties" (Magnenat-Thalmann and Thalmann 2004, p. 200).

This accuracy comes at the cost of computational performance, the main disadvantage of these techniques. The accuracy also renders these models inappropriate for use in dynamic simulations; "the formal and analytical description they require for the mechanical behavior of the material cannot easily be altered to represent transitory and non-linear events. Hence, phenomena such as frequent collisions or other highly variable geometrical constraints cannot be conveniently taken into account" (ibid., p. 200). Hence, continuum models are typically only considered appropriate for static simulations, or simulations where accuracy is paramount. As a result, continuum models have not been considered.

2.1.2.2.2   Discrete Models

According to Choi and Ko (2002, p. 2), "Cloth is not a homogeneous continuum. Therefore modeling

fabrics as a continuum and employing FEM or FDM has several potential drawbacks". As a result several discrete, or particle, models have been proposed.

With these techniques the discretisation in space is carried out by modelling the cloth as a discrete mesh, either regular or triangular, of point masses, called particles. This sacrifices some of the accuracy of continuum models, as the accuracy will depend on the number of particles used. However, this loss in accuracy is traded off against better computational performance; physical models are the only models that can be used for dynamic, real-time simulations.

The discretisation of the cloth has a direct affect on the performance of the simulation; Volino and Magnenat-Thalmann (2001, p. 5) have this to be of order O(n^3). Hence, there is a trade off to be made between accuracy and performance when using discrete models, depending on the use-case.

By far the most popular technique is the mass-spring model. This is because, according to Zink and Hardy (2007, p. 2), "Mass-spring models are the most efficient as well as the simplest of the cloth models" and "is one of the most popular techniques for simulating cloth, especially when interactive frame rates are required". Thus, it has been chosen for this project and will now be described in more detail.

2.1.3   Mass-Spring Models

Mass-spring models were first proposed for use in cloth simulation in Provot (1995). Using these models, the cloth is discretised as a 2-dimensional mesh of point masses, either regular or triangular, connected by linear springs.

2.1.3.1   Provot Model

Using the mass-spring model proposed in Provot (ibid.) the cloth is modelled as a regular mesh of point masses. The points are connected together using three different types of springs:

- Structural springs, connecting particle [i, j] to particles [i + 1, j] and [i, j + 1]. These springs resist structural deformations of the cloth, and provide the overall cloth structure. On their own they are not enough to provide a realistic cloth model; Fig 2.3 shows the results of running a cloth simulation with structural springs only. As can be seen, this does not produce a realistic image

- Shear springs, connecting particle [i, j] to particle [i + 1, j + 1] and particle [i + 1, j] to particle [i, j + 1]. These springs provide shearing resistance for the cloth. By adding shear springs, the realism

(a) Initial configuration   (b) Result of running the simulation
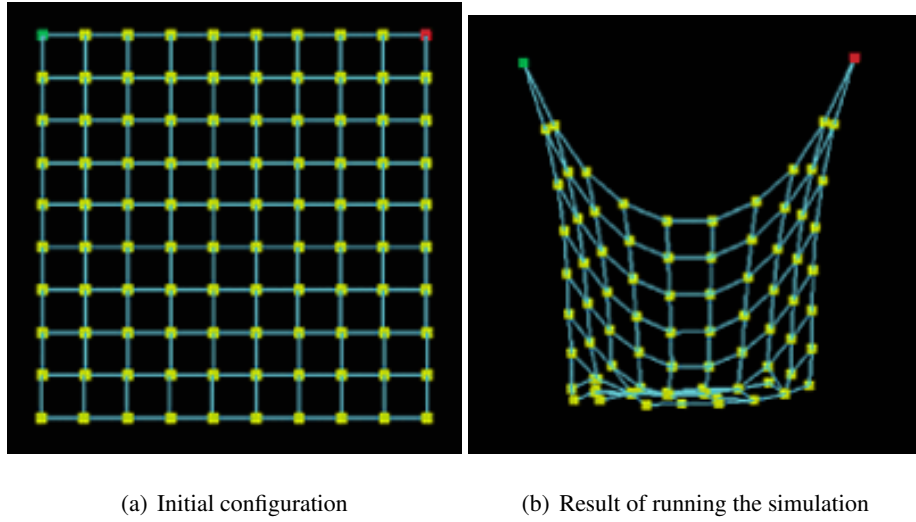
Figure 2.3: Cloth with structural springs only (Lander 2000b, p. 2)

(a) Initial configuration   (b) Result of running the simulation
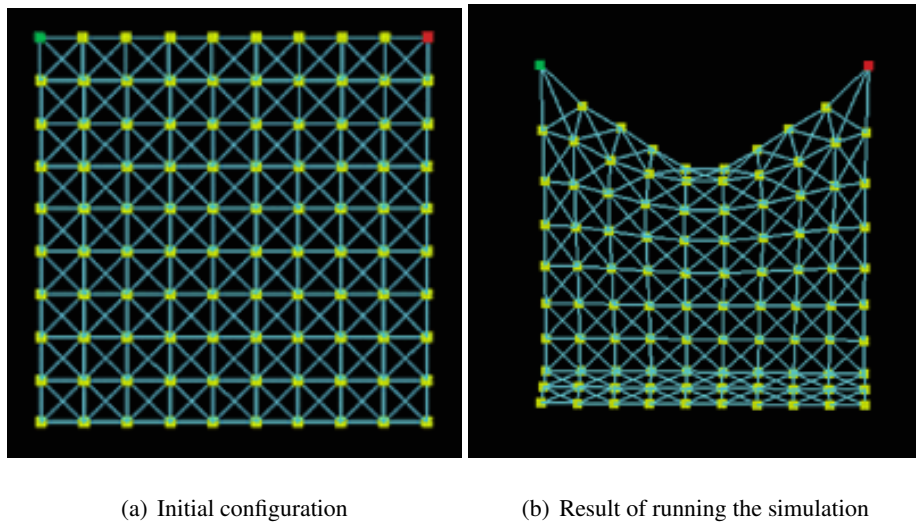
Figure 2.4: Cloth with structural and shear springs (Lander 2000b, p. 2)

of the model is improved, as shown in Fig 2.4

- Bend springs, connecting particle [i, j] to particles [i + 2, j] and [i, j + 2]. These springs model bend resistance

Fig 2.5 shows the arrangement of these springs for a small cloth model.
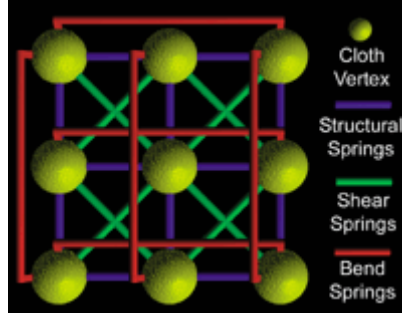
Figure 2.5: Provot cloth model (Lander 2000b, p. 2)

The total number of each type of spring can be calculated with:

$$Num_{structural} = 2((m-1)(n-1)) + (m-1) + (n-1)$$

$$Num_{shear} = 2((m-1)(n-1))$$

$$Num_{flexion} = 2((m-2)(n-2)) + 2((m-2) + (n-2)) \tag{2.2}$$

where:

m and n are the vertical and horizontal dimensions of the mesh

To animate the mesh, forces are applied to the particles and are calculated using Newton's second law:

$$F_{ij} = m_{ij}a_{ij}$$

where:

F_{ij} is the total sum of forces acting on particle ij $\qquad$ (2.3)

m_{ij} is the mass of particle ij

a_{ij} is the acceleration of particle ij

The total force acting on a particle is defined as:

$$F_{total} = \Sigma F_{external} + \Sigma F_{internal} \tag{2.4}$$

$F_{external}$ are external forces acting on the mesh, such as gravity and wind.

Gravity is calculated by:

$$F_g = m_{ij}G$$

where: $\qquad$ (2.5)

G is the gravitational constant

Wind is calculated by:

$$F_{wind} = w(n_{ij} \bullet \overrightarrow{W})$$

where:

n$_{ij}$ is the surface normal of particle ij   (2.6)

$\overrightarrow{W}$ is the wind direction vector

w is the wind constant

F$_{internal}$ are the resultant forces of the springs connecting the mesh.

The spring force is calculated using the Hooke equation (Parent 2012, p. 201):

$$F_{spring} = -k_s(L_c - L_r)\frac{p_2 - p_1}{\| p_2 - p_1 \|}$$

where:

k$_s$ is the spring stiffness coefficient   (2.7)

L$_c$ is the current length of the spring

L$_r$ is the initial, or rest, length of the spring

p$_1$ & p$_2$ are the positions of the two connected particles

Using this equation, the cloth will be modelled with pure elastic springs and will oscillate indefinitely. However, as mentioned in 2.1.1.2 and Provot (1995, p. 1), cloth is a non-elastic medium and therefore the model needs to account for the energy lost due to internal friction.

This is typically modelled as an extra internal damping force, calculated using (Parent 2012, p. 201):

$$F_{damping} = -k_d(\dot{p_2} - \dot{p_1}) \bullet \left(\frac{p_2 - p_1}{\| p_2 - p_1 \|}\right)\left(\frac{p_2 - p_1}{\| p_2 - p_1 \|}\right)$$

where:

(2.8)

k$_d$ is the spring damping coefficient

$\dot{p_1}$ & $\dot{p_2}$ are the velocities of the two connected particles

2.1.3.2 Choi Ko Model

A different mass-spring model was proposed in Choi and Ko (2002) and aims to improve the buckling behaviour of the cloth, resulting in more realistic draping and wrinkling behaviour.

The cloth is modelled in a similar way to the Provot method, but additional bend springs are added, connecting particle [i, j] to particle [i + 2, j + 2] and particle [i + 2, j] to particle [i, j + 2]; Fig 2.6 shows the arrangement of springs.
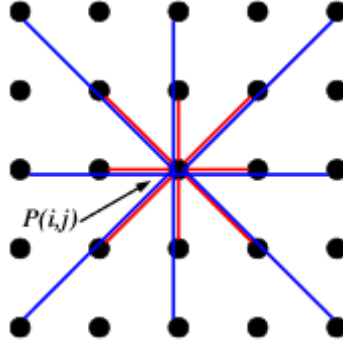
Figure 2.6: Choi Ko cloth model (Choi and Ko 2002, p. 2)

This model uses an energy-based approach, of the general formula 2.9(Bartels 2014, p. 3), to calculate the forces acting on individual particles.

$$F = \left(\frac{\delta E(S)}{\delta x}, \frac{\delta E(S)}{\delta y}, \frac{\delta E(S)}{\delta z} \right)$$

where:

(2.9)

E(S) is an energy function of S, a representation of the cloth's state

Two types of interactions are defined, type 1 and type 2. Type 1 interactions model stretch and shear resistances, the red lines in 2.6, and are represented by a linear spring model. Type 2 interactions model bend forces, the blue lines in 2.6, and helps prevent the so called post-buckling instability problem. The interested reader should see Choi and Ko (2002) for more information on the energy functions for each interaction type.

2.1.3.3   Justification of Choice

Mass-spring models are suitable for use in this project as they are efficient and simple to implement; "Mass-spring models are the most efficient as well as the simplest of the cloth models. This method is one of the most popular techniques for simulating cloth, especially when interactive frame rates are required" (Zink and Hardy 2007, p. 2). As this project is concerned with the real time animation of cloth, mass-spring models are therefore the obvious choice.

Mass-spring models are also the most common method of modelling cloth in video games, used in games such as Alan Wake, (Enqvist 2010, p. 2), and Hitman: Codename 47, (Jakobsen 2005, p. 1), as well as commercial physics engines for games, such as PhysX. Again, since this project is concerned with the simulation of cloth for use in a video game, mass-spring models are the logical choice.

In particular, the Provot model was used for this project as the force-based approach requires the solving

(a) Super-elastic effect   (b) Result of correcting super-elasticity
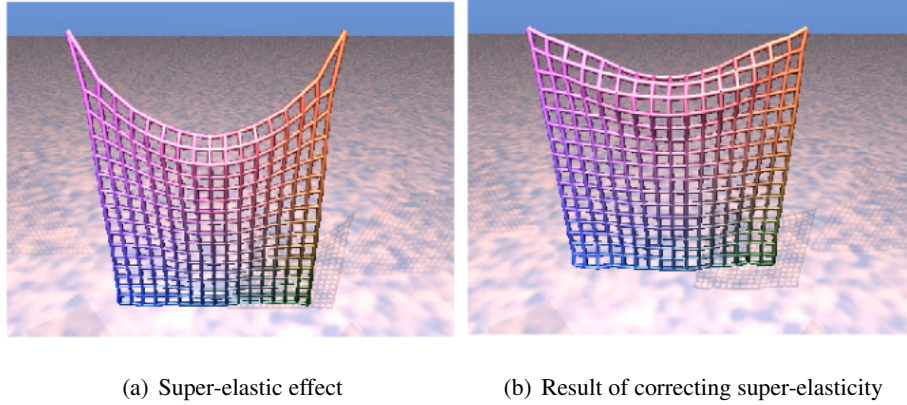
Figure 2.7: Super-elasticity problems (Provot 1995, pp. 4,6)

of a much simpler series of equations than the energy-based approach of the Choi Ko model, and is therefore likely to be more computationally efficient.

One disadvantage of the mass-spring model is that it does not achieve realistic animation of cloth as "mass-spring systems do not model any specific material and are not related to measured properties of real clothes" (Wacker, Thomaszewski, and Keckeisen 2005, p. 3). However, by careful tuning of the spring stiffness coefficients pleasing results can be achieved; Mongus et al. (2012) have shown that, with tuning, mass-spring models can reproduce the drape of a cloth with an accuracy of 97%.

Another disadvantage of mass-spring models is what Provot calls 'super-elasticity'; springs are allowed to deform too much, leading to unrealistic results. This is caused because "the springs are "ideal" and they have unlimited linear deformation rate" (Vassilev, Spanlang, and Chrysanthou 2001, p. 3). To counter this effect, Provot suggests enforcing length constraints on structural and shear springs. First the position of the particles are updated, then the deformation of the springs are calculated. If this deformation value is greater than some threshold, τ_c, then the position of the connected particles are adjusted so the deformation rate equals τ_c. Fig 2.7 shows the super-elasticity problem and the results of employing Provot's corrective method. As can be seen, correcting the super-elasticity results in a much more realistic model.

2.1.3.4 Mass-Spring Models for Video Games

Both the Provot and Choi Ko Mass-Spring models can be separated into two component, the modelling component and the animation component. The modelling component describes how the cloth will be represented internally, i.e. the disrectisation by point masses and the interconnectivity of the springs,

and the animation component details how the cloth will be animated over time; for the Provot model, using the force equations detailed in the previous sections.

For video games, where performance is a key factor, using the force based animation methods in the Provot and Choi Ko models may be prohibitively expensive over a certain mesh size. This results from the fact that the number of springs grows rapidly as the number of particles increases, leading to more internal force calculations per time step. For example, for a cloth represented by a 50 by 50 mesh of particles connected as in the Provot model, there are 14502 springs, and therefore Equations 2.7 and 2.8 must be calculated 14502 times at every time step. For the Choi Ko model, the internal force cost would only rise, as not only are there more springs in their model, but also their force calculations are more expensive. Thus, another approach to animating Mass-Spring models is usually taken for video games, called Position Based Dynamics (PBD).

PBD were first used by Jakobsen (2005) to implement cloth in Hitman: Codename 47 and have since gone on to become the standard for cloth animation in games (Enqvist 2010, p. 2) and commercial physics engines (Kim 2011).

When using PBD, the cloth is modelled either using the Provot method (Enqvist 2010, p. 2) or using a simplified version of the Provot model, where the flexion springs are omitted (Zeller 2005, p. 7; Kim 2011, p. 25). Instead of being modelled as Hooke springs, the spring connections are instead treated as distance constraints of the form

$$\| x2 - x1 \| = d$$

where:

$x2$ and $x1$ are the positions of the particles connected by the constraint

d is the length of the constraint

(2.10)

The work of Jakobsen (2005) was developed in Müller et al. (2006) resulting in a more general PBD model that supports both equality and inequality constraints. For games however, modelling cloth as a mesh of particles connected by simple distance constraints is enough.

To animate the cloth using PBD, external forces are first applied to the cloth, integrated using Verlet integration and the particle positions updated. Since the particles have moved, it is possible that one or more of the spring constraints are violated so they are checked and the positions of the particles corrected so none are violated; this is called constraint relaxation and is shown in Fig 2.8 . The constraints are correct using Equation 2.11(ibid., p. 4); stiffness can also be added to control the appearance of the cloth.
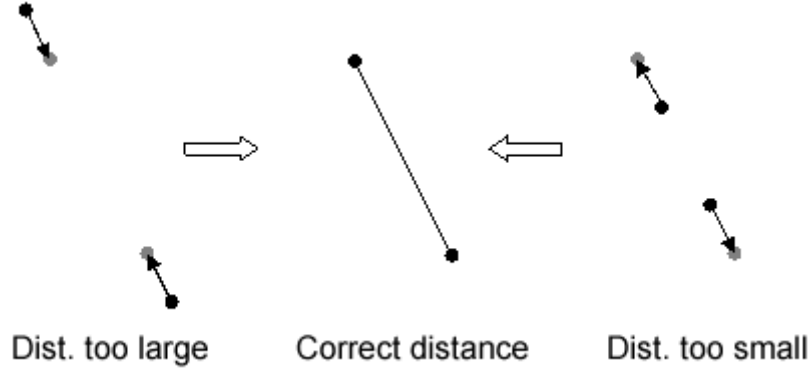
Figure 2.8: Constraint relaxation (Jakobsen 2005, p. 1)

$$\Delta x1 = -\frac{w1}{w1+w2}(\| x2-x1 \| -d)\frac{x2-x1}{\| x2-x1 \|}$$
$$\Delta x2 = \frac{w2}{w1+w2}(\| x2-x1 \| -d)\frac{x2-x1}{\| x2-x1 \|}$$

(2.11)

where:

w1 and w2 are the weights of the respective particles

This method of iteratively checking constraints and relaxing them immediately is called the Gauss-Seidel method and has one main problem; relaxing one constraint may violate other, already examined, constraints and therefore multiple relaxation passes may be needed. According to Jakobsen (2005, p. 1) however, for most cloth only one relaxation pass is necessary for visually pleasing animation, although this is contradicted by (Kim 2011), who suggests that multiple passes are needed when using a Gauss-Seidel approach.

A PBD approach is unconditionally stable, as any instability will be corrected by the relaxation process, and can therefore use a large time step to reduce the performance cost of the simulation. Whilst implicit integrators, discussed below, offer unconditional stability for the traditional Mass-Spring models, they are much more difficult to implement, so the fact that PBD are stable and simple explains their popularity for use in video games. The need for multiple Gauss-Seidel passes can be used to control the performance hit of the cloth as well; the amount of frame time available for cloth simulation could be used to adjust the number of relaxation passes, so that if more time is available, more accurate cloth is produced.

Despite its advantages, PBD was not chosen for this project as it is somewhat of a closed problem for cloth simulation in video games. PBDs are the standard method of animating cloth for games, and have

been implemented efficiently, and parallelised, in commercial physics engines. By contrast, the Provot Mass-Spring model is not conventionally used, as it may be too expensive for certain mesh sizes. However, the research into the performance of the Provot model is either old, or makes no reference to the hardware used, and therefore there is scope for further work to investigate whether performance is still a concern with modern hardware.

2.1.4 Numerical Integration for Mass-Spring Models

As mentioned above, physically-based models for cloth simulation require solving a series of differential equations, discretised in space and time. According to Wacker, Thomaszewski, and Keckeisen (2005, p. 5), "since particle systems already represent a disrectisation in space, only a system of ordinary differential equations has to be solved". For the Mass-Spring model using Newtonian mechanics a series of second order ODEs, of the form 2.12, must be solved (Zink and Hardy 2007, p. 5).

$$\frac{\delta^2 x}{\delta t^2} = M^{-1} F(x, v) \tag{2.12}$$

This can be converted into a coupled series of first order ODEs by separating the position and velocity (ibid., p. 5):

$$\frac{\delta}{\delta t} \begin{pmatrix} x \\ v \end{pmatrix} = \begin{pmatrix} v \\ M^{-1} F(x, v) \end{pmatrix} \tag{2.13}$$

Equations 2.12 and 2.13 cannot be solved analytically, and therefore it is necessary to use a numerical method, or integrator, to approximate them at discrete time intervals.

There are many integration methods that could be chosen, typically classified as either explicit or implicit, and the most popular choices will be described now.

2.1.4.1 Explicit Integrators

Most of the early work on physically-based cloth simulation used explicit integrators as they are simple and easy to implement; they only require information about the state of the system at the previous interval to calculate the current state.

The most commonly used explicit integrators are the Runge-Kutta family of integrators.

2.1.4.1.1 Euler

The first order Runge-Kutta integrator, or explicit Euler, was used in Provot (1995) to approximate a Mass-Spring system.

Equation 2.13 is approximated by (Wang, Hu, and Zhuang 2009, p. 3):

$$v_{i+\Delta t} = v_i + \Delta t F(t_i, v_i)$$

where:

v_i is the velocity of a particle at time interval i

Δt is the time step

(2.14)

When applied to the Provot Mass-Spring model, this gives (Provot 1995, p. 3):

$$a_{i,j}(t + \Delta t) = \frac{1}{m_{i,j}} F_{i,j}(t)$$

$$v_{i,j}(t + \Delta t) = v_{i,j}(t) + \Delta t a_{i,j}(t + \Delta t)$$

$$x_{i,j}(t + \Delta t) = x_{i,j}(t) + \Delta t v_{i,j}(t + \Delta t)$$

where:

$a_{i,j}$, $m_{i,j}$, $v_{i,j}$ and $x_{i,j}$ are the acceleration, mass, velocity and position of particle i, j respectively

(2.15)

The explicit Euler method is computationally cheap but can result in numerical instability if too large a time step is used. Mathematically, the explicit Euler method is stable only if the time step is less than the natural period of the system, approximated as $\pi \sqrt{\frac{m}{K}}$, where K is the maximum stiffness in the system. Vassilev, Spanlang, and Chrysanthou (2001, p. 2) found that in fact explicit Euler is only stable for Δt values less than $0.4\pi \sqrt{\frac{m}{K}}$.

As cloth generally does not stretch easily, this results in high stiffness in the structural and shear springs, which necessitates the use of a small time step if the explicit Euler integrator is chosen. This can impact the overall performance of the simulation, as while this integrator is cheap, the frequency of calculations is high as a result of the time step limitations.

2.1.4.1.2 Midpoint

The explicit Midpoint integrator is a second order Runge-Kutta method and modifies the Euler integrator to give greater stability.

Equation 2.14 is modified to give the following (Wang, Hu, and Zhuang 2009, p. 3):

$$v_{i+\Delta t} = v_i + \Delta t F\left(t_i + \frac{\Delta t}{2}, v_i + \frac{\Delta t}{2} F(t_i, v_i)\right)$$

(2.16)

Since this method requires two derivatives, the computational cost is greater than Euler. However, because the midpoint method affords greater numerical stability (see Fig 2.9), a larger time step can be used which increases the overall simulation performance; Wang, Hu, and Zhuang (ibid.) have shown that the midpoint integrator offers close to twice the simulation performance over explicit Euler.
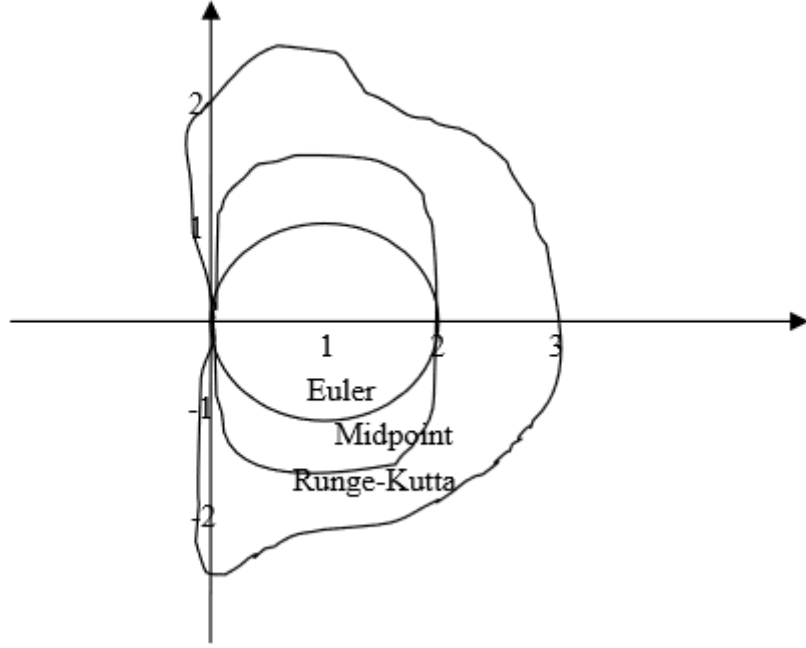
Figure 2.9: Explicit integrator stability regions (Wang, Hu, and Zhuang 2009, p. 4)

2.1.4.1.3 Fourth order Runge-Kutta

The Fourth order Runge-Kutta (RK4) integrator offers greater stability using larger time steps over the midpoint method and is formulated as (Wang, Hu, and Zhuang 2009, p. 3):

$$
\begin{aligned}
v_{i+\Delta t} &= v_i + \frac{\Delta t}{6}(k_1 + 2k_2 + 2k_3 + k_4) \\
k_1 &= F(t_i + v_i) \\
k_2 &= F\left(t_i + \frac{\Delta t}{2}, v_i + \frac{\Delta t}{2}k_1\right) \\
k_3 &= F\left(t_i + \frac{\Delta t}{2}, v_i + \frac{\Delta t}{2}k_2\right) \\
k_4 &= F\left(t_i + \Delta t, v_i + \frac{\Delta t}{2}k_3\right)
\end{aligned}
\tag{2.17}
$$

This integrator has a significantly higher computational cost than the other methods discussed, however Volino and Magnenat-Thalmann (2001, p. 4) have shown that the RK4 supports time steps almost six times larger than the midpoint method. Therefore, given that RK4 is three times as computationally expensive as midpoint, this suggests that this integrator can lead to twice the overall simulation performance. Wang, Hu, and Zhuang (2009, p. 4) have also shown that RK4 offers performance gains over midpoint.

31

2.1.4.1.4 Verlet

Verlet integration is an alternative to the Runge-Kutta family of integrators. It avoids velocity calculations by approximating the velocity of a particle using its previous positions.

A particle's new position is approximated by (Mongus et al. 2012, p. 2):

$$x_{i+\Delta t} = 2x_i - x_{i-\Delta t} + a_{i+\Delta t}\Delta t^2 \tag{2.18}$$

Since Verlet is a velocity less integrator, the linear damping shown in Equation 2.8 will not provide any damping to the system. In order to prevent the system from oscillating infinitely, a damping factor is applied to the approximated velocity, thus Equation 2.18 becomes

$$x_{i+\Delta t} = x_i + dampingFactor(x_i - x_{i-\Delta t}) + a_{i+\Delta t}\Delta t^2 \tag{2.19}$$

This method is computationally fast and reasonably stable, as "velocity is implicitly given and consequently it is harder for velocity and position to come out of sync" (Jakobsen 2005, p. 1). However it does still suffer from time step issues; figures 11 and 13 in Wacker, Thomaszewski, and Keckeisen (2005, pp. 14-15) show that below a certain threshold Verlet integration is less stable than explicit Euler, but more stable over that threshold.

2.1.4.2 Implicit Integrators

According to Baraff and Witkin (1998, p. 1), "Explicit methods are ill-suited to solving stiff equations because they require many small steps to stably advance the simulation forward in time". Therefore they propose an implicit integrator for use in cloth simulation since implicit integrators are unconditionally stable regardless of step size.

However implicit integrators are computationally more expensive than their explicit equivalents, as "they involve the resolution of a large and sparse linear equation system for each iteration" (Volino, Cordier, and Magnenat-Thalmann 2005, p. 4). Since they are unconditionally stable however, this can be countered by simply using a larger time step. The guaranteed stability of these methods also reduces the accuracy of the simulation, as they introduce inherent numerical damping, which increases as the time step increases (see Volino and Magnenat-Thalmann (2001, p. 4)). As such, there is a balance to be found between performance and accuracy of the simulation with implicit integrators.

The most common implicit integrator is the implicit, or backward, Euler method which will be described now. It should be noted that there are many other implicit integrators available.

2.1.4.2.1   Euler

First proposed for use in cloth simulation in Baraff and Witkin (1998), the implicit, or backward, Euler method is an adaptation of the explicit Euler method.

Equation 2.15 is modified to give (Kang, Choi, and Cho 2000, p. 3):

$$v_i^{t+\Delta t} = v_i^t + F_i^{t+\Delta t} \frac{\Delta t}{m_i} \tag{2.20}$$

$F_i^{t+\Delta t}$ cannot be calculated at the current time step, and so must be approximated as (ibid., p. 3):

$$F^{t+\Delta t} = F^t + \frac{\delta F}{\delta x} \Delta x^{t+\Delta t} \tag{2.21}$$

$\Delta x^{t+\Delta t}$ can be written as $\Delta t(v^t + \Delta v^{t+\Delta t})$ and so eq. 2.21 can be rewritten, giving the series of linear equations (ibid., p. 3):

$$\left(I - \frac{\Delta t^2}{m} \frac{\delta F}{\delta x} \right) \Delta v^{t+\Delta t} = F^t \frac{\Delta t}{m}$$

where:
$$\tag{2.22}$$

I is the identity matrix

Thus, implicit Euler involves calculating $\Delta v^{t+\Delta t}$ every iteration using:

$$\Delta v^{t+\Delta t} = \left(I - \frac{\Delta t^2}{m} \frac{\delta F}{\delta x} \right)^{-1} F^t \frac{\Delta t}{m} \tag{2.23}$$

$\frac{\delta F}{\delta x}$ is the negated Hessian matrix, denoted as H, and can be approximated as (ibid., p. 3):

$$H_{ij} = \begin{cases} k_{ij} & \text{if } i \neq j \\ -\sum_{i \neq j} k_{ij} & \text{if } i = j \end{cases}$$

where:
$$\tag{2.24}$$

k_{ij} is the spring stiffness

As a result, the implicit Euler method requires the computation of an n x n matrix each iteration, and thus increasing the size of the mesh greatly impacts the performance of this method.

However, if the stiffness of the springs and mass of the particles are constant throughout the simulation then $\left(I - \frac{\Delta t^2}{m} H \right)^{-1}$ can be precomputed, giving performance gains.

This method has been shown by Volino and Magnenat-Thalmann (2001) to be stable for any time step value, however as the time step increases, the accuracy decreases rapidly over a certain threshold. Using the method described above, it is also not possible to use an adaptive time step or to vary the mass or stiffness of the model as the cost of computing H every iteration is high. As such, many researchers, such as Mesit, Guha, and Chaudhry (2007) and Kang, Choi, and Cho (2000), have presented faster approximation methods for the implicit Euler integrator.

2.1.4.3   Chosen Integration Methods

Four integrations methods were chosen for investigation by this project.

- Explicit Euler. This is the simplest integrator and one of the most popular in the literature but it is also most likely to impact simulation performance due to its reliance on small time steps

- Midpoint. Computationally more expensive than explicit Euler, but stable with larger time steps, therefore offering an interesting comparison between computational cost and simulation performance

- Fourth order Runge-Kutta

- Verlet. Chosen as it is an explicit integrator that is not part of the Runge-Kutta family

Only explicit integrators have been selected as they are considered to be inappropriate when solving stiff differential equations, such as those in cloth, due to the necessity of small time steps.

Chapter 3

Design and Implementation

3.1 Development Methodology

Software development methodologies break the development of a piece of software down into a number of phases with the aim of improving design and code quality as well as aiding in project management. There are a large number of different development methodologies, although they can typically be classified as either sequential, also called waterfall, or cyclical, also called spiral. The choice of which method to use will depend on the specifics of the software project as well as developer preference and team size.

3.1.1 Sequential

The sequential, or waterfall, approach uses a number of strict, sequential phases for developing software; each phase must be completed before the next phase can begin. Fig. 3.1 shows the typical structure of this methodology.

This approach works well for projects were the requirements are strictly defined, the project's subject area well known and the technologies involved well understood by the developers. In this case, the software can be designed well from the start, so there is little need for iterative development. If the project's requirements are likely to change, or the subject area and technologies are ill-understood or new then a waterfall approach is inappropriate. The rigid structure of the waterfall method does not allow requirements to be easily changed, or poor design choices corrected; in order to change requirements or correct poor design the whole development process must be started again, as there is no method of feedback between development phases.
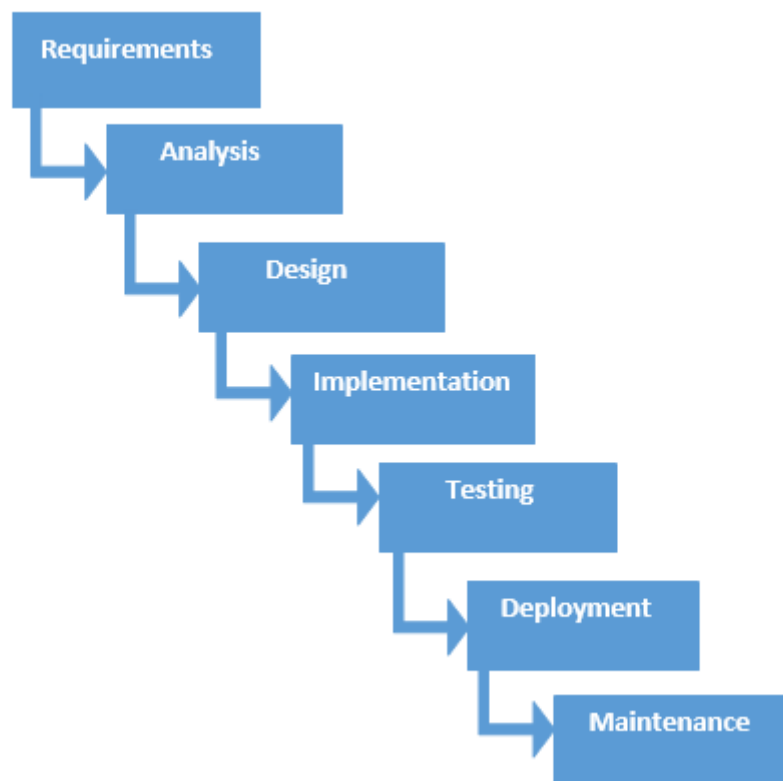
Figure 3.1: Waterfall development methodology (*What is Waterfall Model in software testing and what are advantages and disadvantages of Waterfall Model*)

3.1.2 Cyclical

Cyclical approaches, as the name suggests, develop software using iterative cycles. At the start of each cycle requirements and design are set and at the end, a working software prototype is produced. This prototype is used as feedback for the next cycle, adjusting the requirements and correcting design mistakes and issues as necessary. These methods counteract the disadvantages of the waterfall approach; by using an iterative approach it is easy to add or change requirements or redesign areas of the project.

There are many development methods which are derived from a cyclic approach, including Rapid Application Development (RAD) and Scrum.

RAD is a development method which favours rapid prototyping with minimal planning. Since there is less focus on planning at each iteration it is extremely easy to incorporate design and requirement changes. Prototype development will start earlier than other methods and this enables issues to be caught early, and the design to be altered appropriately. There is a requirement when using RAD of skilled and experience developers and designers, as the prototypes developed must be reusable so as to

Requirement	Type
Must model cloth using the Provot Mass-Spring model	Functional
Must be able to render cloth to the screen	Functional
Must be able to pin particles so they are unaffected by forces	Functional
Must perform in real time	Non-functional

Table 3.1: First cycle requirements

avoid wasting time.

Using Scrum, a project is broken down into sprints and each sprint is timeboxed with a duration, i.e. 24 hours, 4 weeks. At the end of each sprint a working prototype is produced and as the sprints are completed the project is designed and developed over time.

3.1.3 Chosen Methodology

For this project, cyclical methods were preferred over waterfall. This was partly due to the author's preference for cyclical methods and partly because there were some unknowns, particularly related to rendering, that made rigidly designing the system difficult. Using the more agile cyclical methods allowed for some investigative work before finalising the system design.

In particular, RAD was chosen as the development methodology.

3.2 Development

Since RAD was the chosen development methodology, the artefact was developed over several cycles.

3.2.1 First Cycle

In the first cycle the Mass-Spring model was implemented. Springs were implemented using the Hooke equation (Equation 2.7) to calculate the internal spring force with linear damping as an additional internal force using Equation 2.8. Gravity, implemented as Equation 2.5, was the only external force. Rendering of the cloth was also implemented.

Table 3.1 shows the initial requirements of the first development cycle.

Before designing this cycle, an initial investigation into the rendering component was carried out, as the choice between DirectX11 or OpenGL would affect the design of the system.

As this project is not concerned with rendering cloth, but simulating it, it was decided that the cloth would be rendered as a mesh of lines, representing the structural and shear springs (as in Figs 2.4 and 2.7). Since the positions of the particles, and therefore vertices, evolve over time, a DirectX11 implementation would have to use a dynamic vertex buffer and remap the vertex data every frame. This is not an issue in OpenGL, since it is possible to draw vertices directly with the glVertex3f function. It was unknown by the author what the cost of this remapping would be, so simple OpenGL and DirectX11 implementations were created and their performance compared. For a 500 by 500 mesh, with a debug build, the OpenGL implementation rendered the structural and shear springs at 80FPS and the DirectX11 version at 450FPS. Hence, DirectX11 was chosen as the rendering language. It should be noted that the OpenGL implementation was very naive, due to the author's inexperience, and this is most likely the reason for the poor performance. It is probable that a more robust implementation, using more advanced features, would perform much more closely to the DirectX11 implementation.

The initial design can be seen in Fig A.1; the rendering component, constructors, accessors and mutators have been excluded for brevity.

Since DirectX11 was the rendering language, DirectXMath types were used for the key variables in the Particle class. This gives performance gains over manually implementing a 3-dimensional vector and functions, as the functions that operate on DirectXMath types are compiled into SIMD instructions, allowing the calculations to be completed in fewer CPU cycles.

An std::vector was initially used to store the springs as it is not necessary to separate the springs into types, since the internal forces are calculated the same for every spring type. Also, the equations for calculating the amount of each spring (see Equation 2.2) were unknown during the initial design process, so an std::vector was chosen as it would allow an any number of springs to be stored.

During implementation, the initial design had to be adapted as a result of performance concerns; these optimisations will be discussed in the section 3.3.

Fig A.2 shows the final design of this cycle with the optimisation changes. Timing code was also added to allow performance data necessary for testing the hypotheses to be extracted from the cloth. The test plan for this project will be detailed in the next chapter. Code for automating the testing process using an XML file was also added, again, details of this will be discussed in the next chapter.

Requirement	Type
Must implement the Explicit Euler and Verlet integrators	Functional
Must be able to dynamically switch integrators	Functional

Table 3.2: Second cycle requirements

3.2.2 Second Cycle

During the second development cycle the model developed in the first cycle was adapted to use different integration methods. The explicit Euler and Verlet integrators were implemented as described in 2.1.4.1. Wind was also added as an additional external force.

The requirement for this development cycle are shown in Table 3.2.

The initial design of this development cycle can be seen in Fig A.3. For brevity, only the changes introduced for this cycle are shown for the classes developed previously; it can be assumed that the Particle and Cloth classes are unchanged other than the documented additions.

Two separate designs were initially proposed, one using static classes and storing a function pointer for the appropriate integrator, and the second using an interface and virtual functions. For the interface design, the inheriting classes were designed using the Singleton design pattern. Since particles are passed as parameters to the integrate function, there is no need for each particle to have their own instance of a particular integrator. Therefore it makes sense for integrators to be Singletons, and this helps to reduce the memory footprint of the application as well as the cost of dynamically switching integrators; as each integrator only needs to be dynamically allocated once, rather than for every particle.

The two different designs were suggested as the aim was to use the most efficient implementation possible and it was unknown during the design process which would be more efficient. As such, both designs were implemented and then some tests run using the explicit Euler integrator to determine which was most efficient. Compared with implementing explicit Euler directly in Particle, both implementations increased total update time by approximately 0.4ms for a 50 by 50 mesh on a debug build. This translated to an approximate drop of 4-5 FPS, and was expected due to the fact that both designs must call accessors to access Particle's data.

Compared with each other, the results were more variable. For some runs the static class design was more efficient and for others the interface design more so. Ultimately, the efficiency difference was

small, at most a 0.1ms difference between them, so the conclusion was reached that both designs were equally efficient. However, the explicit Euler integrator is the cheapest integrator, so for more expensive integrators, such as RK4, a wider performance gap may be found. Therefore these experiments will be run again during the third development cycle using RK4 and the design retroactively changed if a significant efficiency gulf is found.

Since both designs were equally efficient, the interface design was chosen as the author felt that it was, ostensibly, a better quality approach than using static classes. Using interfaces means Particle conforms much more to the Open/Closed SOLID principle; Since Particle stores a pointer to the interface, and only calls virtual functions, new integrators can easily be added and used without any changes needed in Particle.

One minor optimisation was made to the initial design and is documented in the next section. As a result of this optimisation, the chosen design now performs almost as well as coding the integrator directly in Particle.

Wind was originally intended to be calculated using a static normal assigned at Particle creation, however on reflection it was realised that this would not work, as the normal of the particles will change as they move over time. Therefore it is necessary to calculate the surface normal for the particles every time step. Using the code downloaded from Mosegaard (2009) as a reference, the particles are split into triangles and the normal calculated with the equation below.

$$
\begin{aligned}
\overrightarrow{P1ToP2} &= p2 - p1 \\
\overrightarrow{P1ToP3} &= p3 - p1 \\
\overrightarrow{normal} &= \overrightarrow{P1ToP2} \times \overrightarrow{P1ToP3}
\end{aligned}
\tag{3.1}
$$

Equation 2.6 had to be modified slightly as well in order to give a vector, rather than a scalar, force. Again, using Mosegaard (ibid.) as a reference, the equation was modified to:

$$
F_{wind} = n_{ij}(w(\parallel n_{ij} \parallel \bullet \overrightarrow{W}))
\tag{3.2}
$$

This change is support by Provot (1995, p. 3), who arrives at a similar equation for calculating a wind force.

The final design can be seen in Fig A.4. In addition to the optimisation changes, another change was made as a result of poor understanding of the integration equations. Initially the design was to store the

time step in the integrator classes and have the time step checking code in the integrate function. The algorithm would then proceed as follows for every frame:

```
/* In update */
```
timeSinceLastIntegration += deltaTime

for *every spring* **do**
| calculateInternalForce

end

for *every particle* **do**
| addGravity

end

if *timeSinceLastIntegration >= timeStep* **then**

   for *every particle* **do**
   | do integration calculations

   end

   timeSinceLastIntegration = 0.0

end

Algorithm 1: Original integration algorithm

Thus, forces were calculated and added every frame, resulting in a huge performance decrease as mesh size increased and overly elastic cloth as the time step was increased so the integration wasn't calculated every frame. By examining the integration equations again, it was realised that calculating the forces should be included as part of the integration step, and therefore only performed at every time step, rather than every frame. As such, the timeStep variable was moved from the integrators to a global variable, and the time step checking code moved to the global update function (not shown in the design diagrams). Now, Cloth's update function is called every time step, rather than every frame, and the cloth behaves as expected as the time step is varied.

3.2.3 Third Cycle

In the final development cycle the Midpoint and RK4 integrators were implemented.

The initial design is shown in Fig A.5. As with the second phase, only those changes introduced in this phase are shown.

In order to implement both Midpoint and RK4, it was necessary to make additional changes to the algorithm flow. Following the changes detailed in the previous section, the cloth animation algorithm would proceed as follows every time step:

```
/* In Cloth.update */
for every spring do
 | calculateInternalForce
end
for every particle do
    addGravity

    if flag scenario then
     | addWind
    end

    do integration calculations
end
```

Since both integrators require multiple derivations, i.e. multiple calculations of the total force, it was necessary to redesign the system.

The integrate function is now passed a Cloth object rather than a Particle and Cloth has a new function, calcForces, which calculates the total force in the mesh. This allows an integrator to calculate the total force multiple times if necessary, but requires it to loop through every particle in order to apply the appropriate integration calculations. As such, the integrator classes are also friend classes of Cloth, allowing them access to the particles array directly. This breaks the Open/Closed principle slightly, so removing the friend relationship and requiring integrators to call accessors may be a better approach. The friend design was kept in order to give as much performance as possible, but it should be noted that caching the particle array in a local variable would lead to only one accessor call per time step, which would most likely result in near identical performance to the friend approach.

Since integrate is now passed a Cloth object, the chosen integrator is stored outside of Cloth and Particle, in the global encapsulating class (not shown in the diagrams for brevity), and integrate is called every time step in place of Cloth's update method.

As mentioned in the previous section, the performance of the static class and interface designs were compared again, in order to see if a larger performance delta appeared with a higher cost integrator. The

results of this comparison were similar to those of the second cycle. The results were still very variable, but ultimately there was less than a frame difference between both implementations. Therefore, the interface design was kept and the final design can be seen in A.6.

Unit testing was also added during this cycle, in order to validate the integrator implementations. The force, velocity (where appropriate) and positions of the particles at the end of an integration step are compared with values calculated manually; an accuracy of four decimal places is used to account for the small floating point rounding errors inherent in computing.

3.3   Profiling and Optimisation

3.3.1   First Cycle

Several optimisations were made to the design of the first development cycle as a result of profiling the application.

Firstly the std::vector was replaced with dynamically allocated arrays in the Cloth class. Iterating though the vector to calculate the spring forces proved prohibitively expensive for meshes over a certain size, even when calcSpringForce was an empty function; a 100 by 100 mesh was the largest mesh that supported real time frame rates, running at 40FPS on a debug build. Profiling showed that std::vector iterator functions were the most expensive execution path, as a range-based for loop was used to iterate over every spring. This can be seen in Fig B.1 in the appendices. Hence, the vector was replaced with dynamically allocated arrays and the equations listed in 2.2 identified. Fig B.2 shows the profiling results using dynamic arrays. As can be seen, the high cost execution paths have moved away from iterating over the springs and into calculating the spring forces themselves.
Switching to arrays gave a 4x FPS increase, for the same mesh size, and a 2x increase in the maximum real time mesh size.

Secondly, profiling showed there were optimisations to be made in calcSpringForce.
The profile in Fig B.3 shows that calcSpringForce was the most expensive code path, and within it, addForce and XMLoadFloat3 were the most expensive functions. This results from the fact that XM-FLOAT3s are used in Particle for variables such as position. XMFLOAT3s must be converted into

XMVECTORs using XMLoadFloat3 in order to be able to use the DirectXMath vector functions. Therefore, the position and velocity of every particle had to be converted every frame in order to implement Equations 2.7 and 2.8. Similarly, addForce must call XMLoadFloat3 and XMStoreFloat3 to first convert totalForce into an XMVECTOR for use in addition, and then convert the resultant XMVECTOR back into an XMFLOAT3. Again, this had to be done every frame, hence why Fig B.3 shows that XMLoadFloat3 and XMStoreFloat3 are the two most expensive functions in the entire system. As a result, XMVECTORs were used instead of XMFLOAT3s, removing the need for conversions, and giving reasonable performance gains.

Fig B.3 also shows that calls to the overloaded subtraction and multiplication operators were other expensive code paths. These simply call the appropriate DirectXMath function, and so calls to operators were replaced with direct calls to the DirectXMath function. For example,

```
XMVECTOR length = p1->getPosition() - p2->getPosition();
```

became

```
XMVECTOR length = XMVectorSubtract(p1->getPosition(), p2->getPosition());
```

Fig B.4 shows the the profiling results after these changes were added. The most expensive code paths now are all DirectXMath functions directly involved in calculating Equations 2.7 and 2.8.

Implementing both of these changes awarded performance gains of 40FPS for a debug build with a 50 by 50 mesh.

A final optimisation step was changing the accessors and mutators in Particle to return and pass by reference. This improved performance slightly, giving gains of roughly 5FPS.

3.3.1.1 Second Cycle

One optimisation was made to the initial design of cycle two.

The VerletIntegrator and ExplicitEulerIntegrator classes were made friend classes of Particle. This allows the integrators to access Particle's private member variables directly, removing the overhead of having to call accessors. This change resulted in small performance increases for both integrators, reducing overall update time be approximately 0.3ms, for a 50 by 50 mesh on a debug build, which translated to an increase of 3-4FPS. This increase was also enough to move from unstable to stable cloth when using Verlet integration.

Chapter 4

Test Plan

4.1 Test Data

To evaluate the hypotheses, a number of data fields will be captured from the simulation

- Simulation frame rate. This will be affected by the cost and frequency of the integration calculations and is essential to capture to determine if the simulation is running in real time

- Average time spent in the various functions such as calcSpringForce and update. Extracting these timings will give a better understanding of where the time each frame is spent

The data mentioned above will be extracted by simulating the cloth in two different scenarios.

The first, or sheet, scenario will simulate a sheet hanging from a washing line. The top left and right particles of the cloth will be pinned, so as to be unaffected by any forces, and gravity applied as the sole external force.

The second scenario will simulate a flag on a flag pole flapping in the wind. Particles on the left edge of the cloth will be pinned with gravity and a wind force acting as external forces. The addition of wind will result in much more movement in the cloth so this scenario provides data on performance of a more active simulation.

4.2 Test Parameters

Mass-Spring models for cloth simulation have a number of different parameters which affect realism and performance, and are notoriously difficult to tune.

4.2.1 Mesh Size

This is the discretisation of the cloth, i.e. the number of particles used to represent the cloth, and is represented by two integers representing the number of rows and columns; the total number of particles in the cloth is therefore *rows × columns*.

Increasing mesh size will result in a more realistic simulation but there will be direct impacts on performance as a result. Adding more particles adds more springs, and therefore more calculations are needed every time step to calculate the internal forces. Adding more particles also increases the number of integration calculations needed every time step and both of these factors combined will result in a performance hit for the simulation.

Several different mesh sizes will be used when evaluating the project hypotheses. Data will be extracted for each integrator at each mesh size. This will allow a comparison of the performance impact of the integrators when mesh size is varied.

4.2.2 Integrator Time Step

The time step will vary from integrator to integrator and must be set carefully in order to maintain the stability of the cloth.

Varying the time step will affect the performance of the simulation as it will vary the frequency with which the integration calculations must be performed.

The maximum stable time step will be used along with a number of smaller time steps. This will allow a direct comparison of performance impact as time step decreases; the maximum time step value will be found by investigating the point at which the integrators become unstable.

4.2.3 Spring and Damping Coefficients

Varying the spring and damping coefficients of the springs will affect the realism of the simulation. If the stiffness is set too low, then the particle displacement will increase and may result in unrealistic deformations of the cloth. On the other hand, if the stiffness is set too high then this can lead to no displacement in the cloth at all. For damping, if it is set too low then the cloth will oscillate too much and appear too elastic, if set too high then the cloth will appear as if moving through a viscous fluid, such as oil.

Varying stiffness may also have an impact on the simulation's performance; increasing the stiffness may

require the use of smaller time steps in order to maintain stability, depending on the chosen integrator.

4.2.4 Particle Mass

Since this project is not concerned with truly accurate cloth modelling, the particles' mass will be defined uniformly; that is, a total mass will be defined for the cloth and then divided by the number or particles to give the mass of an individual particle.

Varying the mass of the particles may have an impact on simulation performance. As a result of Equation 2.5, increasing the mass of a particle will increase its displacement due to gravity and therefore, the stiffness of the springs may need to be increased in order to maintain the realism of the simulation.

Since this project is primarily concerned with measuring the performance of different integrators, mesh size and time step are the key parameters. As such, mass and spring and damping coefficients will be kept the same for each mesh size. In this way only one parameter will change between tests and therefore the true effect of the parameter on performance can be measured. The downside of keeping mass and the coefficients constant is that it may not lead to the most realistic cloth, however this is acceptable because the focus is on measuring performance rather than appearance.

4.3 Test Process

As the previous section details, the first stage of the testing process will be investigations into suitable values for the various test parameters. Following this, the test data will be extracted for every combination of mesh size and time step, in both the flag and sheet scenarios.

This, second, testing phase will be automated, using an XML file to detail the specific integrator and test parameters to use. The XML file will take the following form:

```xml
<test_list>
  <test id=''''>
    <integrator type='''' time_step=''''/>
    <cloth_params height='''' width='''' mass='''' wind_constant=''''>
      <top_left_position x='''' y='''' z='''' />
      <mesh_size rows='''' columns='''' />
      <structural spring_coefficient='''' damping_coefficient='''' />
```

```xml
        <shear spring_coefficient='''' damping_coefficient='''' />

        <flexion spring_coefficient='''' damping_coefficient='''' />

        <wind direction x='''' y='''' z='''' />

      </cloth_params>

    </test>

  </test_list>
```

Each test element extracted from the test_list will be run in both the flag and sheet scenario. Scenarios will be run for a maximum of one minute, and when the run is completed, the appropriate test data will be extracted and stored in a CSV file.

Chapter 5

Data Analysis and Evaluation

This chapter will present and analyse the data gathered with the test plan detailed in the previous chapter. It will also evaluate the project hypotheses using the gathered data.

5.1 Chosen Parameters

The first stage of the data collection process was to choose suitable values for the parameters detailed previously.

5.1.1 Mesh Size

The maximum mesh size used was 300 by 300; this is the largest mesh size the can be run at real time frame rates with the most expensive integrator (RK4). This maximum was decreased by 50 in both dimensions, to a minimum size of 50 by 50, to give the six mesh sizes below.

- 300 by 300

- 250 by 250

- 200 by 200

- 150 by 150

- 100 by 100

- 50 by 50

5.1.2 Time Step

The maximum time step was 20ms. This was the largest time step where at least one integrator was still stable for a 50 by 50 mesh. This values was decreased by 5ms giving the ranges of five time steps listed below.

- 20ms

- 15ms

- 10ms

- 5ms

- 1ms

5.1.3 Mass and Spring and Damping Coefficients

These parameters were kept constant for every mesh size to avoid changing more than one variable between tests. Values were chosen that gave a reasonable cloth appearance. There are some visual issues, such as too much oscillation, with the values chosen at the larger mesh sizes but this is acceptable due to the focus of the project. The values used are as follows:

- Mass = 100

- Structural Stiffness = 20

- Structural Damping = 7.5

- Shear Stiffness = 20

- Shear Damping = 7.5

- Flexion Stiffness = 5

- Flexion Damping = 2.5

For Verlet, a constant damping factor of 0.5% was used.

5.2 Results

5.2.1 Explicit Euler

Fig C.1 shows the average simulation frame rate for every time step at every mesh size, in the sheet scenario. The graph shows two things, firstly that as mesh size increases average frame rate decreases and secondly that as time step increases average frame rate increases.

The data shows that varying mesh size can have a dramatic effect on the frame rate, this is shown well by Fig C.2. This graph uses the average FPS for a 1ms time step, so that only one variable is changed. It has a strong negative correlation, which supports the conclusion that mesh size has a large effect on performance. Also, it clearly shows a dramatic frame rate decrease as mesh size is increased to 100 by 100 and 150 by 150; for a 100 by 100 mesh the decrease is approximately 1.4 times and for 150 by 150 approximately 5.4 times.

The decrease in frame rate can be explained by examining where the time each frame is spent. Fig C.6 shows that the majority of the frame time is spent in the update function for a 300 by 300 mesh using a 1ms time step. This is the worst case test, but the conclusion is reflected across all other mesh sizes and time steps. By plotting the average time spent in the update function against mesh size, it is possible to explain why the frame rate decreases. Fig C.4 shows this graph; as with Fig C.2 it shows data for a 1ms time step. This shows a strong positive correlation, thus it can be concluded that update time increases with mesh size. If the time for each update increases with mesh size, then the total time for each frame must increase also, thus reducing the frame rate of the simulation.

Digging a little deeper, Fig C.7 shows that calculating the internal forces, i.e. the spring forces, is the most expensive part of each update. By plotting this against mesh size, shown in Fig C.5, a strong positive correlation is again observed. This is easy to explain. As mesh size increases, the number of particles increases, and therefore the number of springs also increases. More springs means that Equations 2.7 and 2.8 must be calculated more, hence the time spent on internal forces increases.

The increase in update time with mesh size also explains the increase in frame rate as the time step increases. As the time step increases, the expensive update function is called less frequently, so overall frame time is decreased, thus increasing the frame rate. Fig C.3 shows the average frame rate plotted against the time step for a 300 by 300 mesh. This graph shows a positive correlation, thus supporting that frame rate increases with time step. It also shows that frame rate only increases once the time step

exceeds some threshold; this is also shown in Fig C.1. Again, this result can be explained by examining the average update time. For the 300 by 300 mesh, the average update time was approximately 6ms, and frame rate only increased once the time step reaches 10ms. The reason for this should be obvious; both the 1ms and 5ms time steps are less than the total update time, therefore the update function will still be called every frame.

When looking at the results in the figures above, it is also important to look at the stability of each test. The stability of each test was evaluated subjectively, and the results are listed in Table 5.1 As can be seen, for the sheet scenario, explicit Euler was really only stable with a 1ms time step, with the exception of the 50 by 50 mesh, where it was stable with a 5ms time step as well.

The data for the flag scenario shows similar correlations to the sheet scenario. Figs C.8 and C.9 show that as mesh size increases FPS decreases, with the same initial dramatic decreases as the sheet scenario; the decrease for a 100 by 100 mesh is approximately 2.3 times and approximately 5 times for 150 by 150. As with the sheet scenario, the majority of the frame time is still spent within update (see Fig C.13) and Fig C.11 displays a strong positive correlation as well.

Fig C.14 shows a slightly different time breakdown within the update function. Calculating the internal forces is still the most expensive part, but the cost of calculating external forces has risen significantly over the sheet scenario; an approximate increase of 6.7 times. This is because the flag scenario includes wind as an additional external force. In order to apply wind, the particles must be split into triangles and the surface normal of every triangle calculated at every time step.

Figs C.8 and C.10 also show that as time step increases the FPS increases with it. They also support the conclusion that frame rate only increases once the time step exceeds the total update time; again the frame rate for the 300 by 300 mesh only increased at 10ms, because the average update time was approximately 8ms.

The stability of the flag scenario tests, listed in Table 5.2 are also similar to the sheet scenario, with the only difference being that a 5ms time step and 100 by 100 mesh was stable for the flag scenario.

Mesh Size	Time Step (ms)	Stable/Unstable
50 by 50	1	Stable
50 by 50	5	Stable
50 by 50	10	Unstable
50 by 50	15	Unstable
50 by 50	20	Unstable
100 by 100	1	Stable
100 by 100	5	Unstable
100 by 100	10	Unstable
100 by 100	15	Unstable
100 by 100	20	Unstable
150 by 150	1	Stable
150 by 150	5	Unstable
150 by 150	10	Unstable
150 by 150	15	Unstable
150 by 150	20	Unstable
200 by 200	1	Stable
200 by 200	5	Unstable
200 by 200	10	Unstable
200 by 200	15	Unstable
200 by 200	20	Unstable
250 by 250	1	Stable
250 by 250	5	Unstable
250 by 250	10	Unstable
250 by 250	15	Unstable
250 by 250	20	Unstable
300 by 300	1	Stable
300 by 300	5	Unstable
300 by 300	10	Unstable
300 by 300	15	Unstable
300 by 300	20	Unstable

Table 5.1: Stability results for explicit Euler (sheet)

Mesh Size	Time Step (ms)	Stable/Unstable
50 by 50	1	Stable
50 by 50	5	Stable
50 by 50	10	Unstable
50 by 50	15	Unstable
50 by 50	20	Unstable
100 by 100	1	Stable
100 by 100	5	Stable
100 by 100	10	Unstable
100 by 100	15	Unstable
100 by 100	20	Unstable
150 by 150	1	Stable
150 by 150	5	Unstable
150 by 150	10	Unstable
150 by 150	15	Unstable
150 by 150	20	Unstable
200 by 200	1	Stable
200 by 200	5	Unstable
200 by 200	10	Unstable
200 by 200	15	Unstable
200 by 200	20	Unstable
250 by 250	1	Stable
250 by 250	5	Unstable
250 by 250	10	Unstable
250 by 250	15	Unstable
250 by 250	20	Unstable
300 by 300	1	Stable
300 by 300	5	Unstable
300 by 300	10	Unstable
300 by 300	15	Unstable
300 by 300	20	Unstable

Table 5.2: Stability results for explicit Euler (flag)

5.2.2 Verlet

5.2.3 Midpoint

5.2.4 Fourth Order Runge-Kutta

5.3 Evaluation

5.3.1 Null Hypothesis

5.3.2 Alternative Hypothesis

Appendix A

Class Diagrams

A.1 First Cycle Design
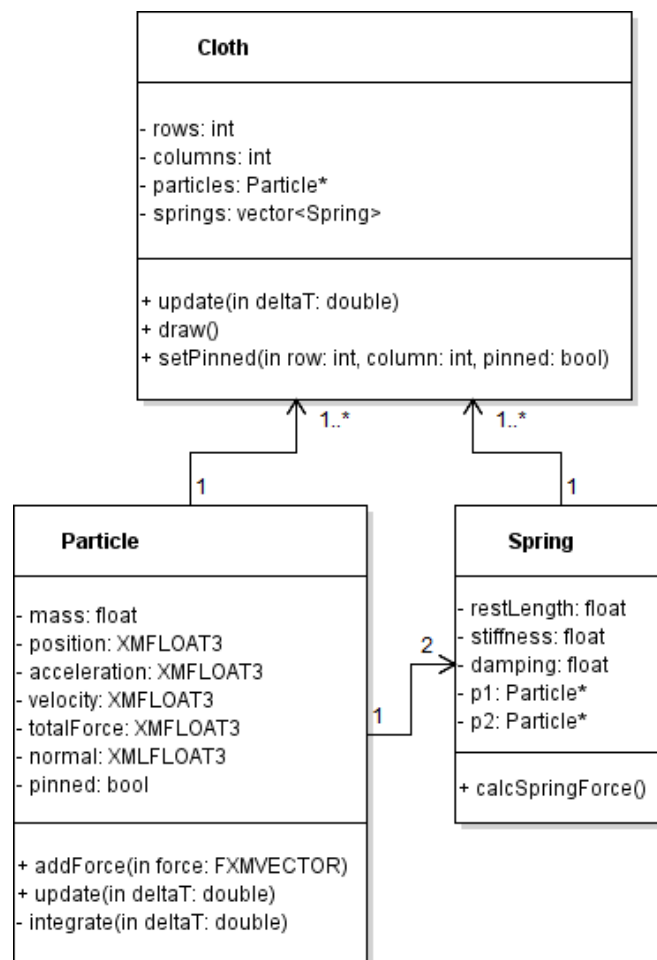
Figure A.1: Initial design for the first development cycle
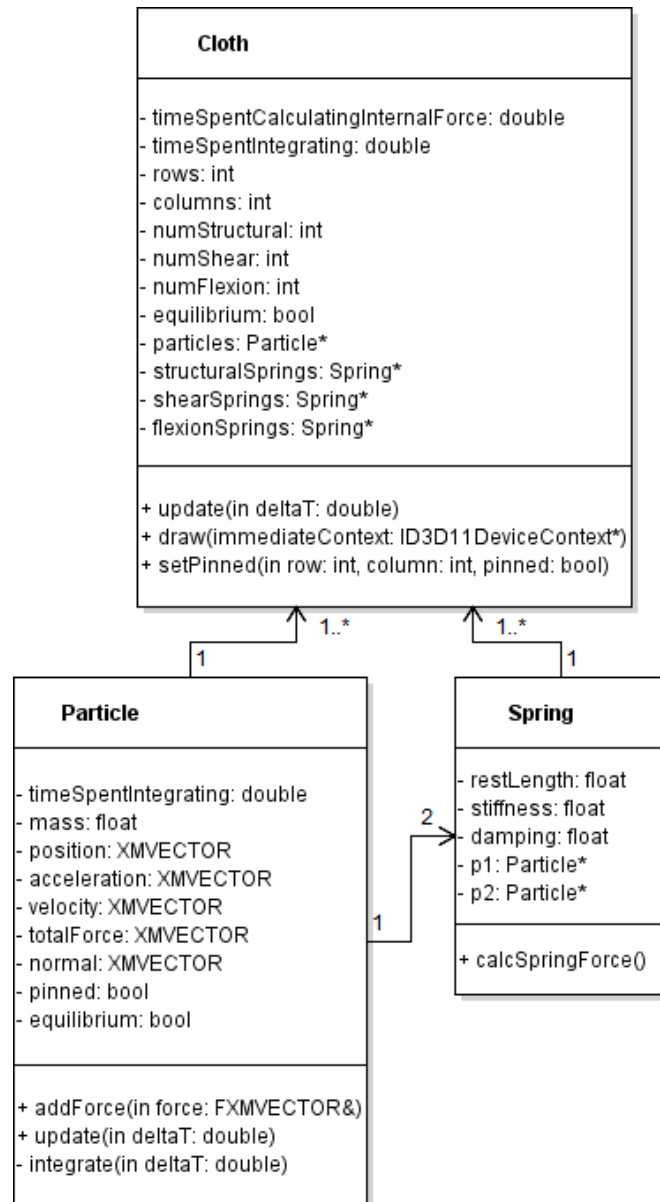
Figure A.2: Final design for the first development cycle

Cloth

+ setIntegrator(integrator: IIntegrator*)
+ setIntegrator(integrator: void (*)(Particle&, double))

VerletIntegrator

- <<static>> instance: std::unique_ptr<IIntegrator>
- timeStep: double

+ <<static>> getInstance(): IIntegrator*

1..*
1

Particle

- previousPosition: XMVECTOR
- integratorInterface: IIntegrator*
- integratorFPointer: void (*)(Particle&, double)

+ getPreviousPosition(): XMVECTOR&
+ getTotalForce(): XMVECTOR&
+ setIntegrator(integrator: IIntegrator*)
+ setIntegrator(integrator: void (*)(Particle&, double))

«interface»
IIntegrator

+ virtual setTimeStep(timeStep: double)
+ virtual integrate(particle: Particle&, deltaT: double)

0..* 1

ExplicitEulerIntegrator

- <<static>> instance: std::unique_ptr<IIntegrator>
- timeStep: double

+ <<static>> getInstance(): IIntegrator*

<<static>>
ExplicitEuler

- timeStep: double

+ setTimeStep(timeStep: double)
+ integrate(particle: Particle&, deltaT: double)

<<static>>
Verlet

- timeStep: double

+ setTimeStep(timeStep: double)
+ integrate(particle: Particle&, deltaT: double)

Figure A.3: Initial design for the second development cycle

58
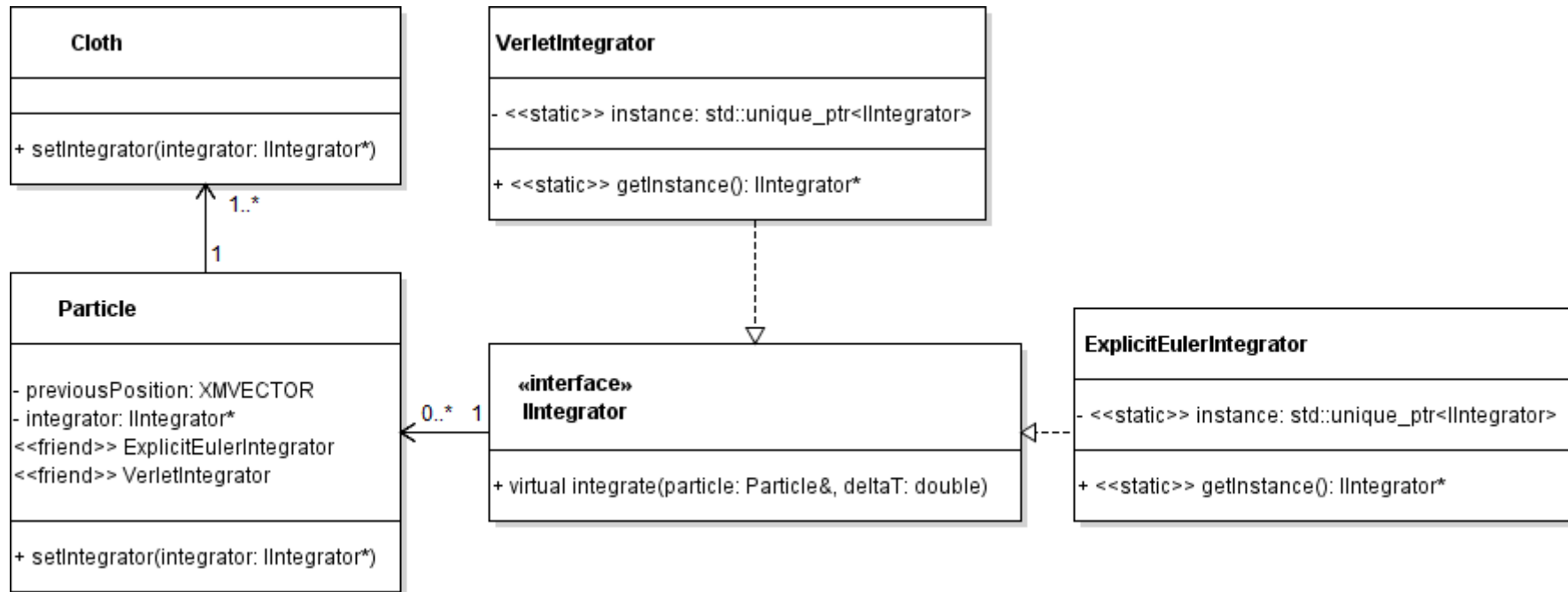
Figure A.4: Final design for the second development cycle

A.3 Third Cycle Design
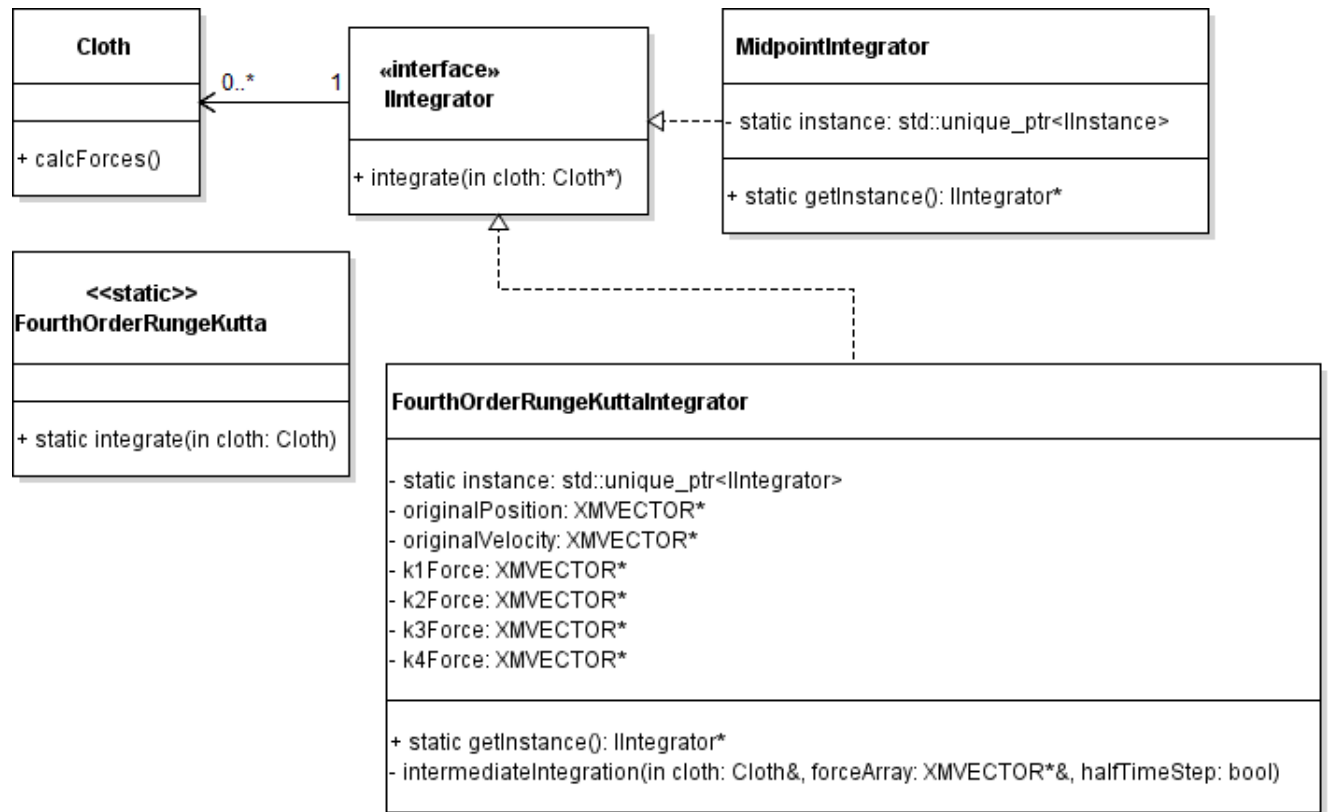
Figure A.5: Initial design for the third development cycle

Cloth

+ calcForces()

0..*   1

«interface»
IIntegrator

+ integrate(in cloth: Cloth*)

MidpointIntegrator

- static instance: std::unique_ptr<IInstance>

+ static getInstance(): IIntegrator*

FourthOrderRungeKuttaIntegrator

- static instance: std::unique_ptr<IIntegrator>
- originalPosition: XMVECTOR*
- originalVelocity: XMVECTOR*
- k1Force: XMVECTOR*
- k2Force: XMVECTOR*
- k3Force: XMVECTOR*
- k4Force: XMVECTOR*

+ static getInstance(): IIntegrator*
- intermediateIntegration(in cloth: Cloth&, forceArray: XMVECTOR*&, halfTimeStep: bool)

Figure A.6: Final design for the third development cycle

Appendix B

Profiling Results

B.1   First Cycle

Hot Path

Function Name	Inclusive Samples %	Exclusive Samples %
Cloth::update	93.00	1.11
std::_Vector_const_iterator<std::_Vector_val<std::_Simple_types<Spring> > >::operator!=	25.13	3.47
std::_Vector_iterator<std::_Vector_val<std::_Simple_types<Spring> > >::operator*	22.37	3.92
std::_Vector_iterator<std::_Vector_val<std::_Simple_types<Spring> > >::operator++	17.06	3.65
Spring::calcSpringForce	9.74	4.57

Figure B.1: Profiling results using a std::vector to store springs

Hot Path

Function Name	Inclusive Samples %	Exclusive Samples %
wWinMain	99.12	0.00
Application::update	96.81	1.91
Cloth::update	77.81	2.23
Spring::calcSpringForce	41.99	20.32
Particle::addForce	17.71	3.88

Figure B.2: Profiling results using dynamic arrays to store springs

Hot Path

Function Name	Inclusive Samples %	Exclusive Samples %
Spring::calcSpringForce	89.51	5.09
Particle::addForce	23.05	5.12
DirectX::XMLoadFloat3	12.17	12.17
DirectX::operator-	9.13	4.39
DirectX::operator*	8.63	4.26

Related Views: Call Tree   Functions

Functions Doing Most Individual Work

Name	Exclusive Samples %
DirectX::XMLoadFloat3	18.00
DirectX::XMStoreFloat3	8.45
Particle::addForce	5.86
DirectX::XMVectorAdd	5.75
Spring::calcSpringForce	5.19

Figure B.3: Profiling results for unoptimised calcSpringForce

Hot Path

Function Name	Inclusive Samples %	Exclusive Samples %
🔥 DirectX::XMVectorScale	8.88	8.88
🔥 DirectX::XMVectorSubtract	7.28	7.28
🔥 DirectX::XMVector3Length	6.53	6.53
🔥 DirectX::XMVector3Dot	4.80	4.80
🔥 Particle::getPosition	4.77	4.77

Related Views: Call Tree   Functions

Functions Doing Most Individual Work

Name	Exclusive Samples %
DirectX::XMVectorScale	11.54
DirectX::XMVectorAdd	9.86
Spring::calcSpringForce	9.74
DirectX::XMVectorSubtract	7.64
Particle::addForce	6.87

Figure B.4: Profiling results for optimised calcSpringForce

Appendix C

Test Results

C.1   Explicit Euler

C.1.1   Sheet Data
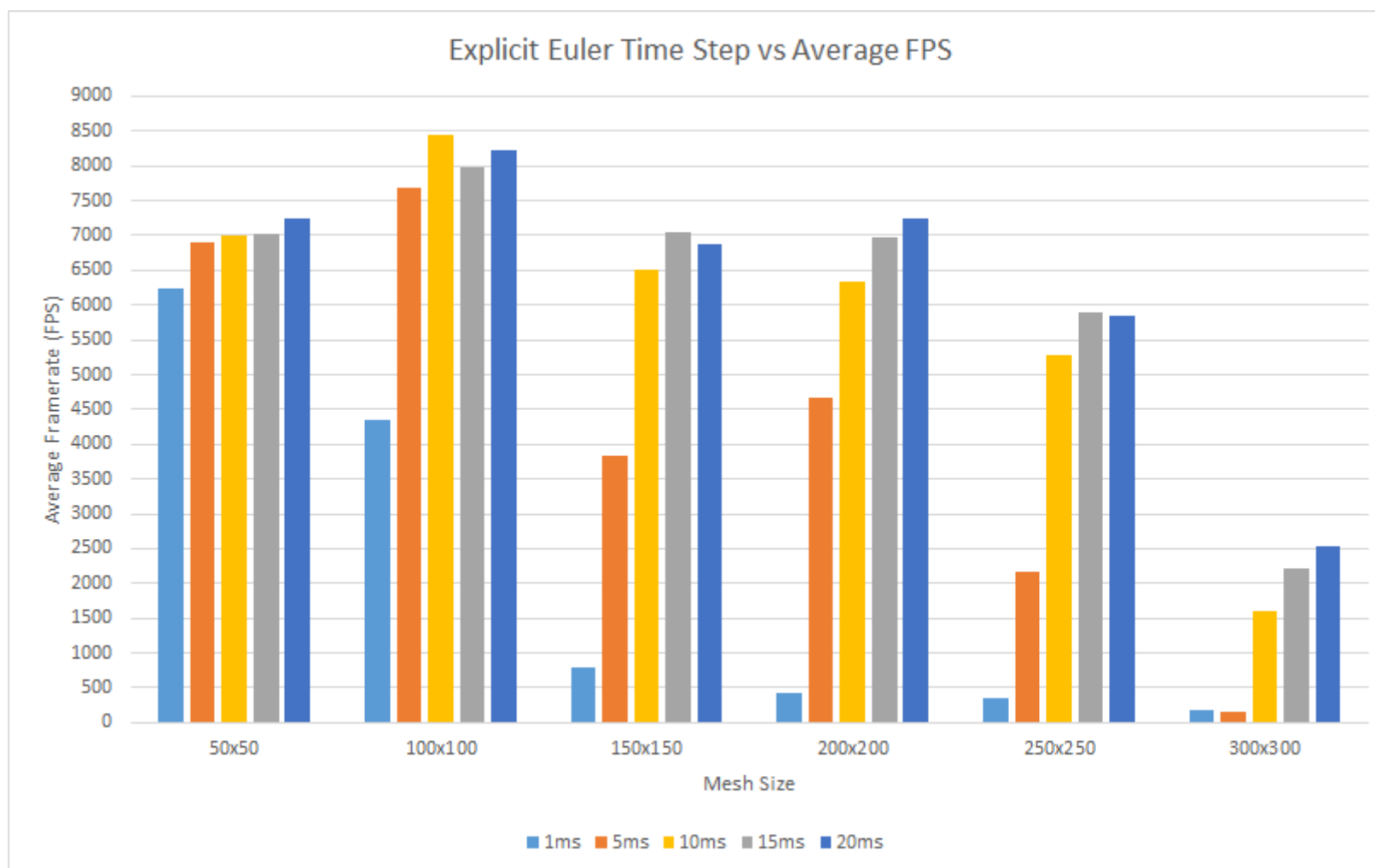
Figure C.1: Explicit Euler time step against average FPS (sheet)
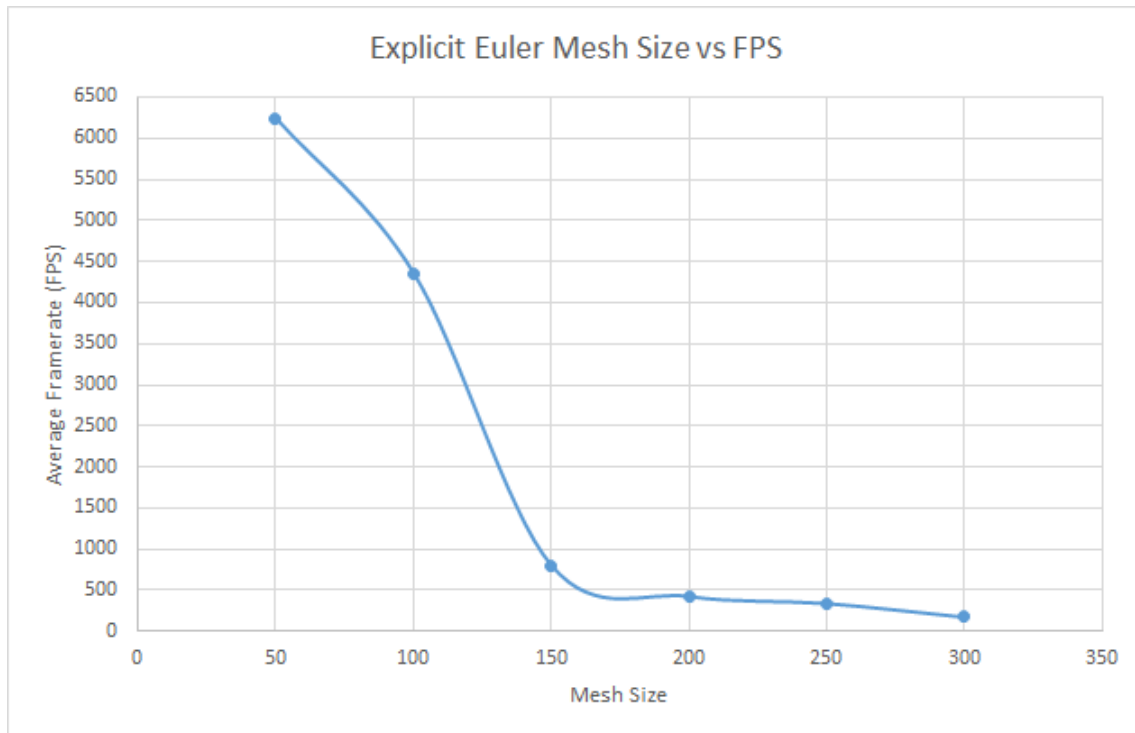
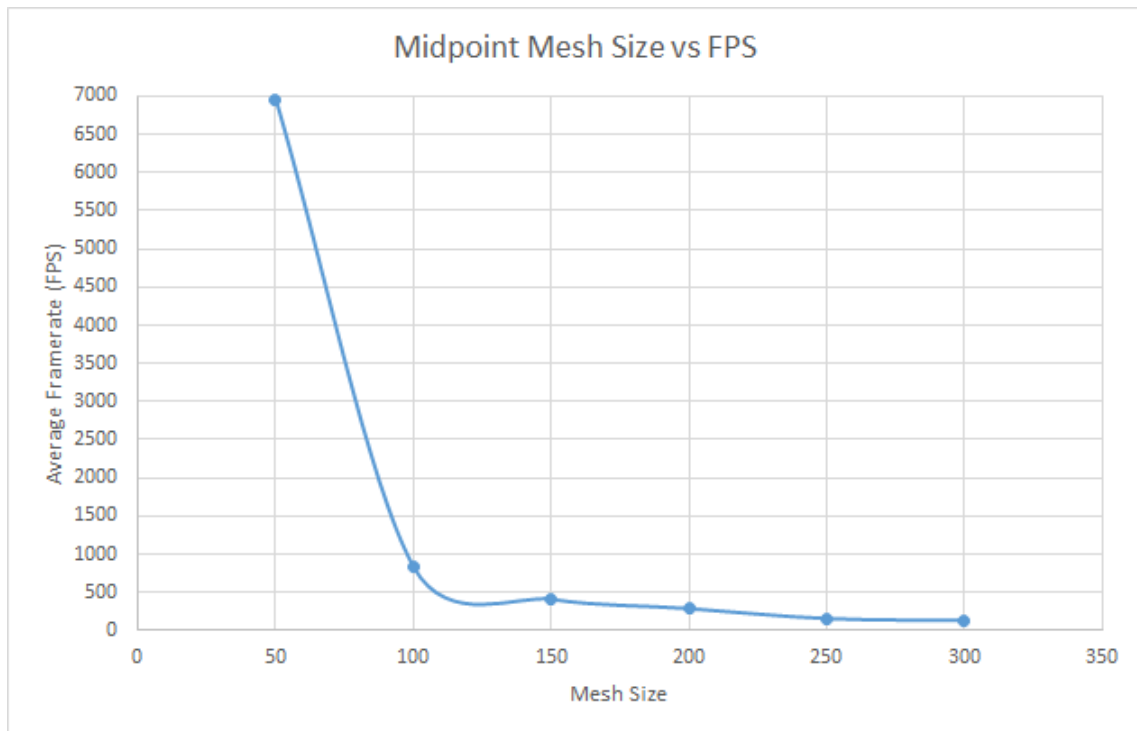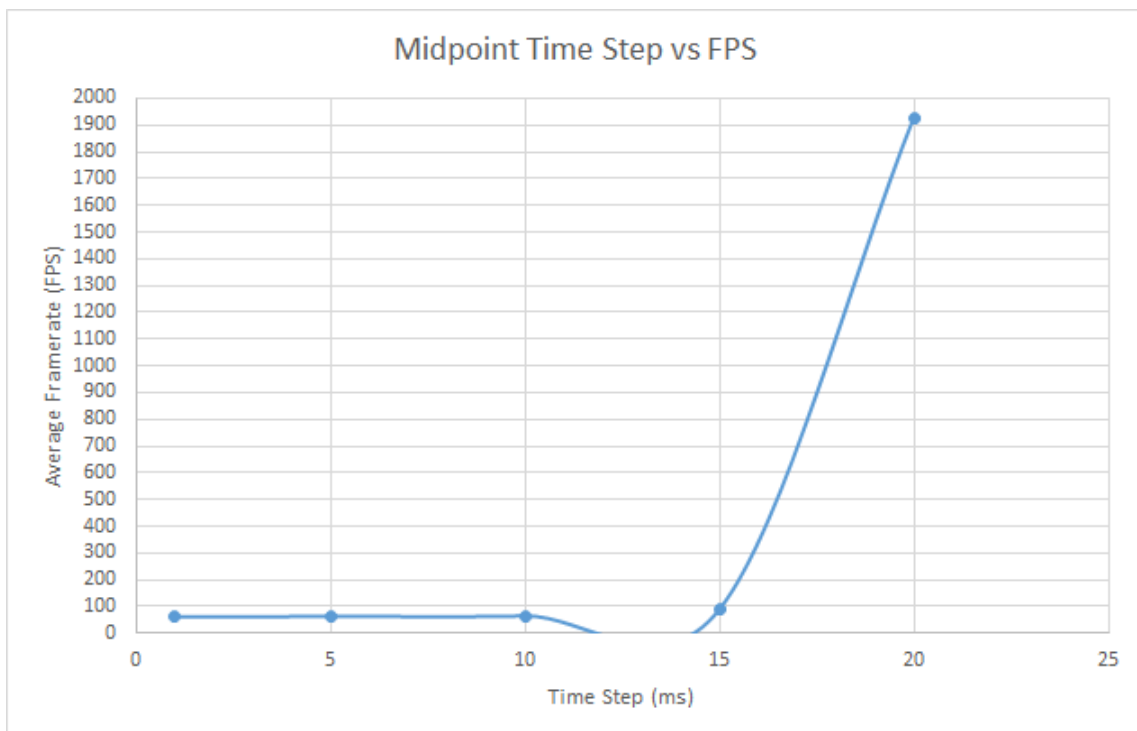Figure C.2: Explicit Euler mesh size against average FPS (sheet)
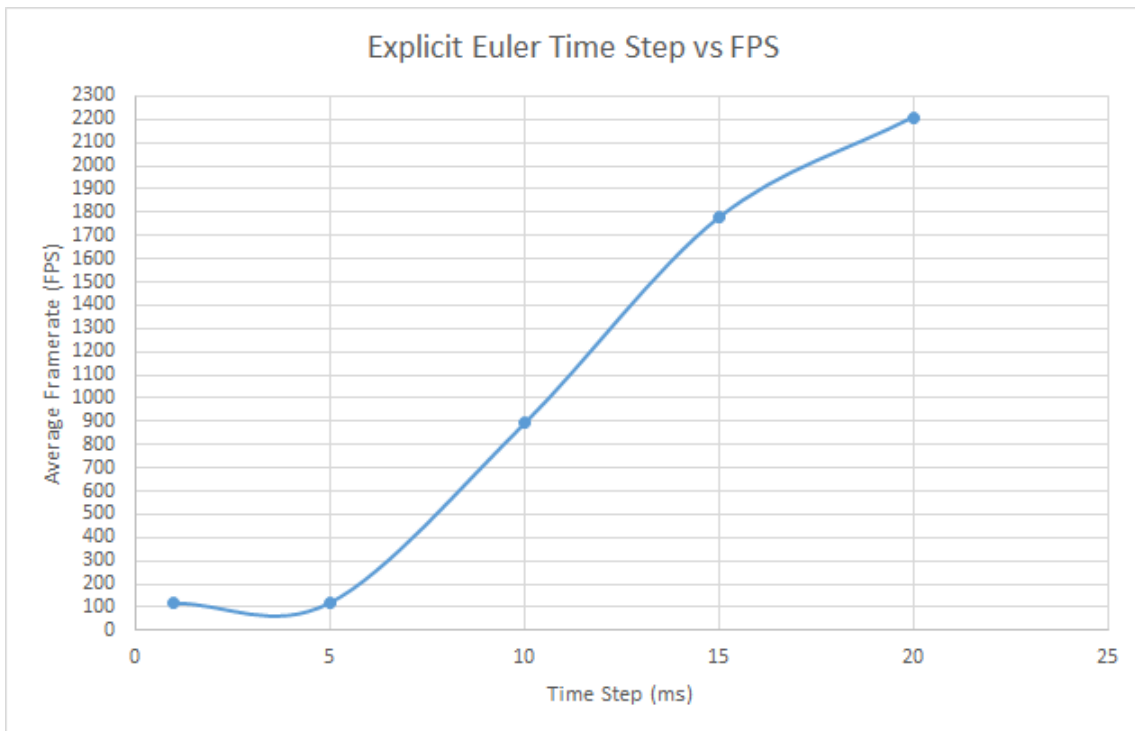
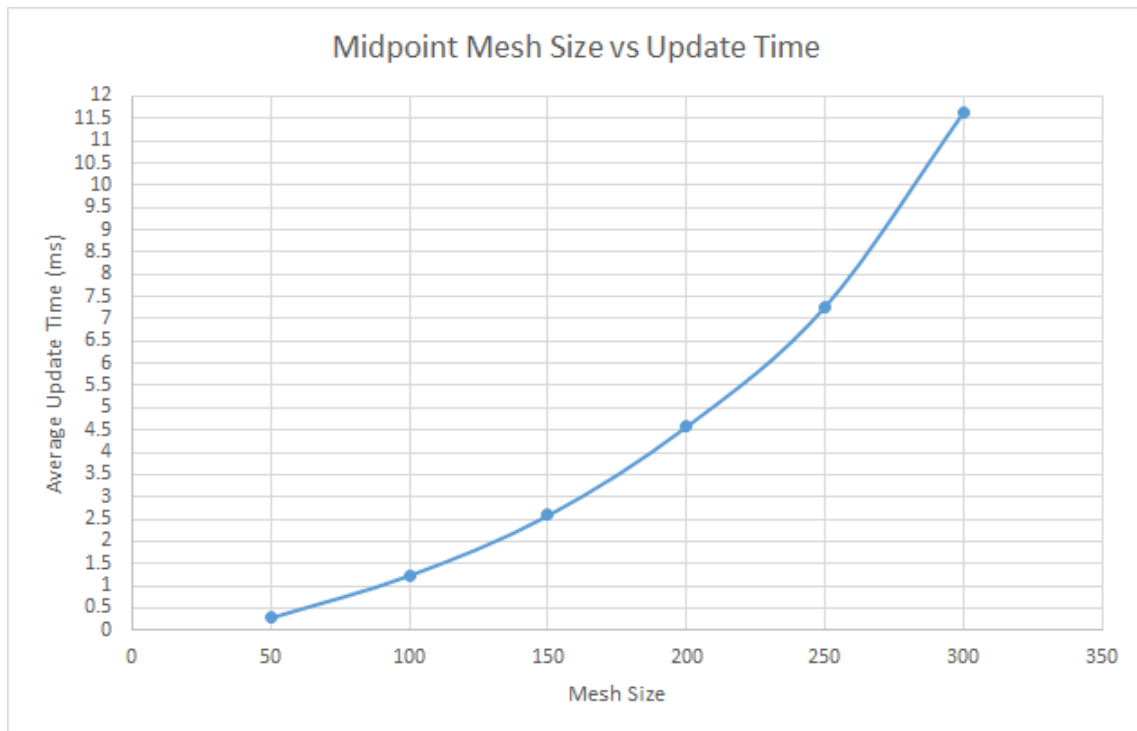Figure C.3: Explicit Euler time step against average FPS for a 300 by 300 mesh (sheet)
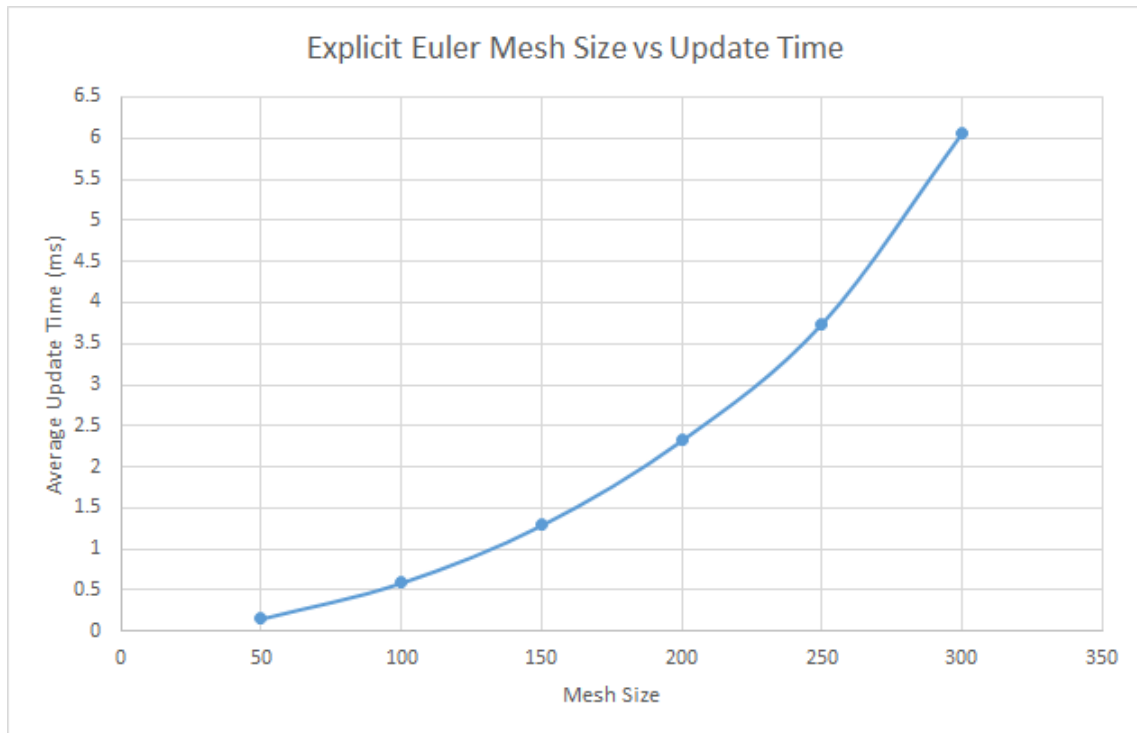
Figure C.4: Explicit Euler mesh size against average update time (sheet)
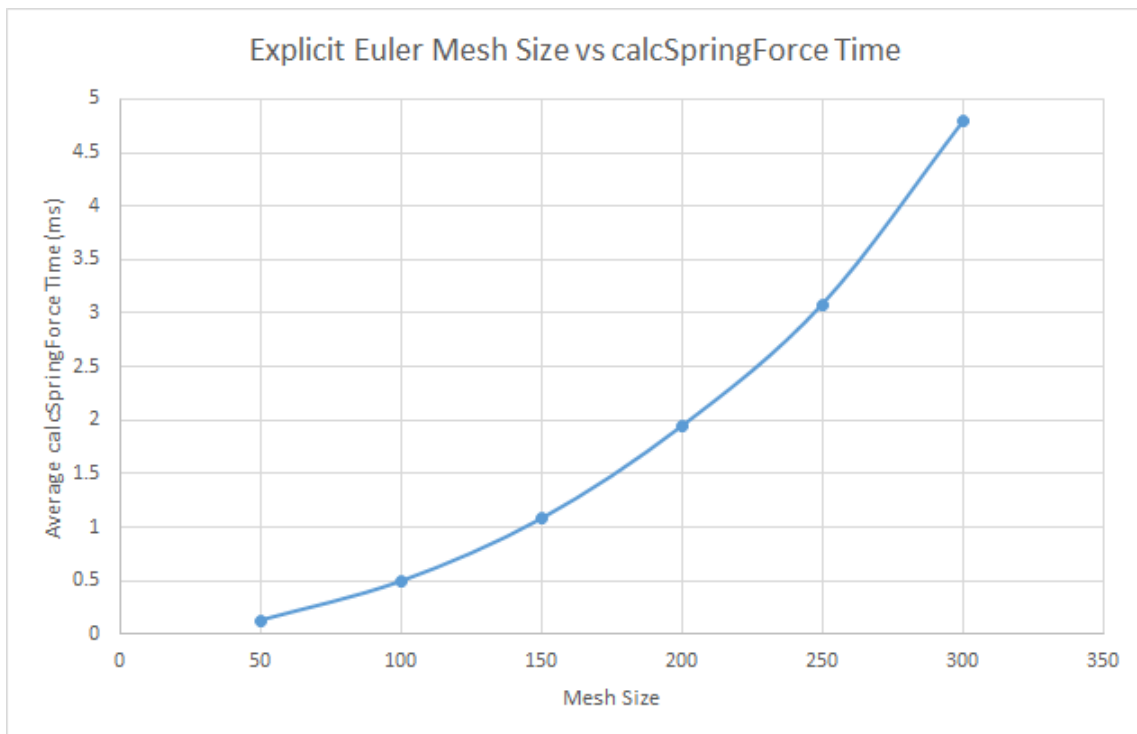
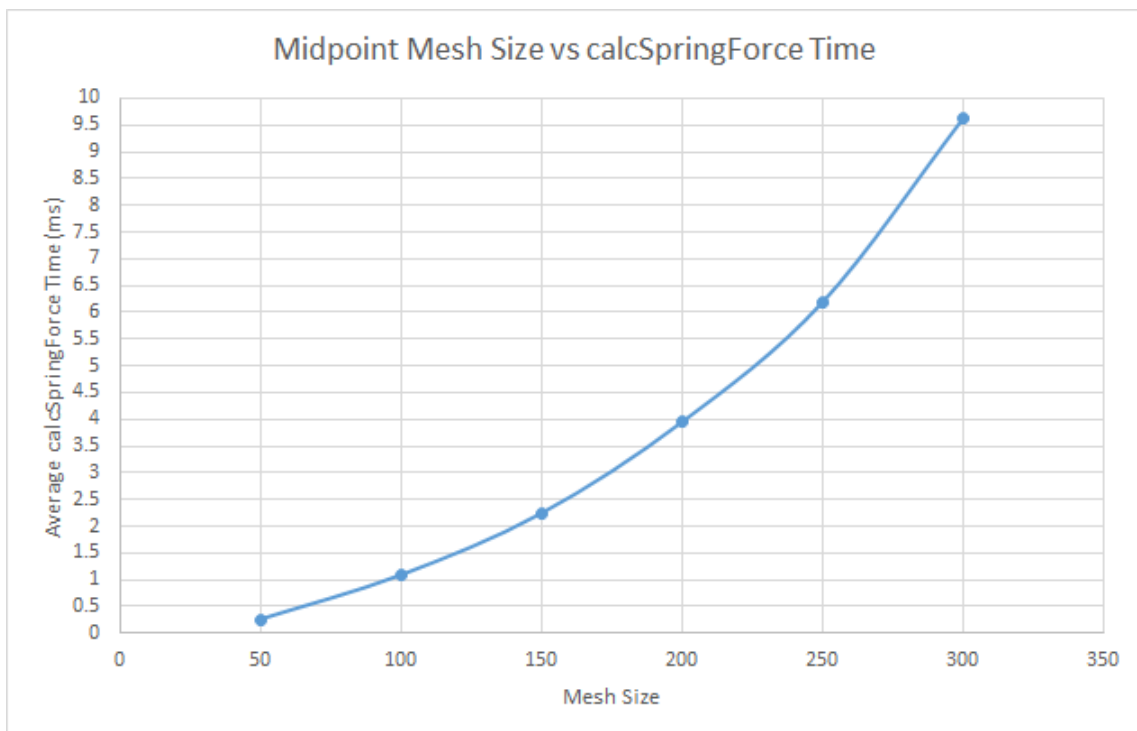Figure C.5: Explicit Euler mesh size against average internal force time (sheet)
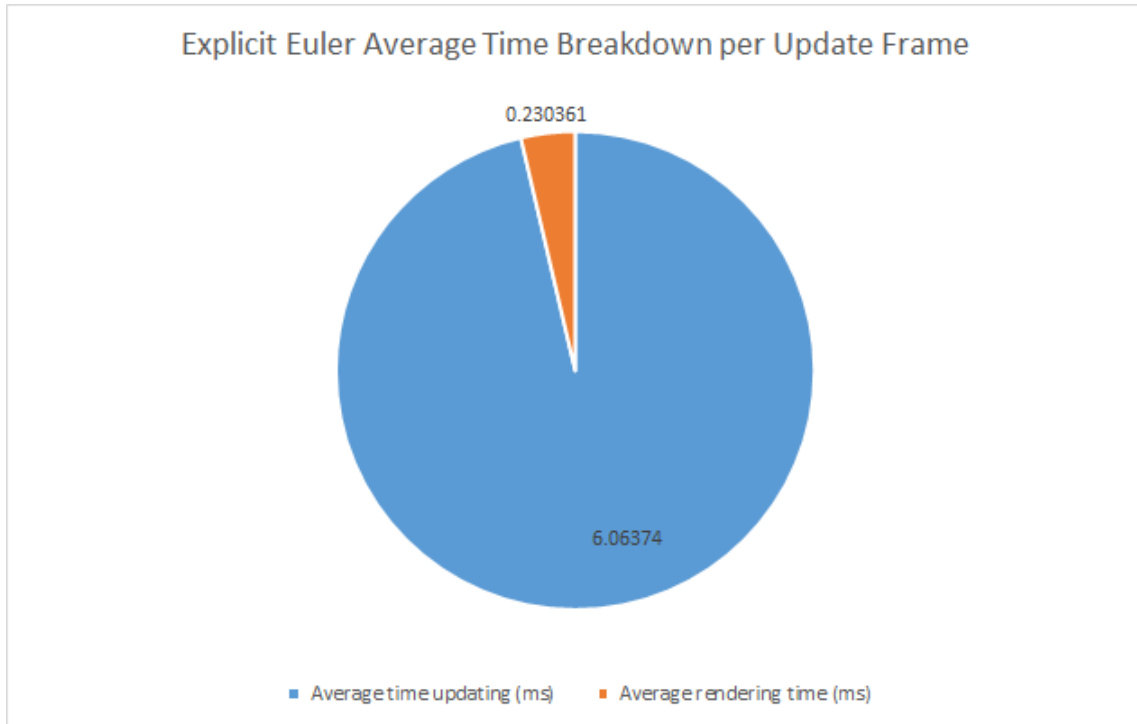
Figure C.6: Explicit Euler frame time breakdown (sheet)
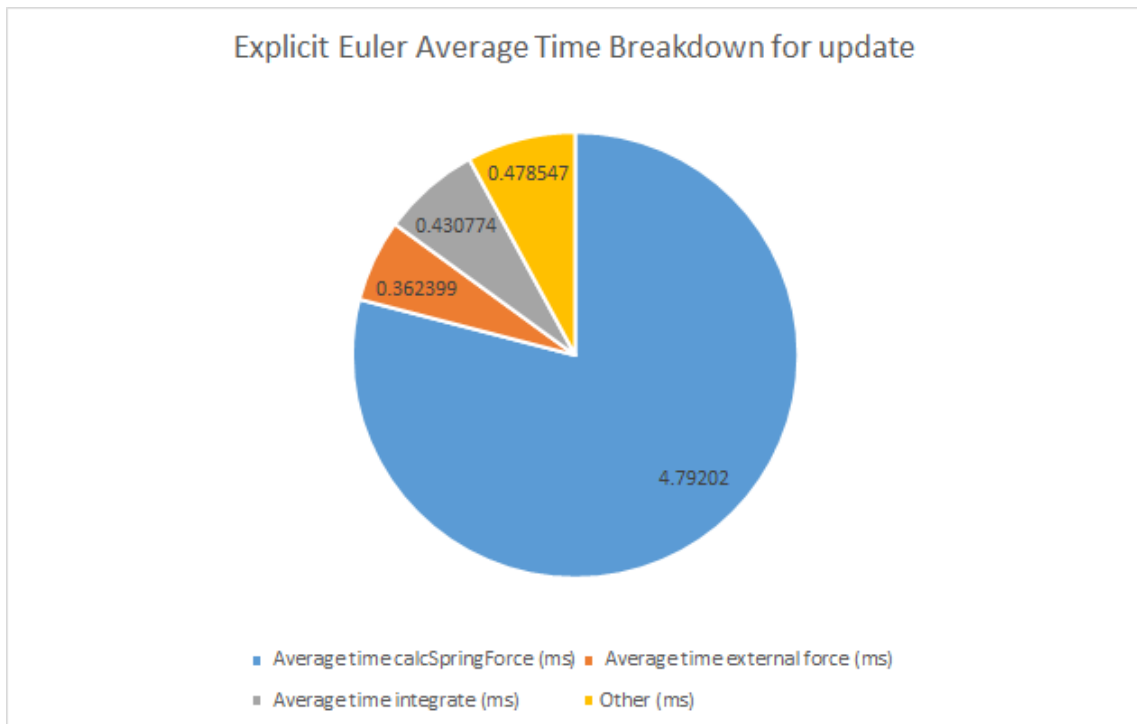
Figure C.7: Explicit Euler update time breakdown (sheet)
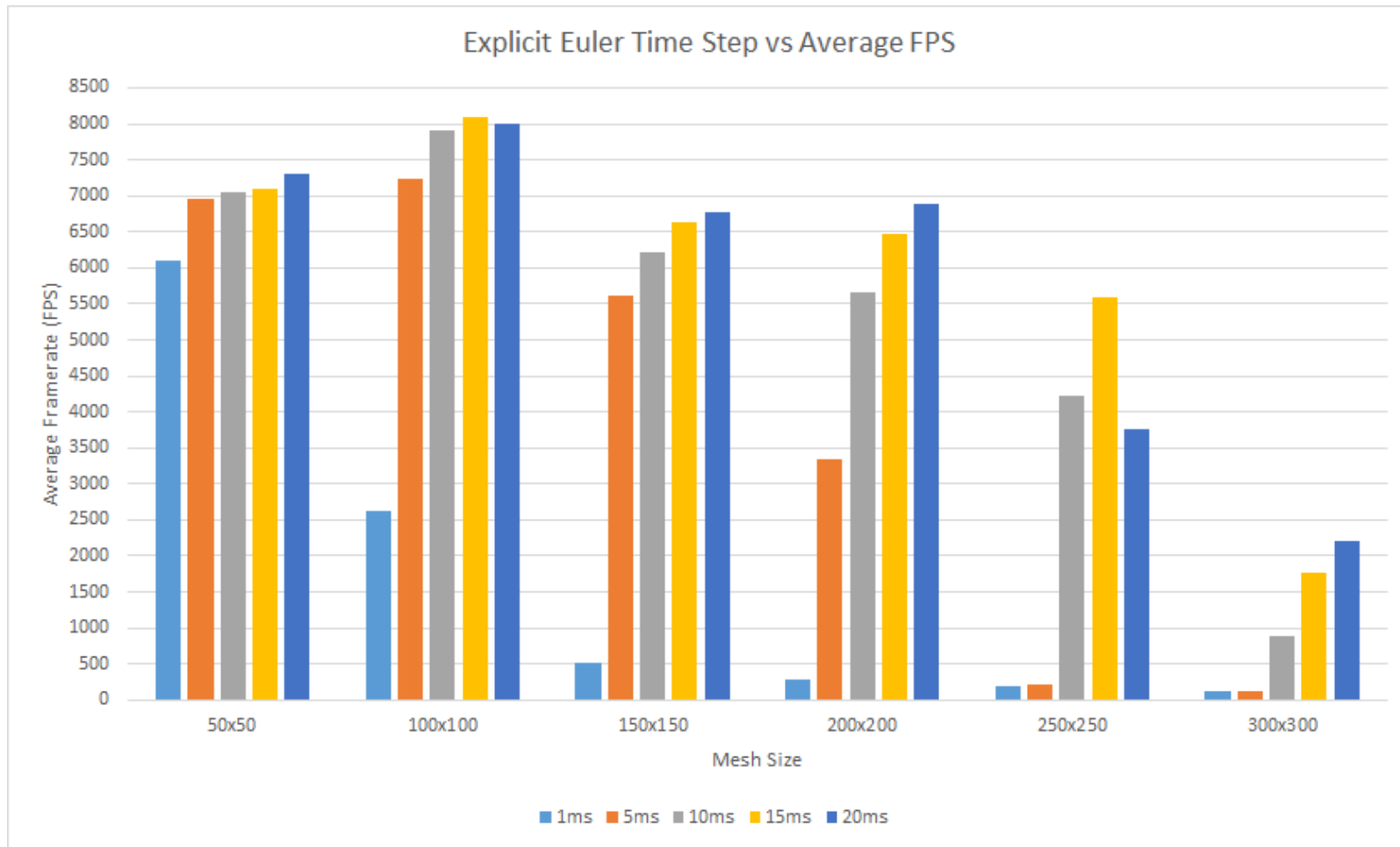
Figure C.8: Explicit Euler mesh size against average FPS (flag)
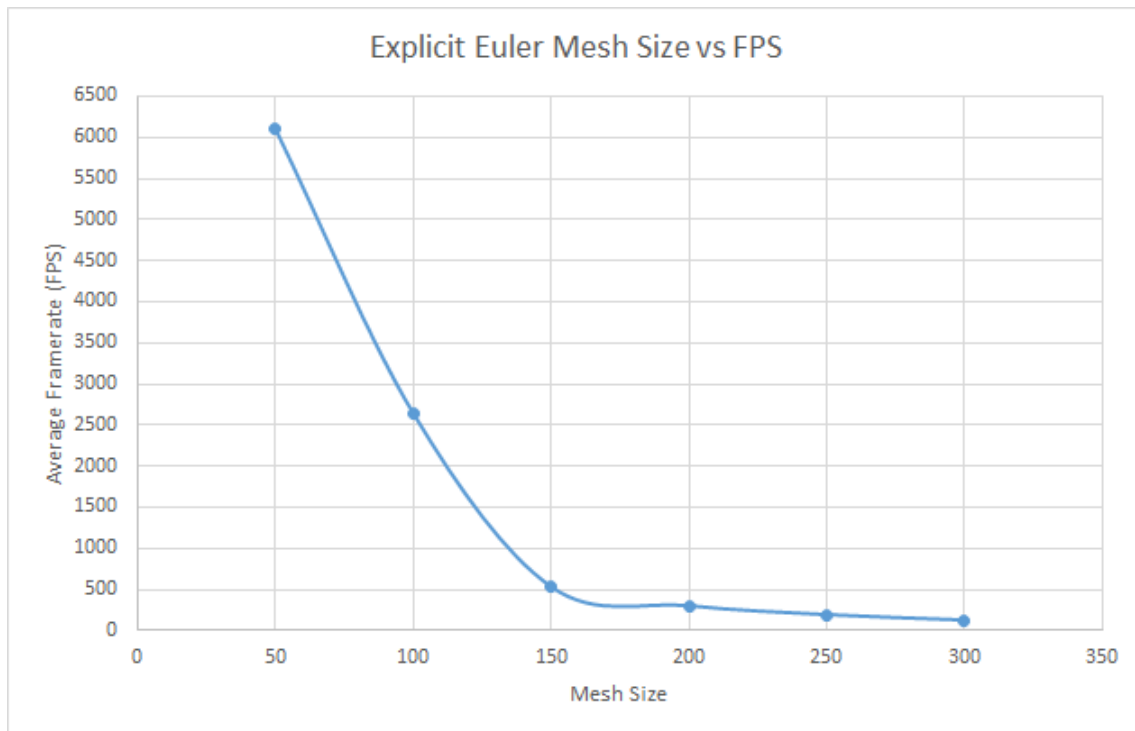
Figure C.9: Explicit Euler mesh size against average FPS (flag)
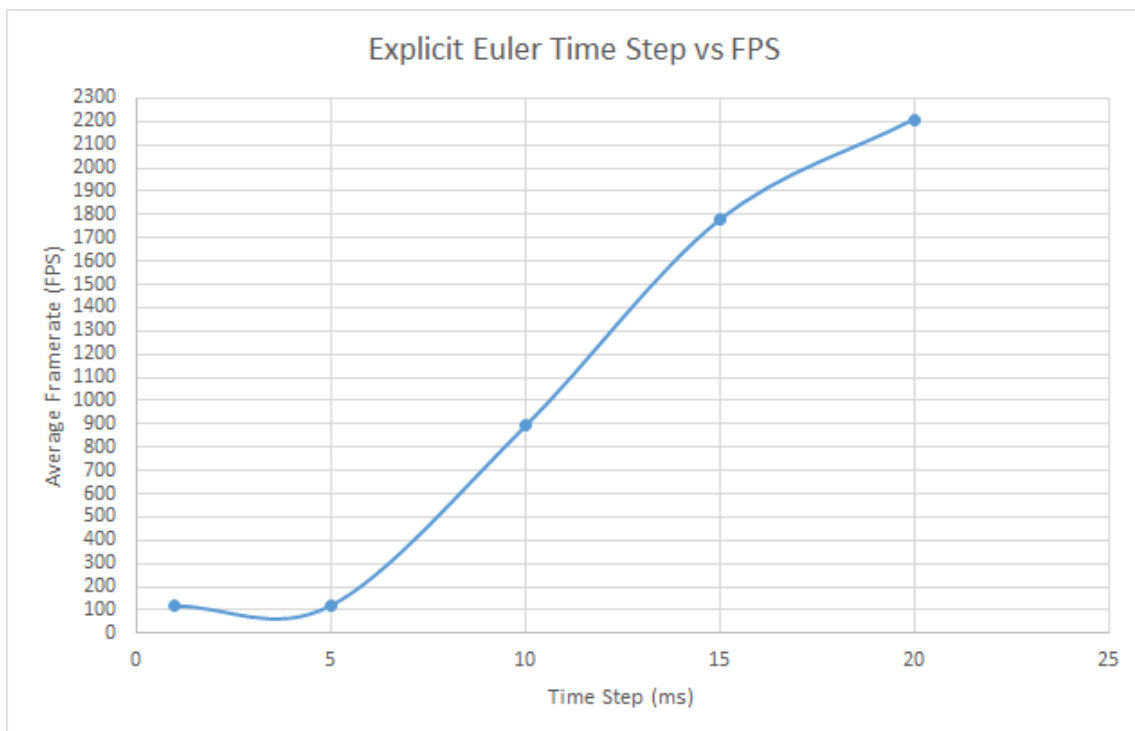
Figure C.10: Explicit Euler time step against average FPS for a 300 by 300 mesh (flag)
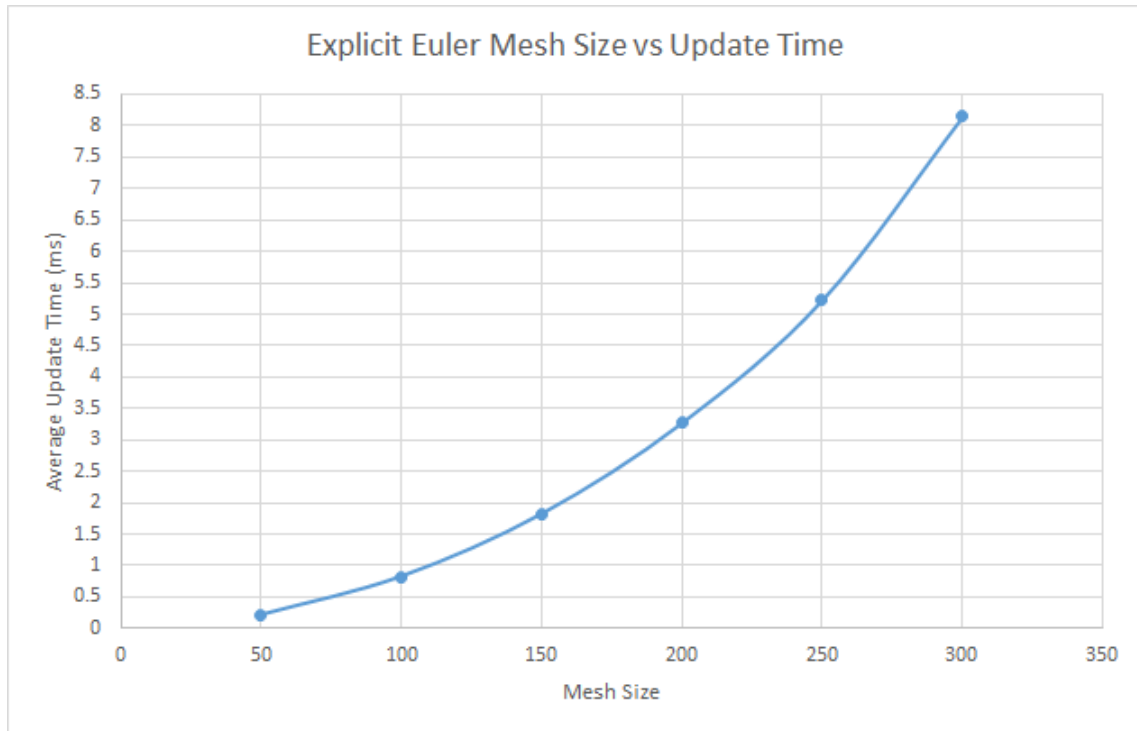
Figure C.11: Explicit Euler mesh size against average update time (flag)
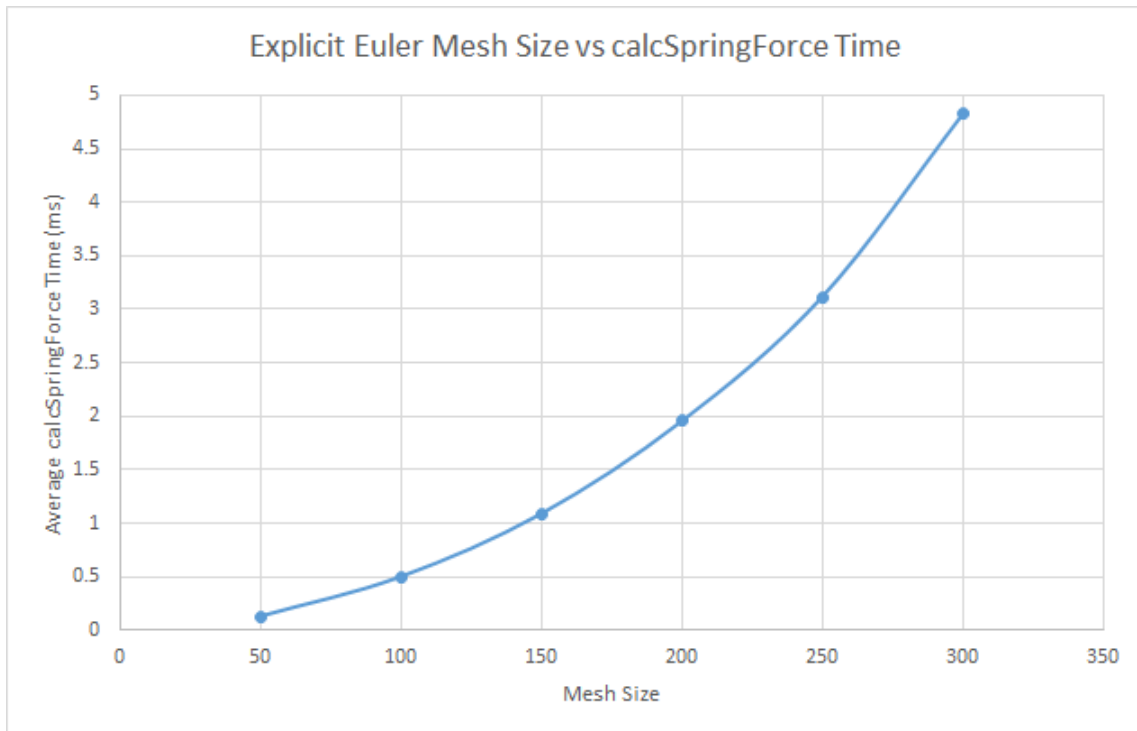
Figure C.12: Explicit Euler mesh size against average internal force time (flag)
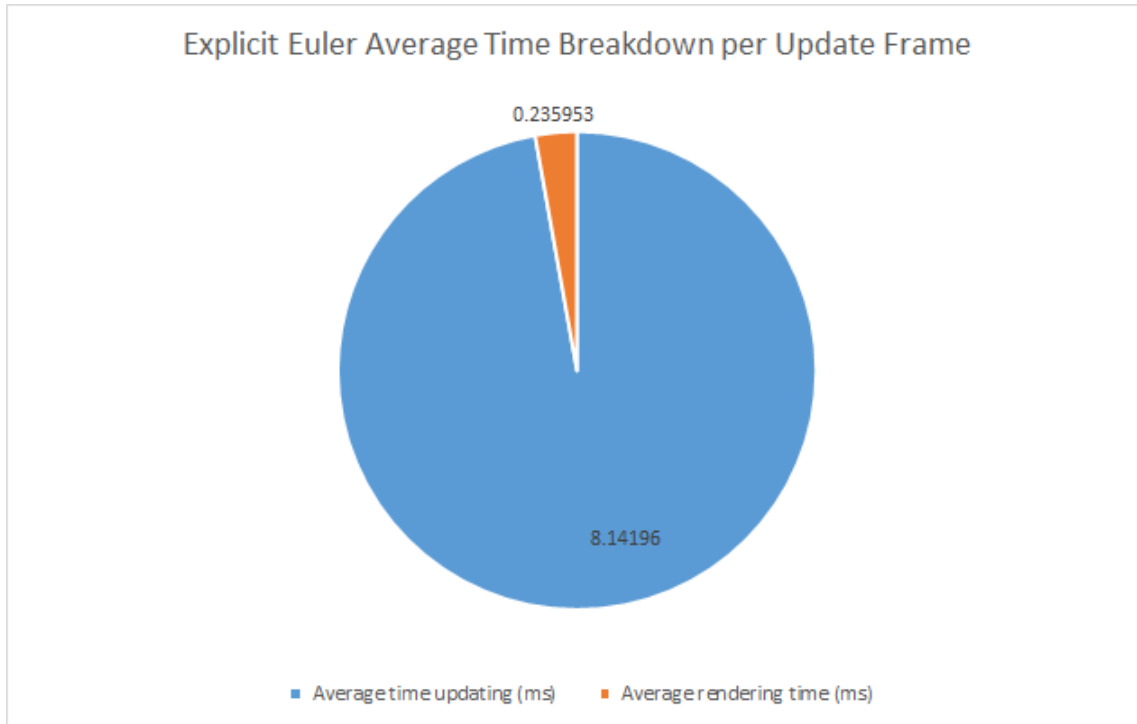
Figure C.13: Explicit Euler frame time breakdown (flag)
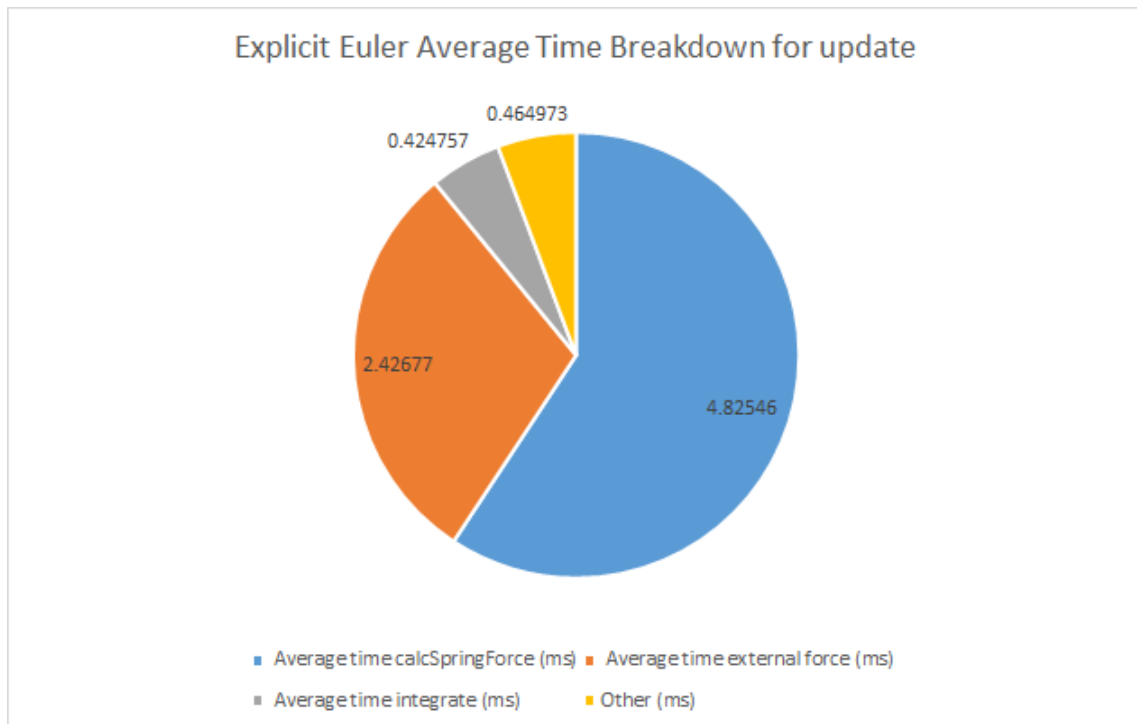
Figure C.14: Explicit Euler update time breakdown (flag)

C.2 Verlet

C.2.1 Sheet Data
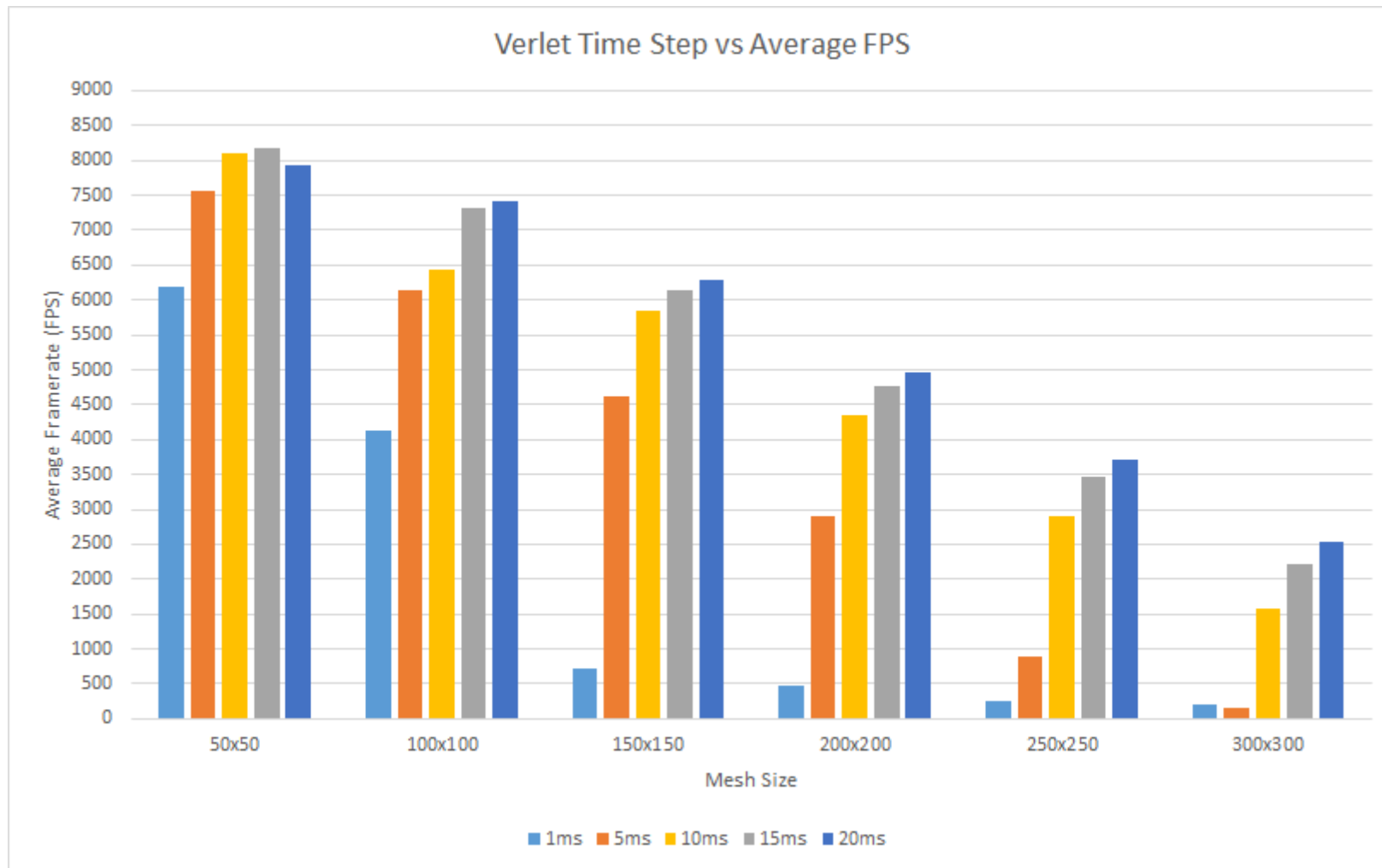
Figure C.15: Verlet time step against average FPS (sheet)
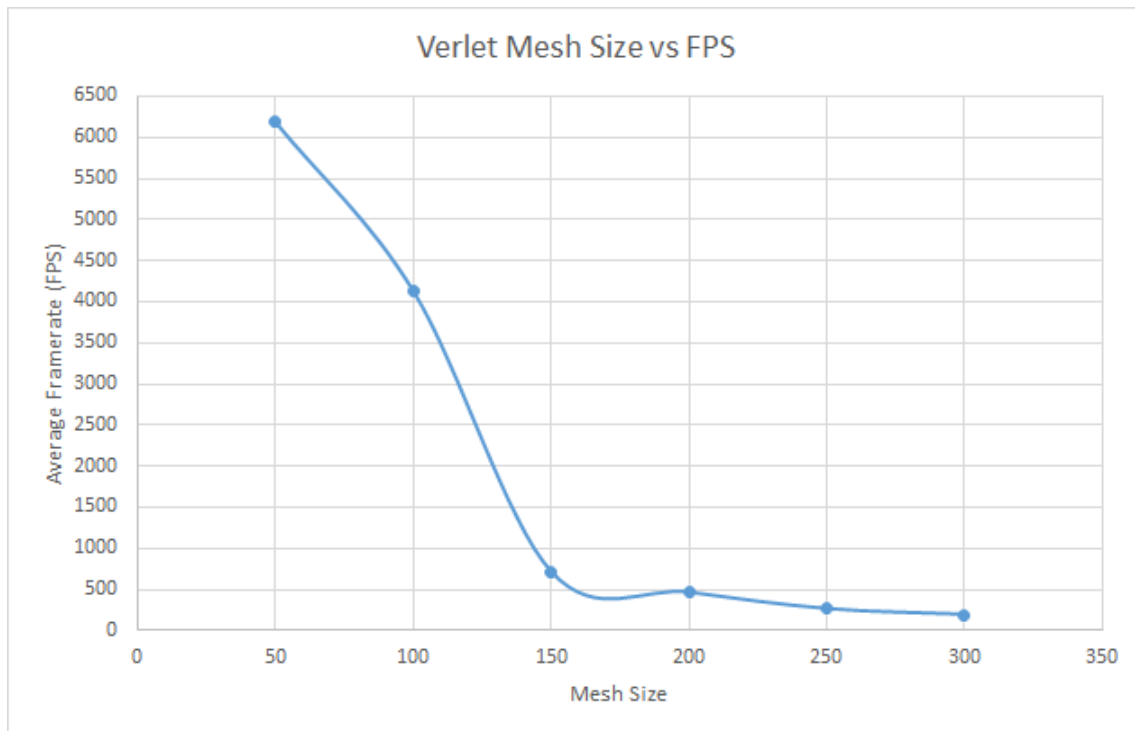
Figure C.16: Verlet mesh size against average FPS (sheet)
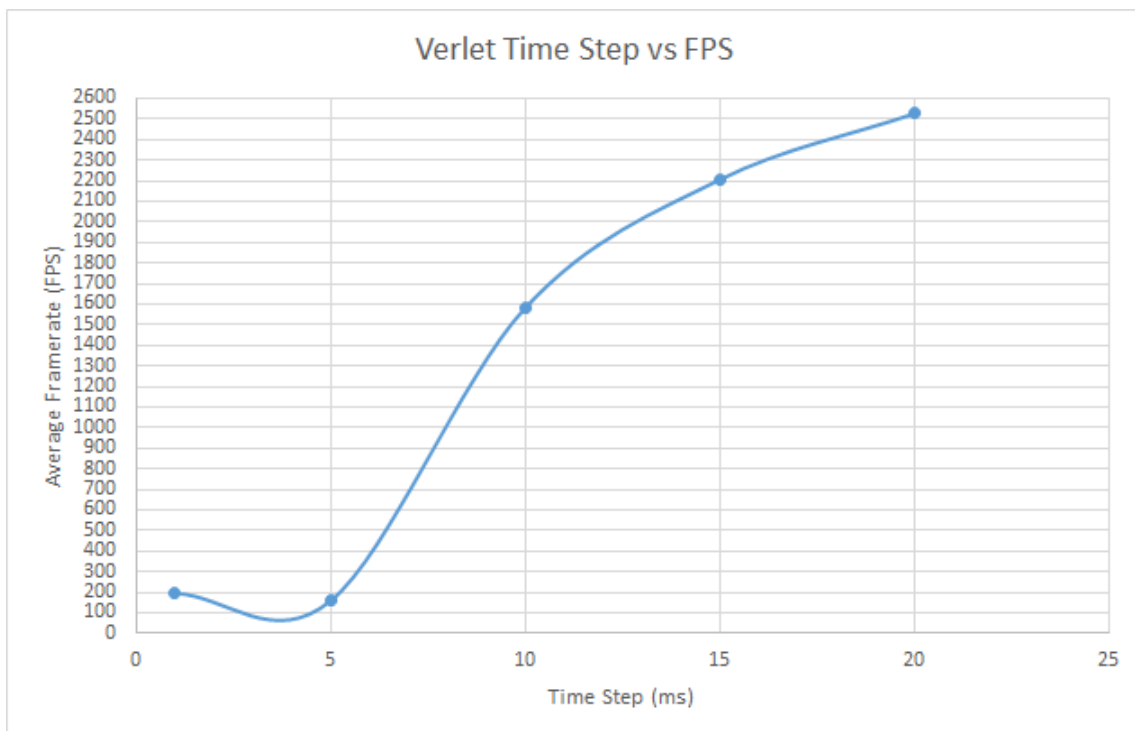
Figure C.17: Verlet time step against average FPS for a 300 by 300 mesh (sheet)
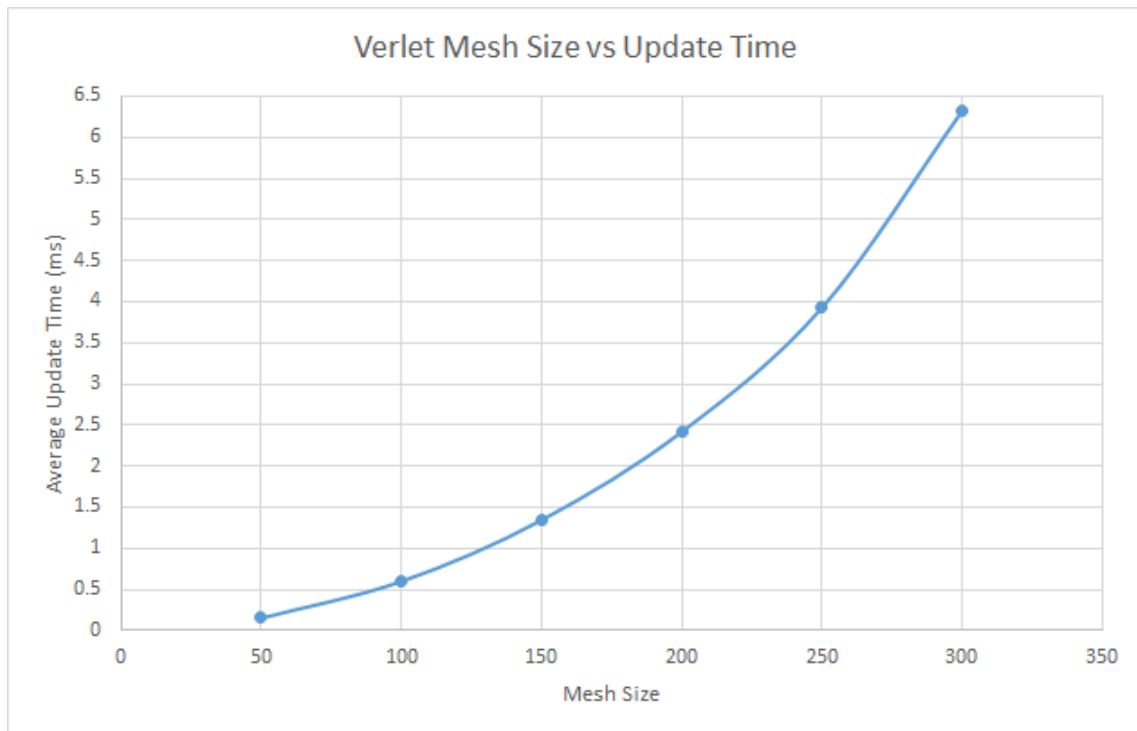
Figure C.18: Verlet mesh size against average update time (sheet)
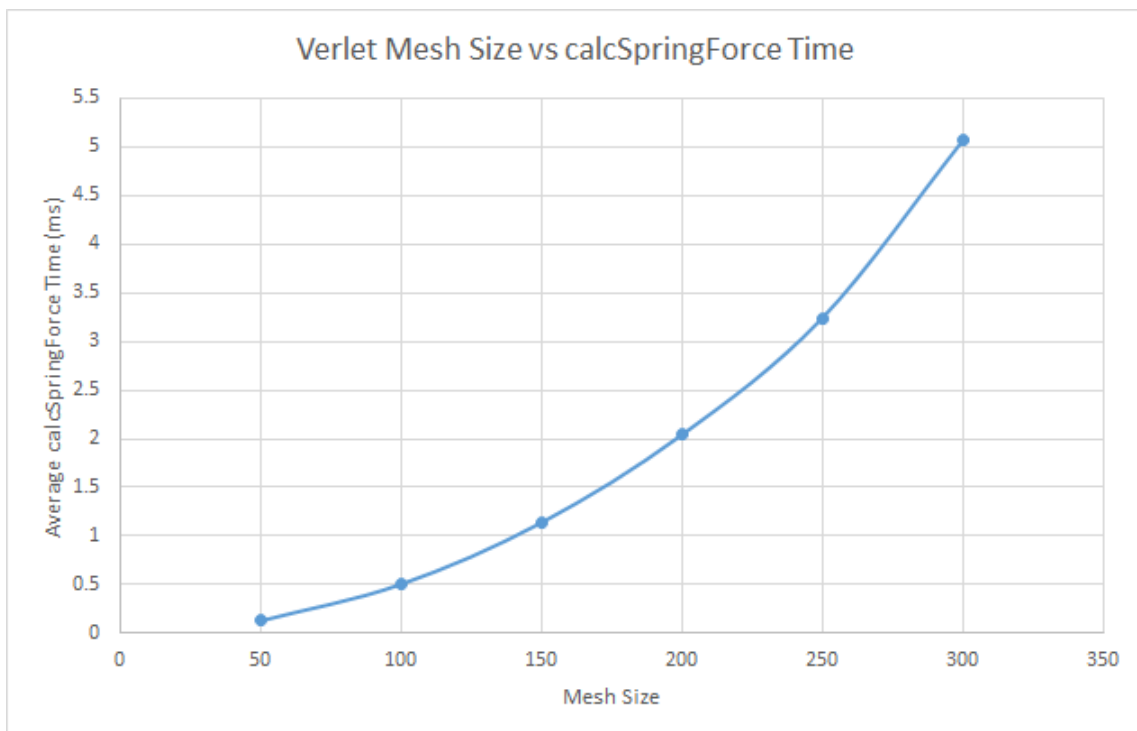
Figure C.19: Verlet mesh size against average internal force time (sheet)
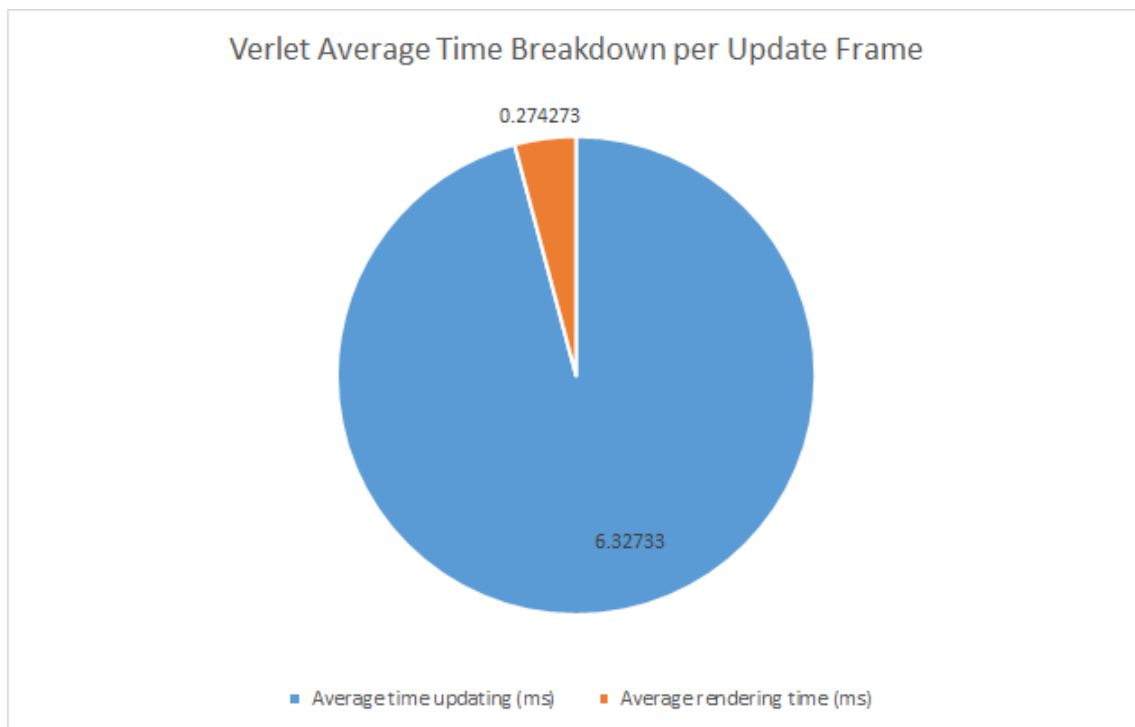
Figure C.20: Verlet frame time breakdown (sheet)
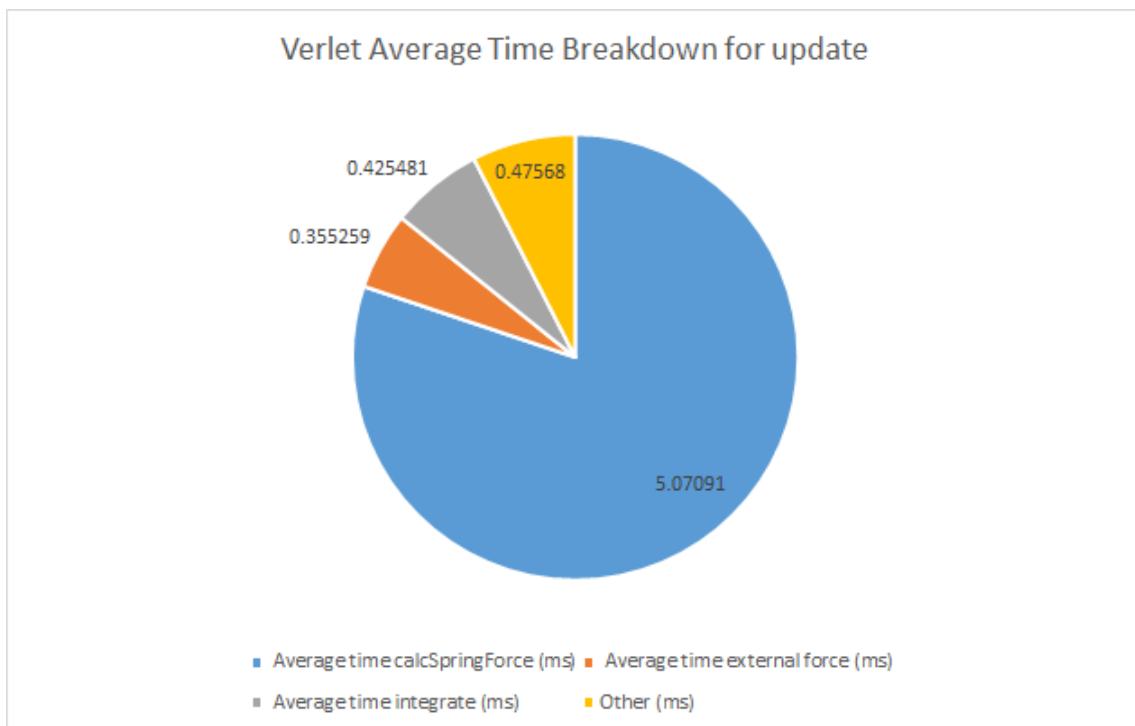
Figure C.21: Verlet update time breakdown (sheet)
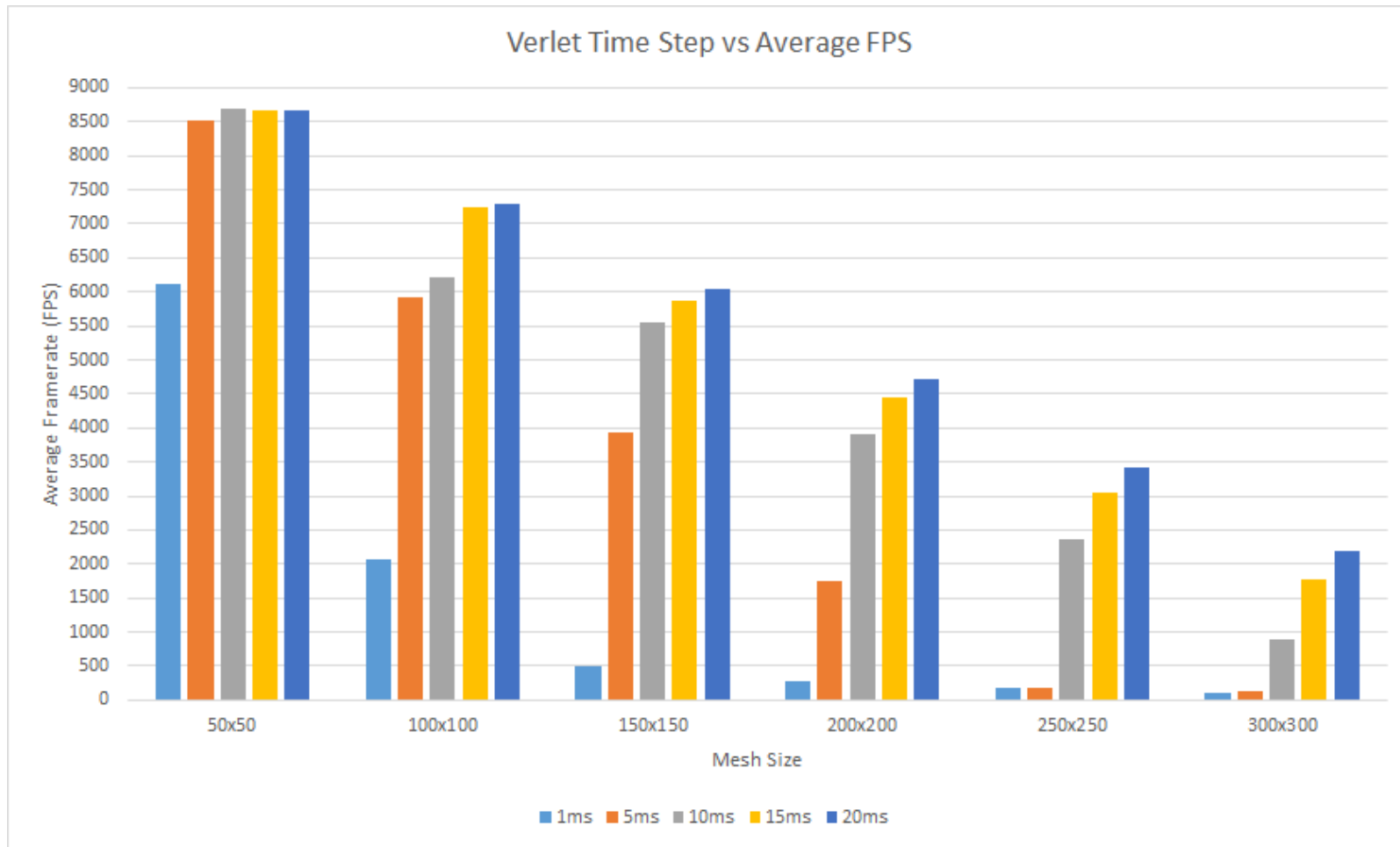
Figure C.22: Verlet mesh size against average FPS (flag)
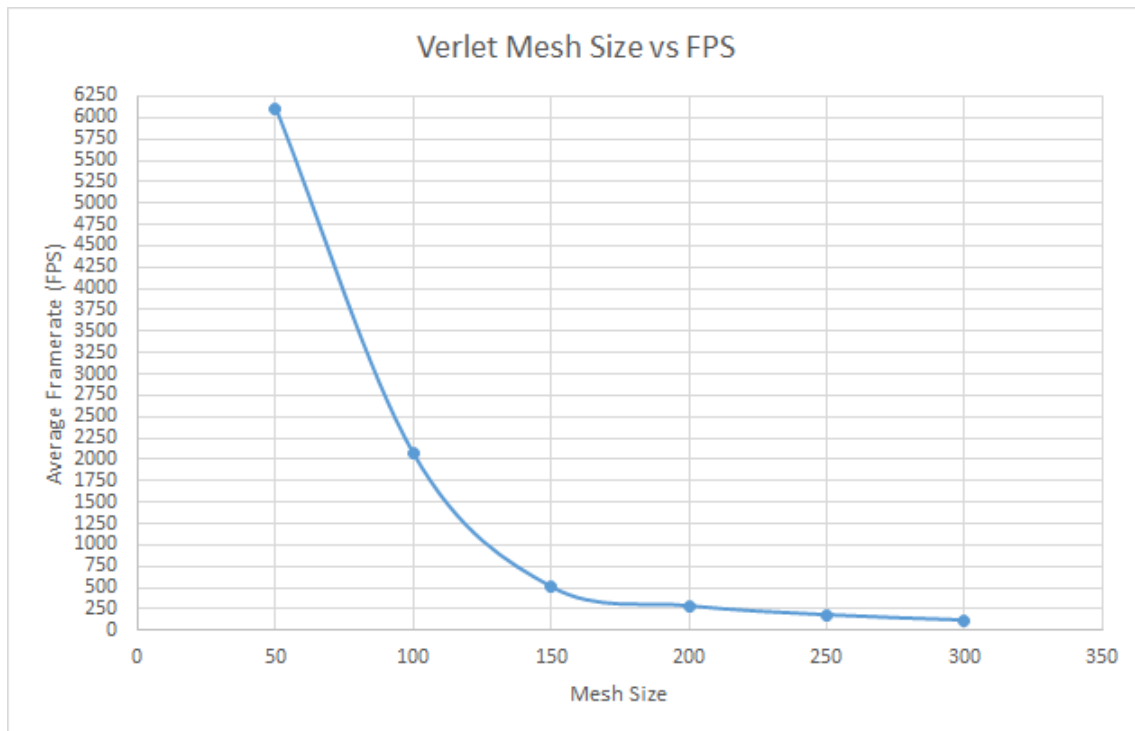
Figure C.23: Verlet mesh size against average FPS (flag)
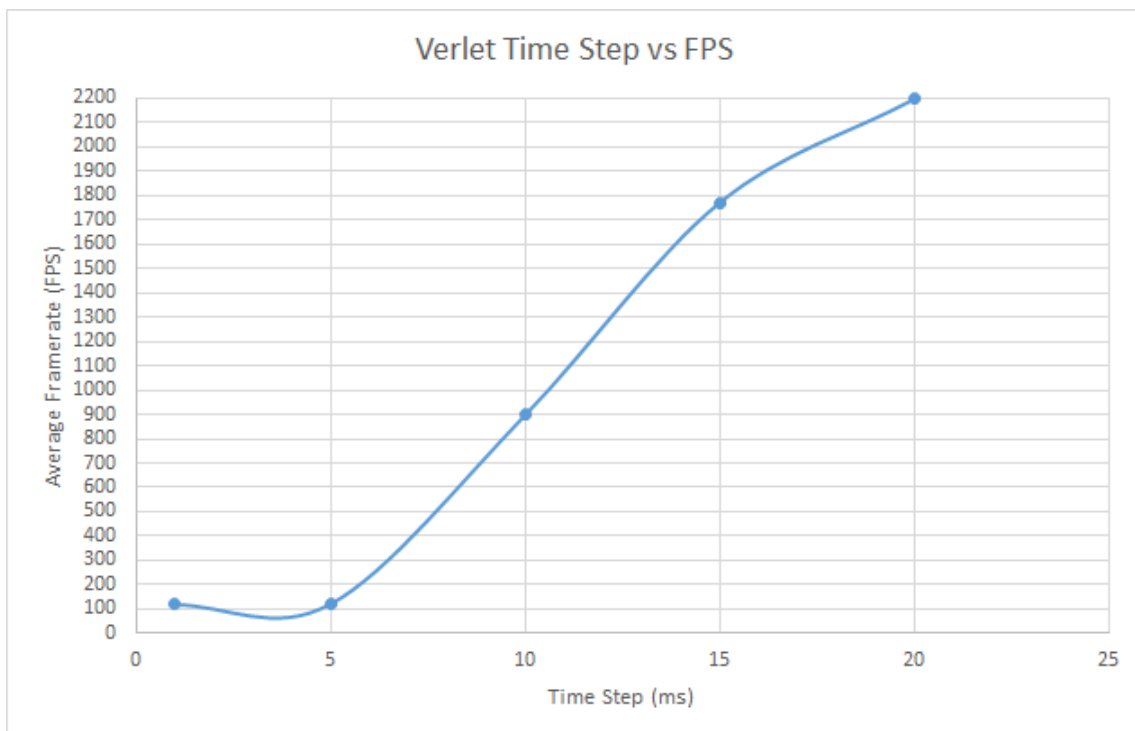
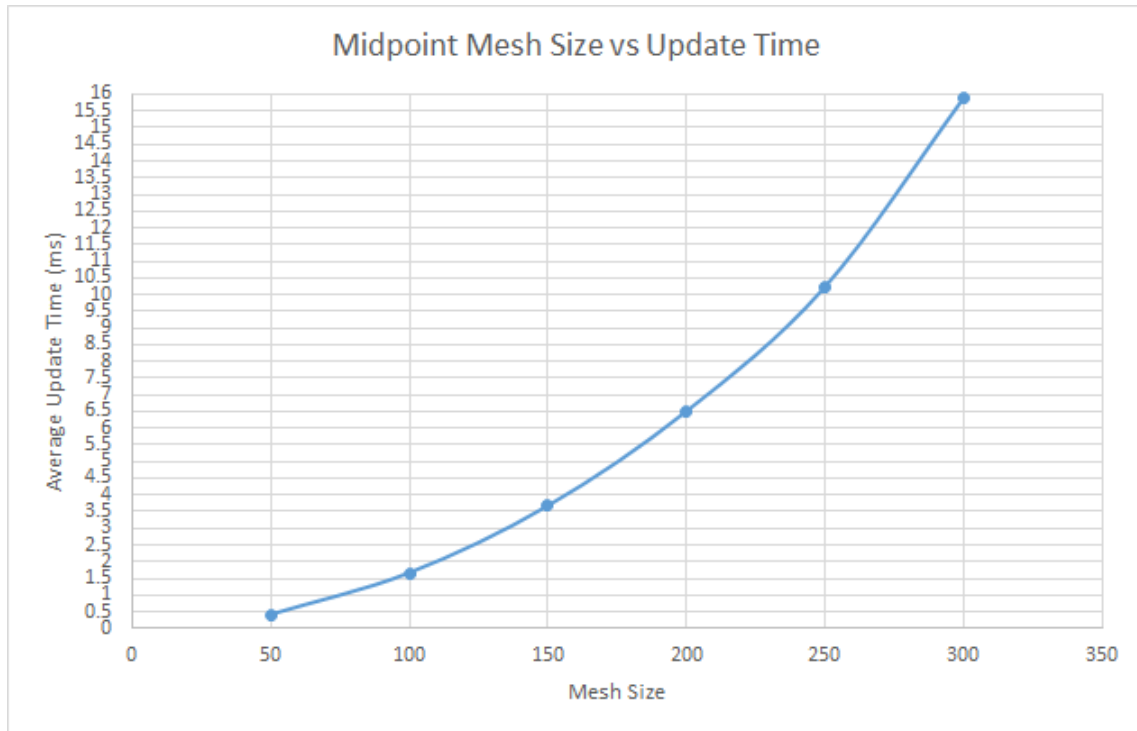Figure C.24: Verlet time step against average FPS for a 300 by 300 mesh (flag)
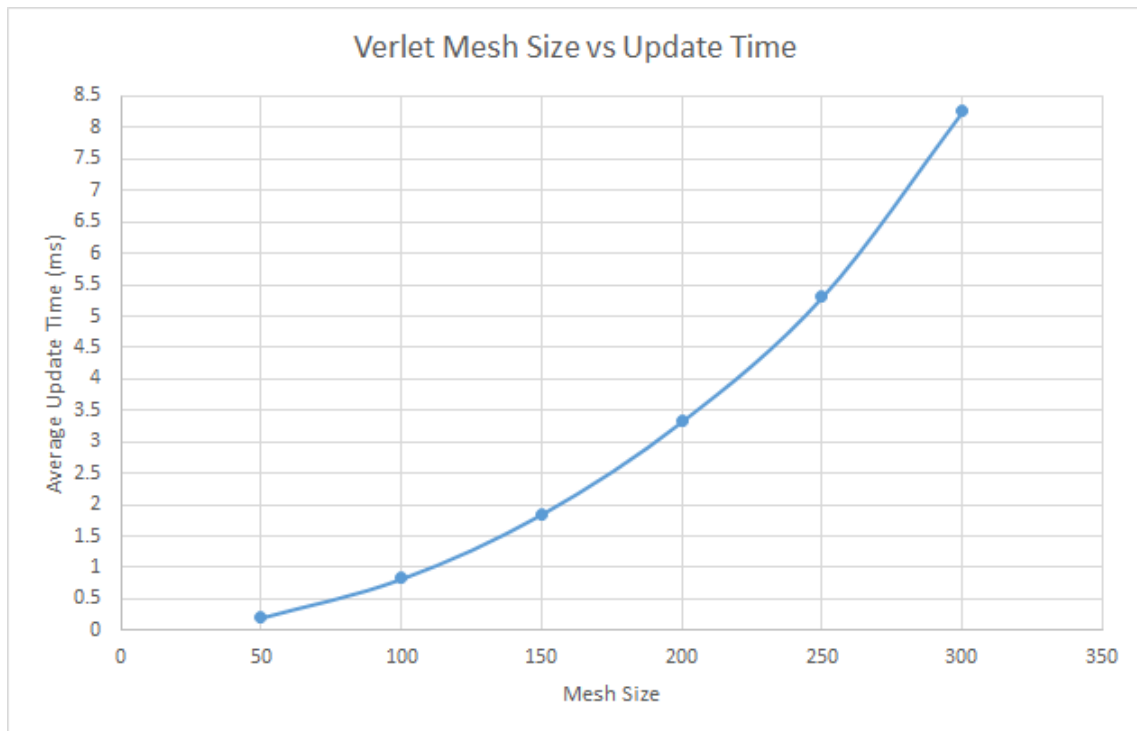
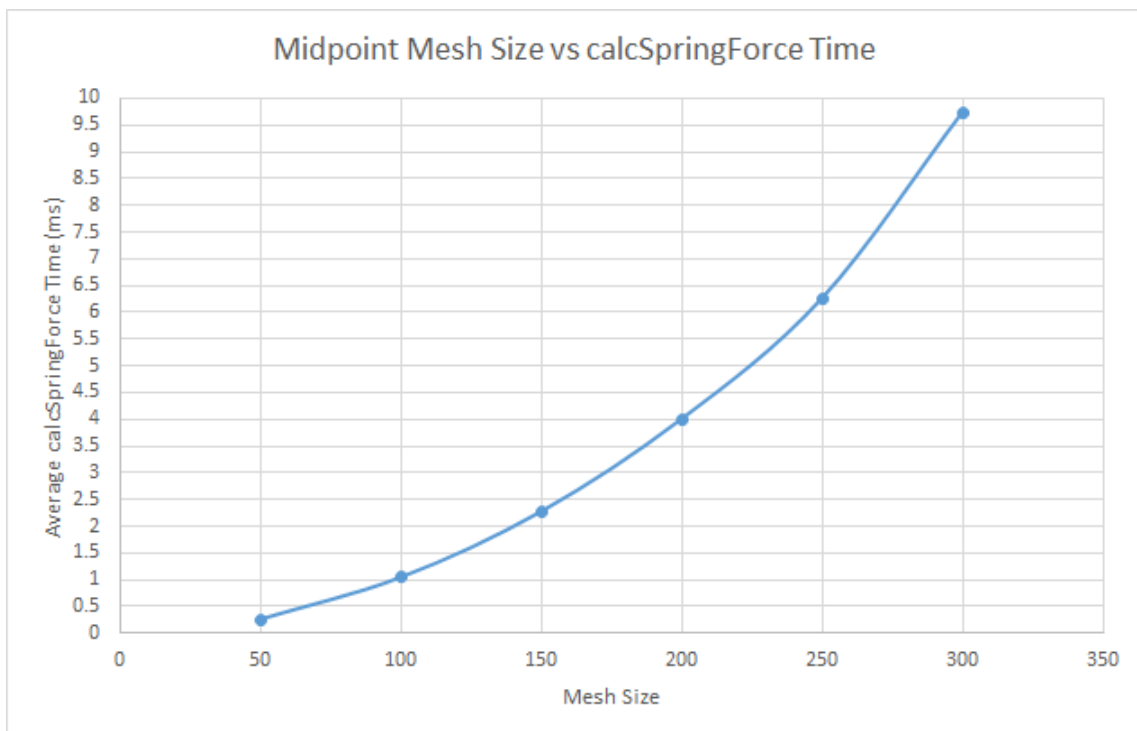Figure C.25: Verlet mesh size against average update time (flag)
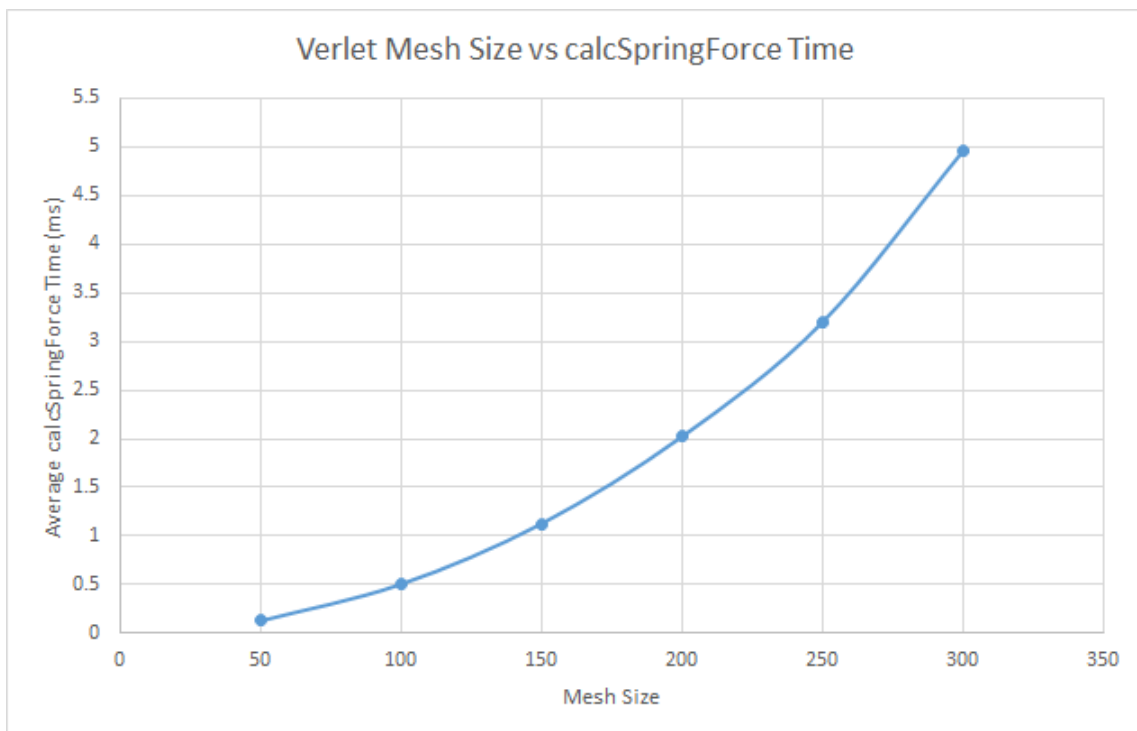
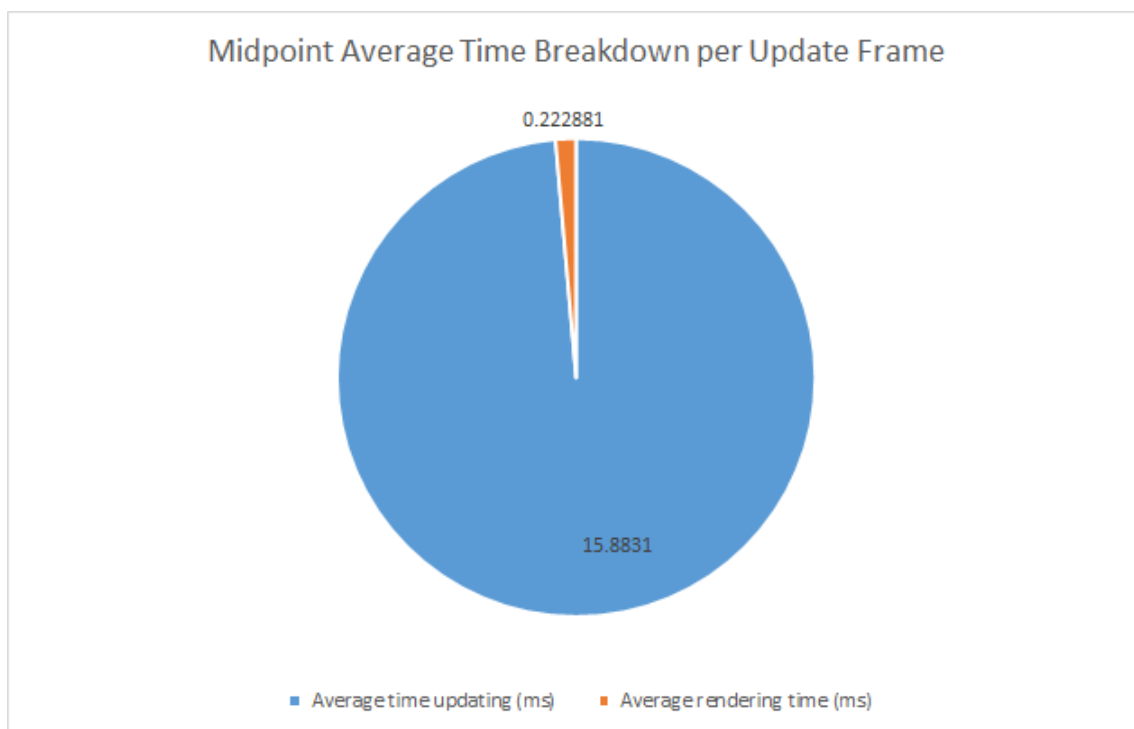Figure C.26: Verlet mesh size against average internal force time (flag)
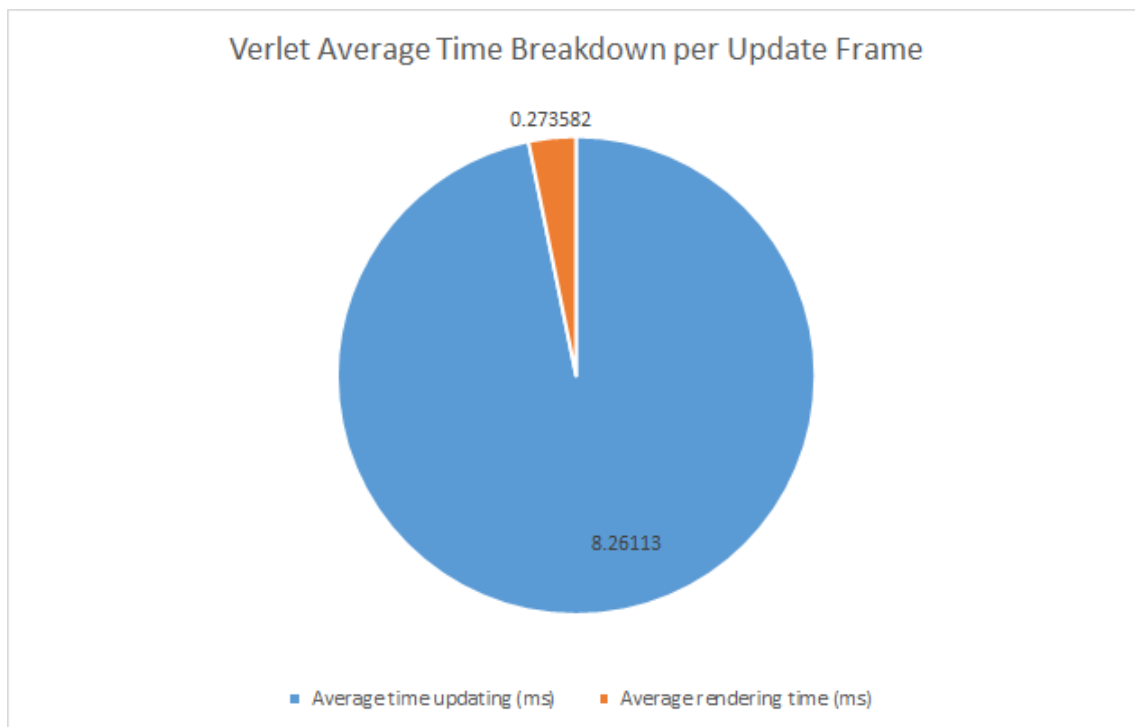
Figure C.27: Verlet frame time breakdown (flag)
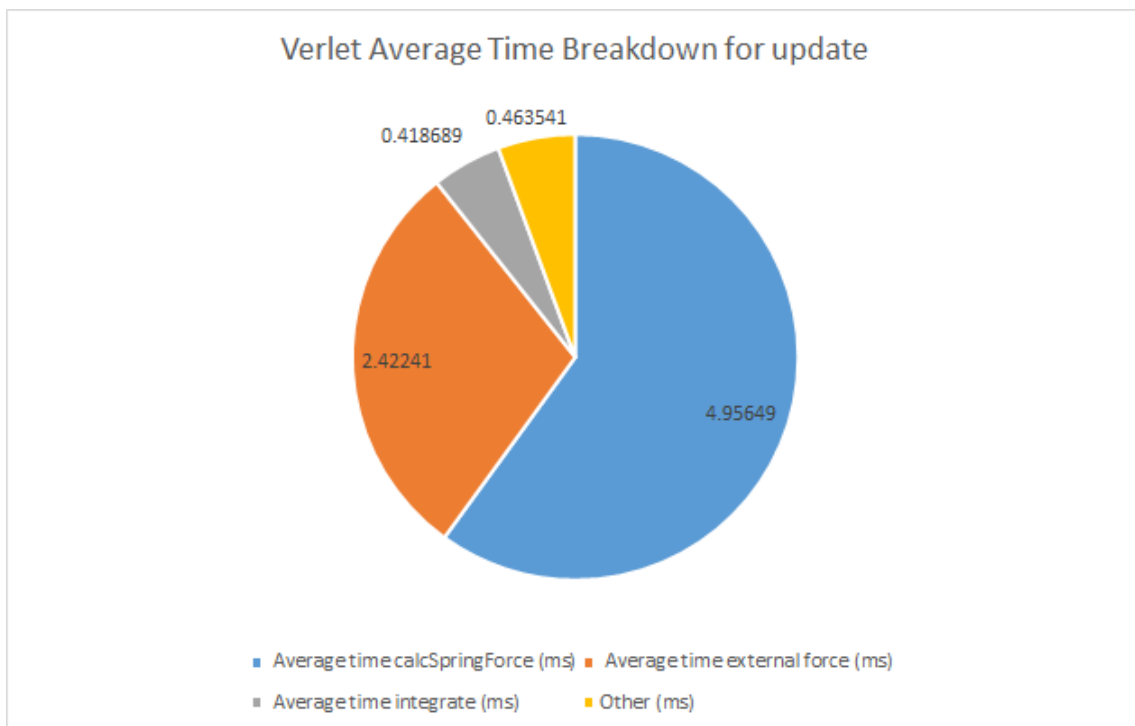
Figure C.28: Verlet update time breakdown (flag)

C.3 Midpoint

C.3.1 Sheet Data
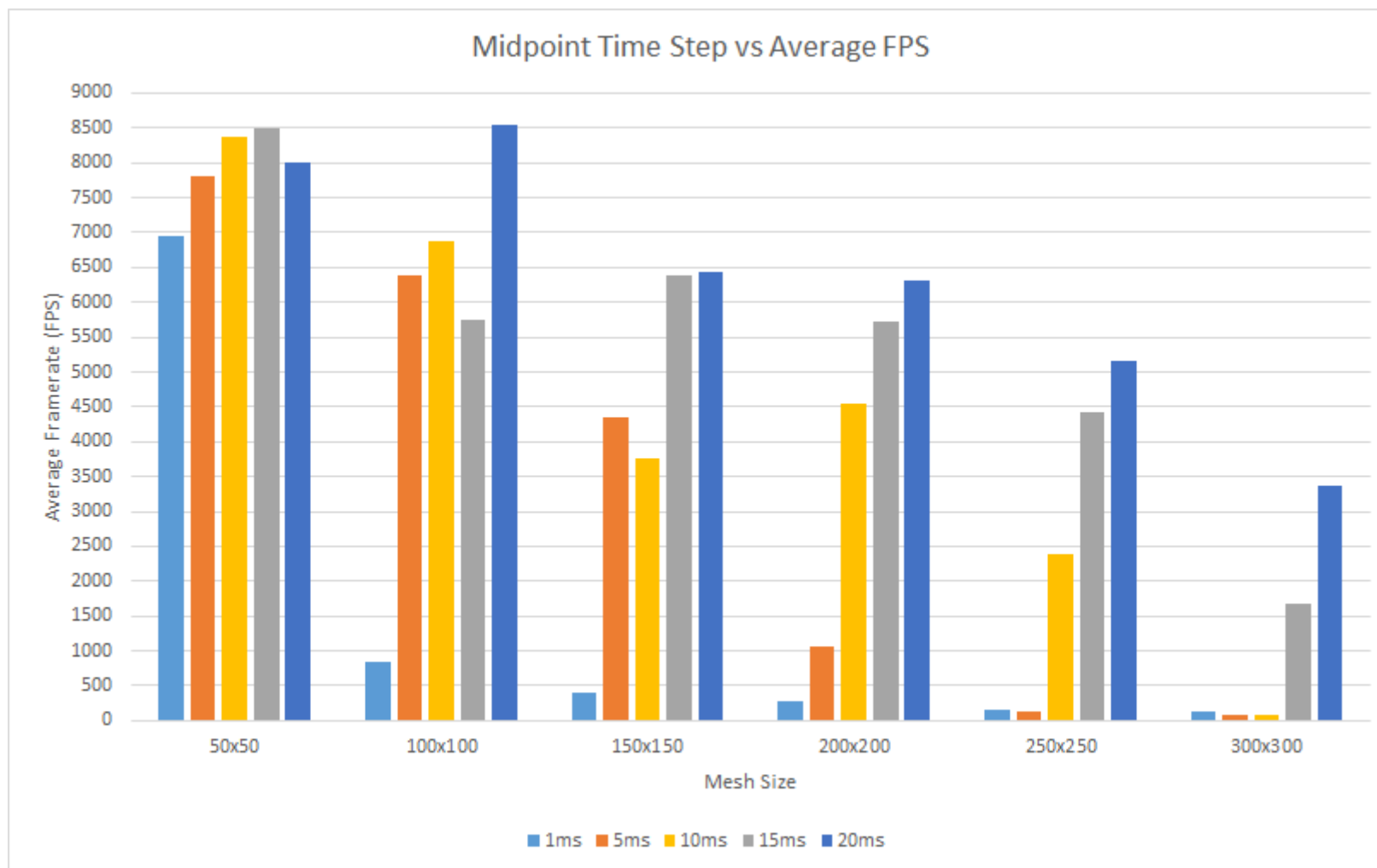
Figure C.29: Midpoint time step against average FPS (sheet)

Figure C.30: Midpoint mesh size against average FPS (sheet)

Figure C.31: Midpoint time step against average FPS for a 300 by 300 mesh (sheet)

Figure C.32: Midpoint mesh size against average update time (sheet)

Figure C.33: Midpoint mesh size against average internal force time (sheet)
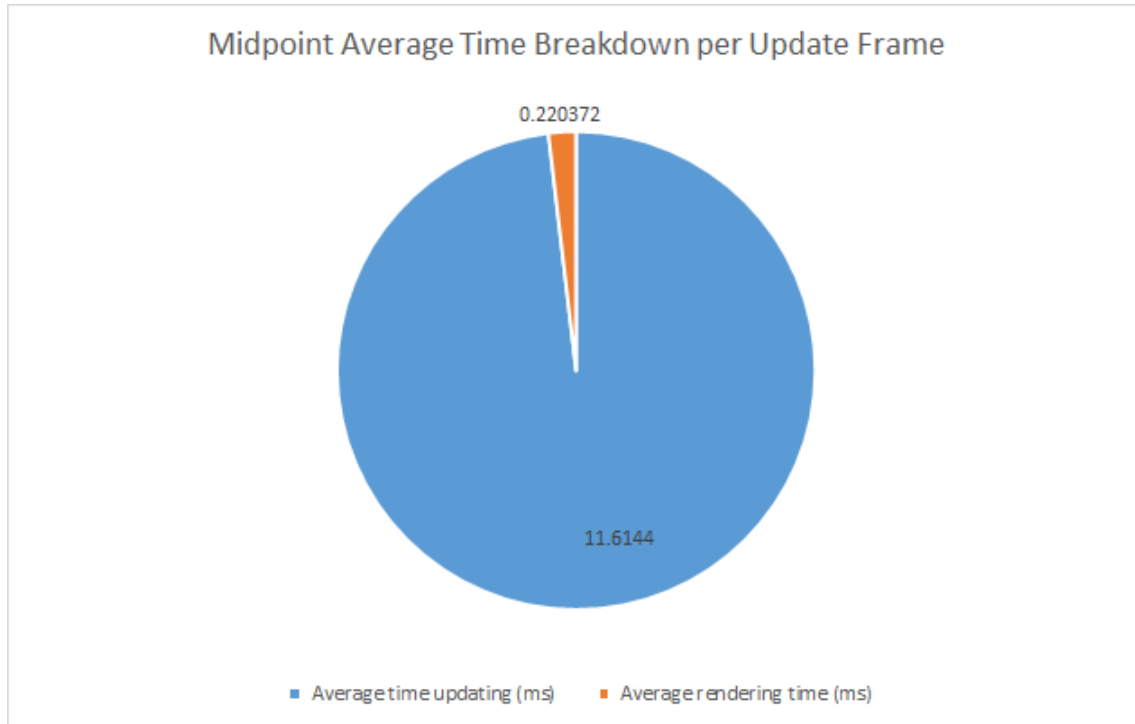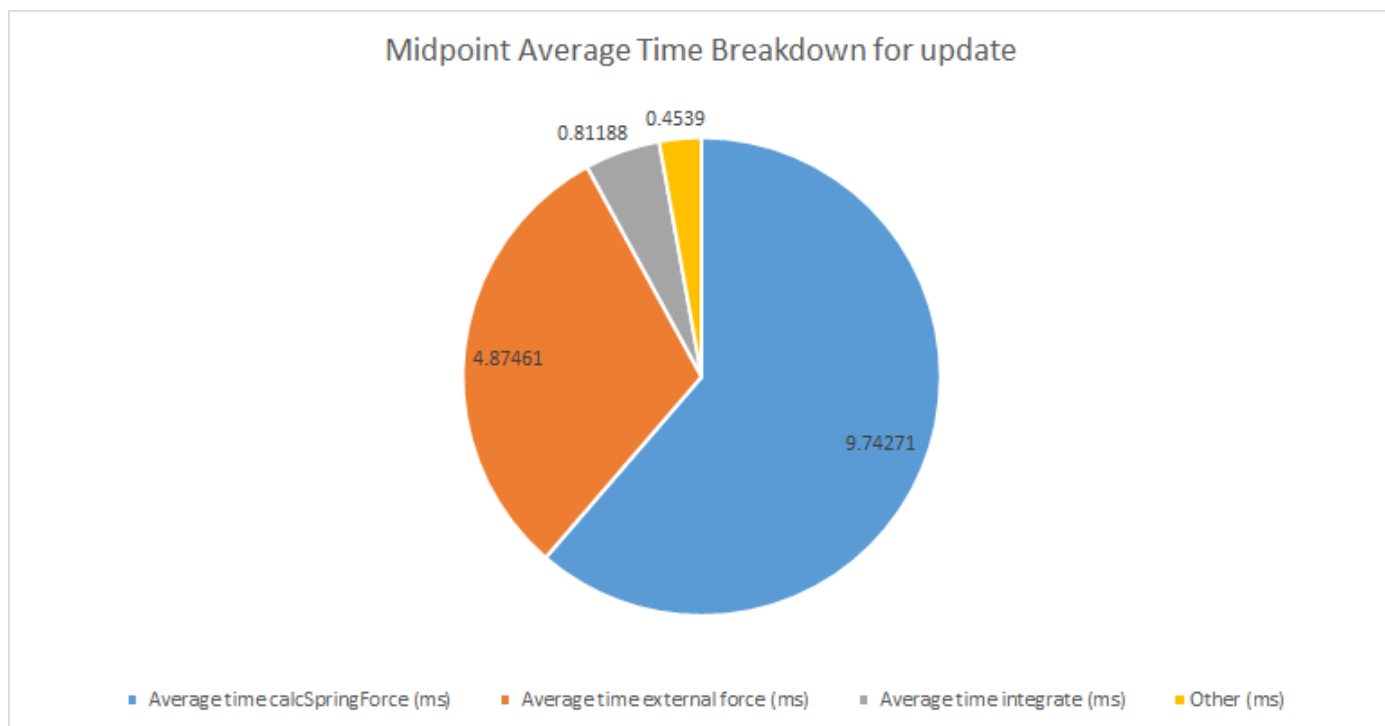
Figure C.34: Midpoint frame time breakdown (sheet)
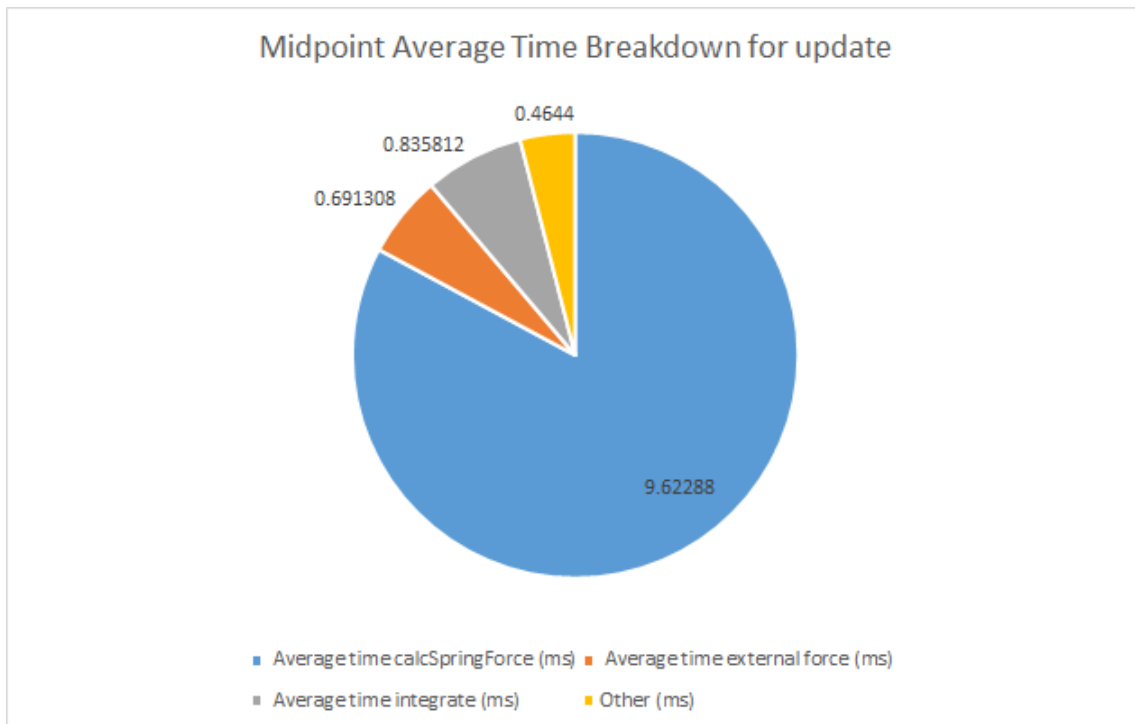
Figure C.35: Midpoint update time breakdown (sheet)

C.3.2 Flag Data
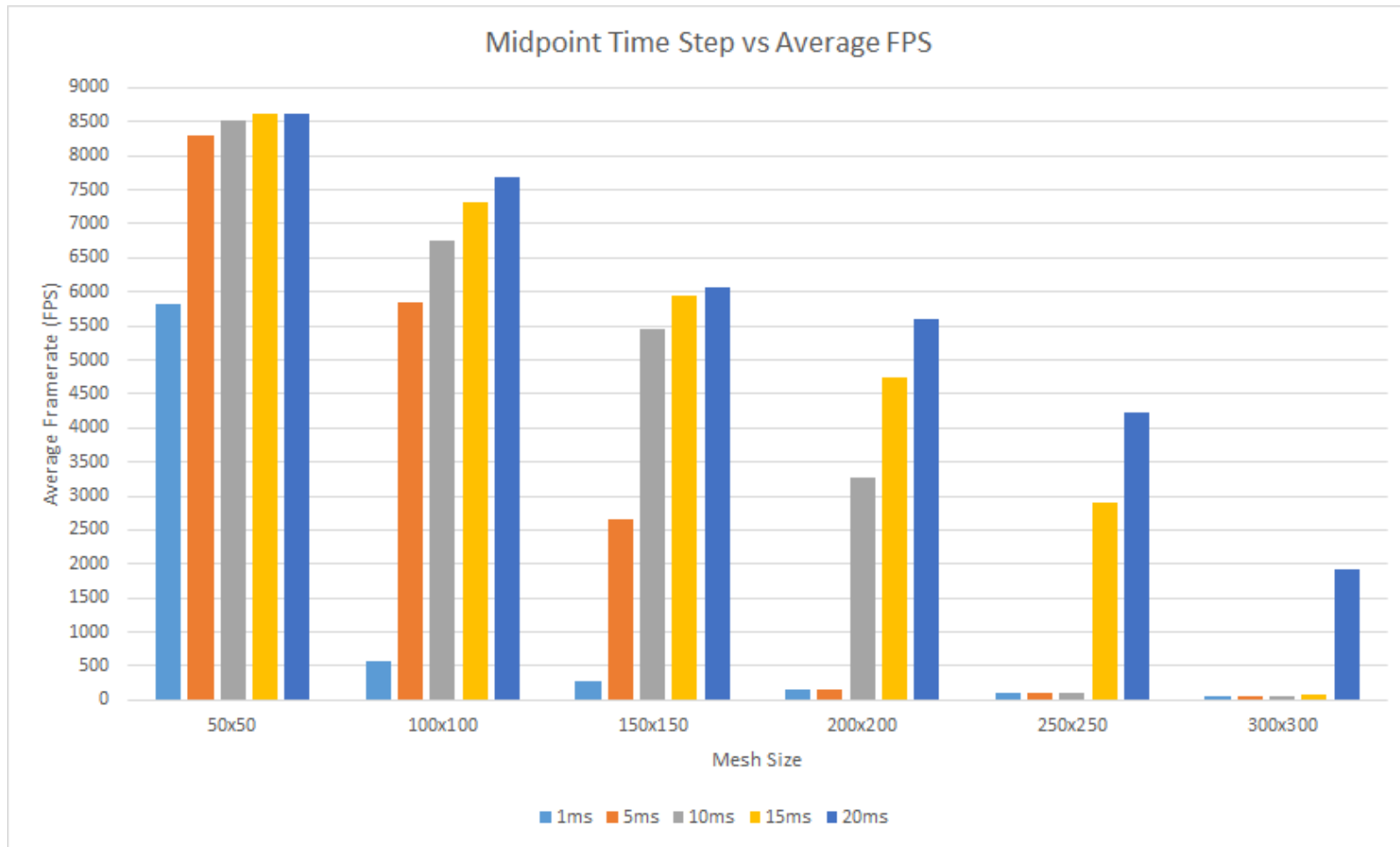
Figure C.36: Midpoint mesh size against average FPS (flag)
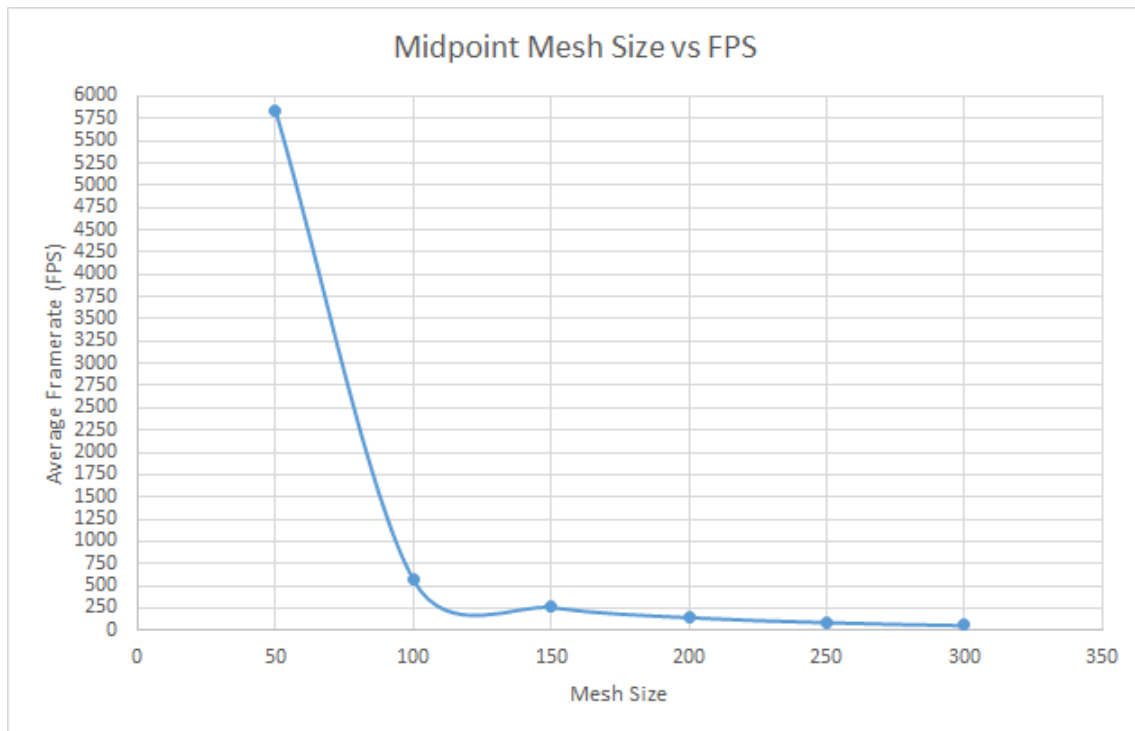
Figure C.37: Midpoint mesh size against average FPS (flag)
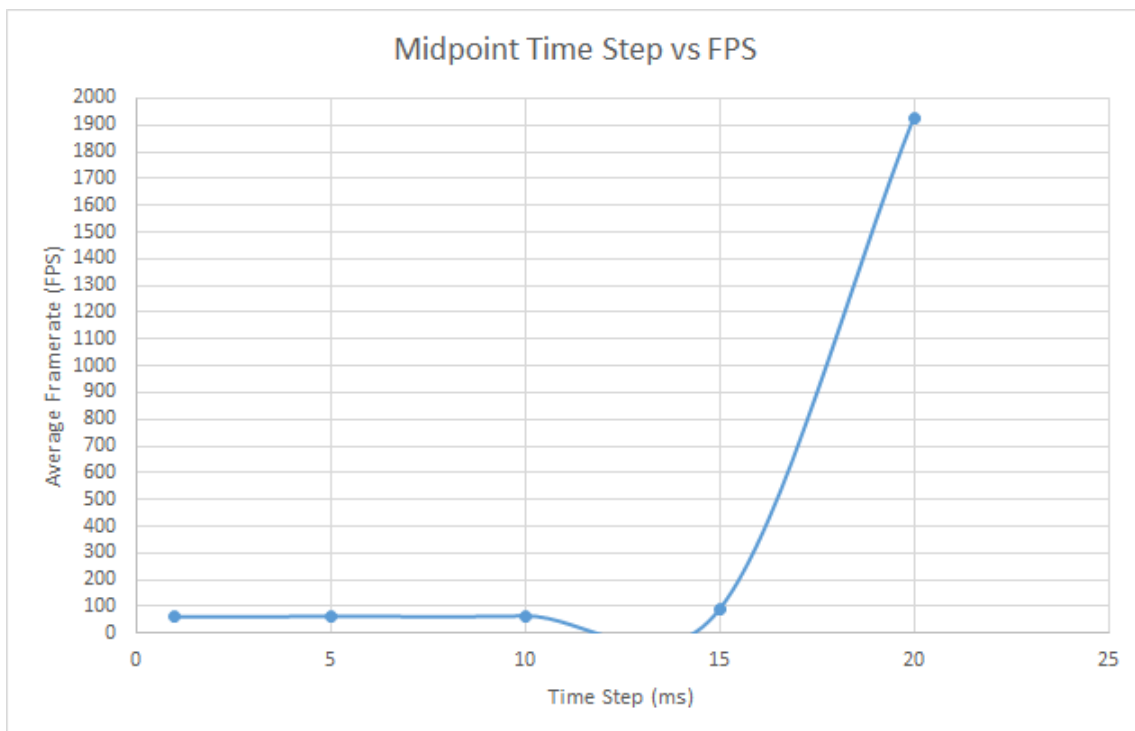
Figure C.38: Midpoint time step against average FPS for a 300 by 300 mesh (flag)

Figure C.39: Midpoint mesh size against average update time (flag)

Figure C.40: Midpoint mesh size against average internal force time (flag)

Figure C.41: Midpoint frame time breakdown (flag)

Figure C.42: Midpoint update time breakdown (flag)

C.4   Fourth Order Runge-Kutta

C.4.1   Sheet Data
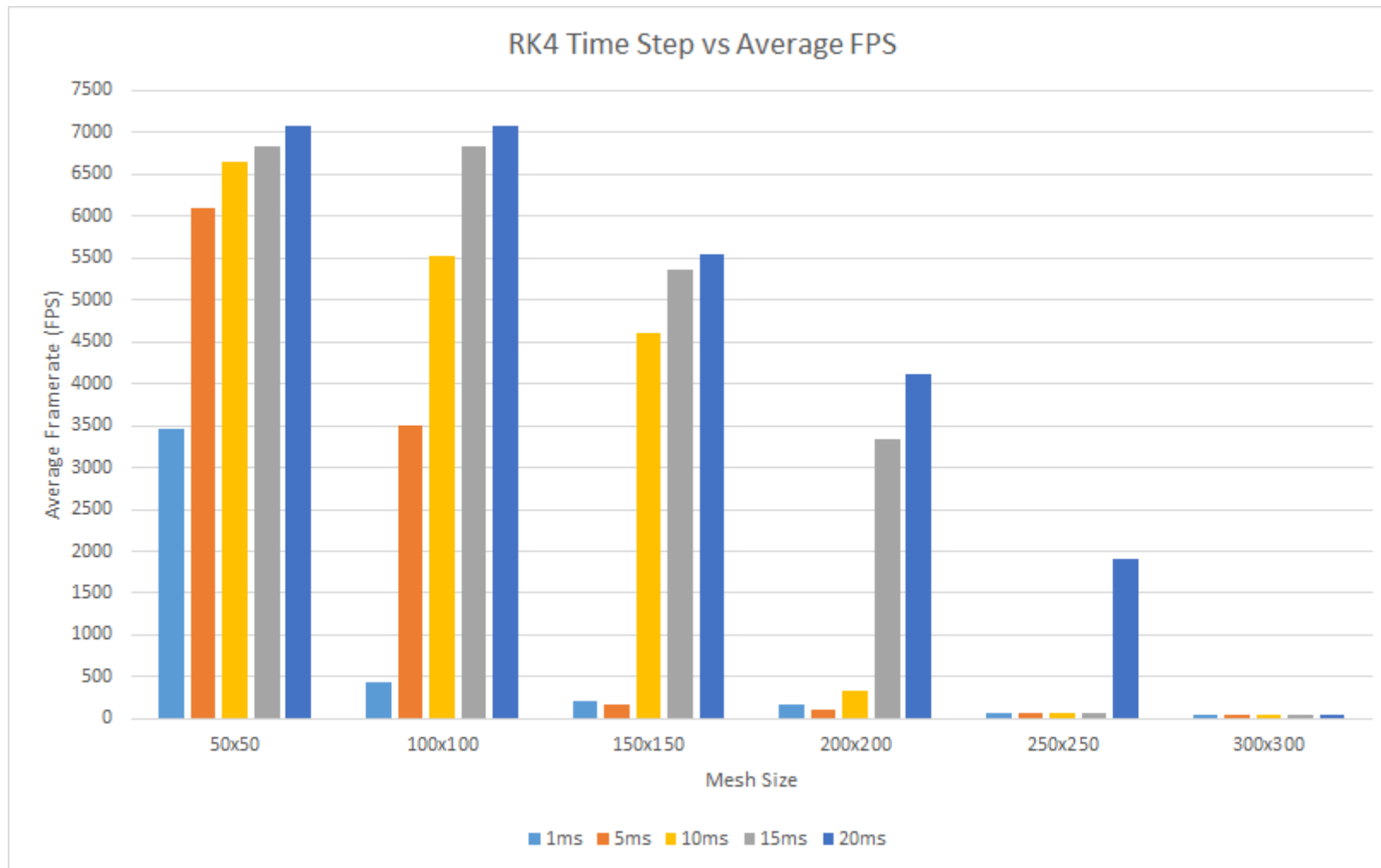
Figure C.43: Fourth Order Runge-Kutta time step against average FPS (sheet)
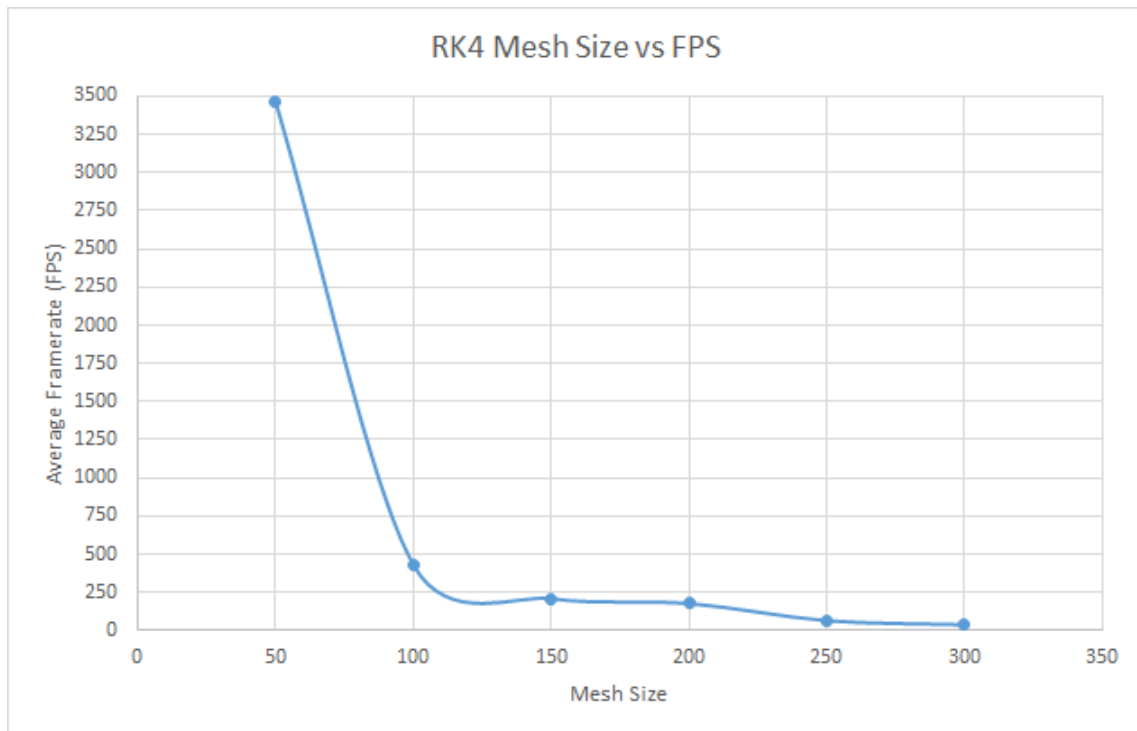
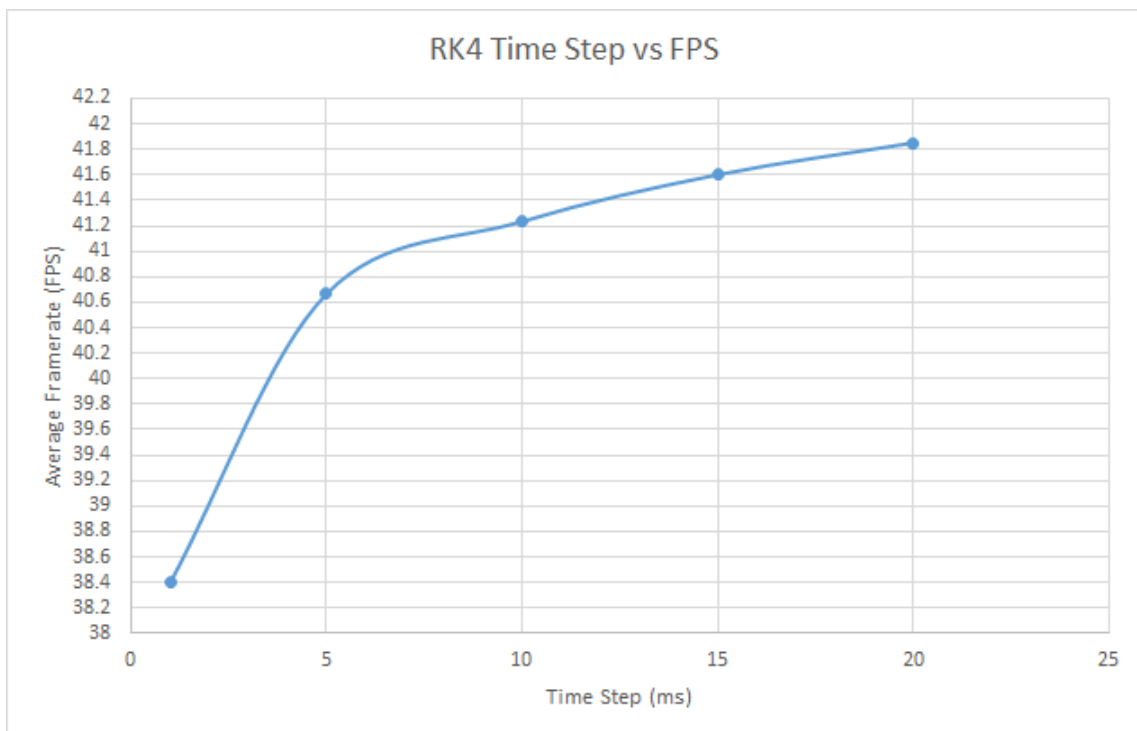Figure C.44: Fourth Order Runge-Kutta mesh size against average FPS (sheet)

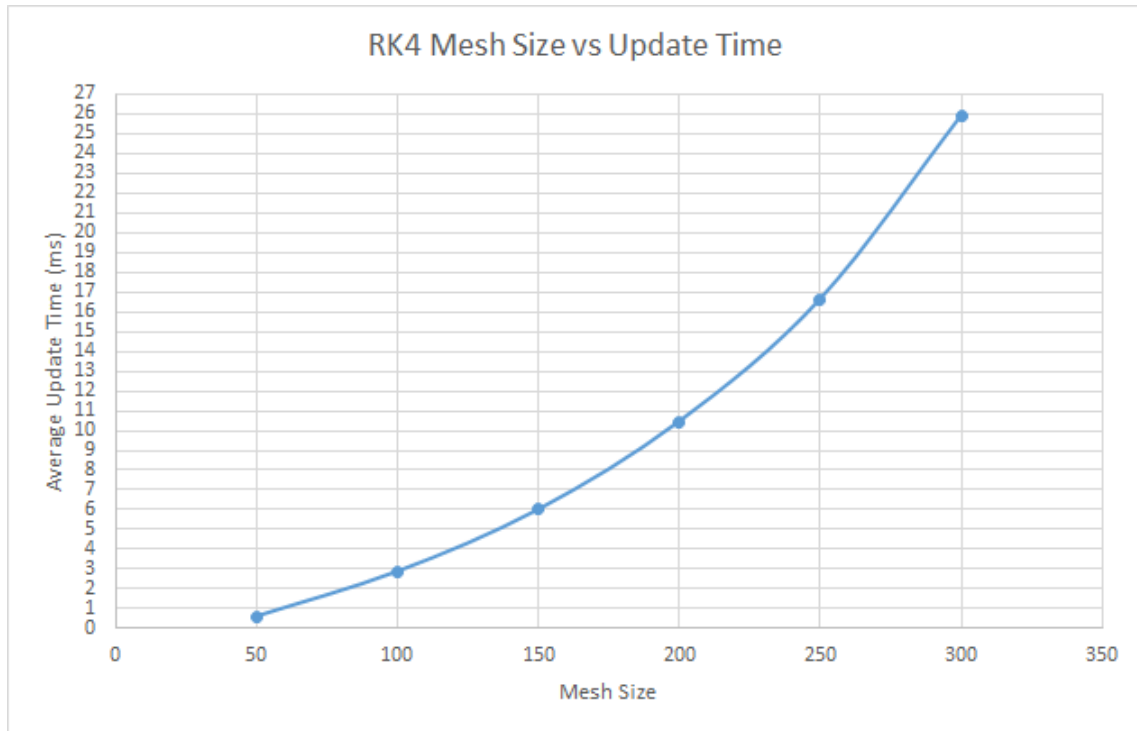Figure C.45: Fourth Order Runge-Kutta time step against average FPS for a 300 by 300 mesh (sheet)

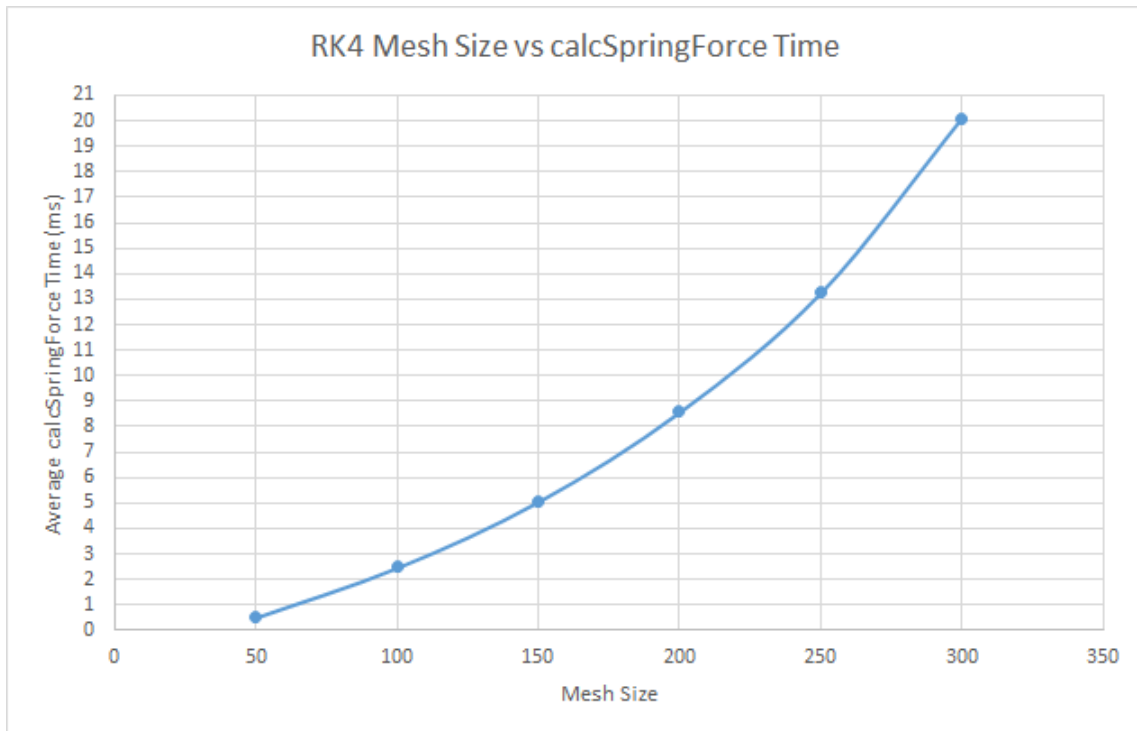Figure C.46: Fourth Order Runge-Kutta mesh size against average update time (sheet)

Figure C.47: Fourth Order Runge-Kutta mesh size against average internal force time (sheet)
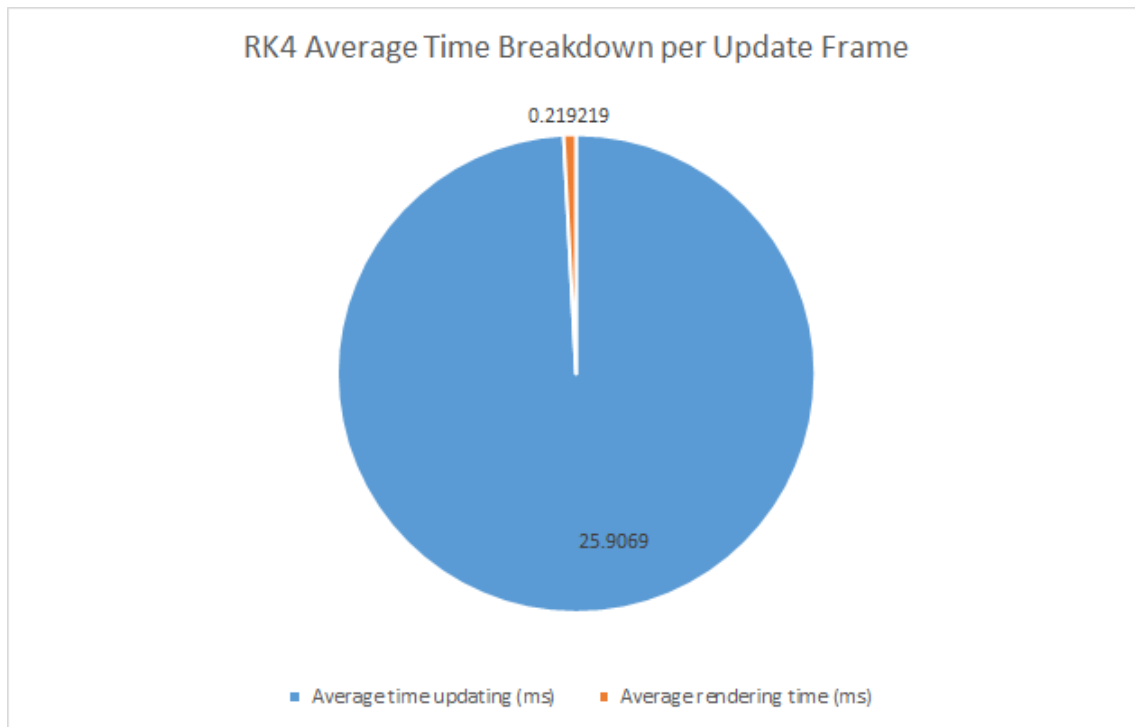
96

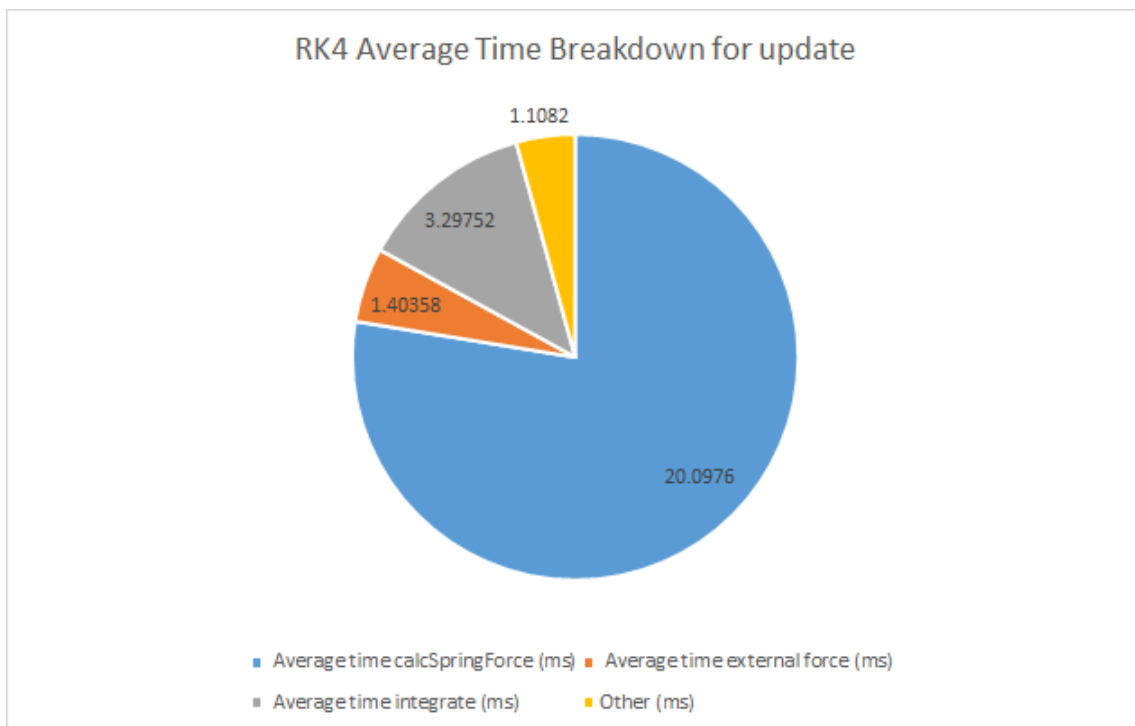Figure C.48: Fourth Order Runge-Kutta frame time breakdown (sheet)

Figure C.49: Fourth Order Runge-Kutta update time breakdown (sheet)
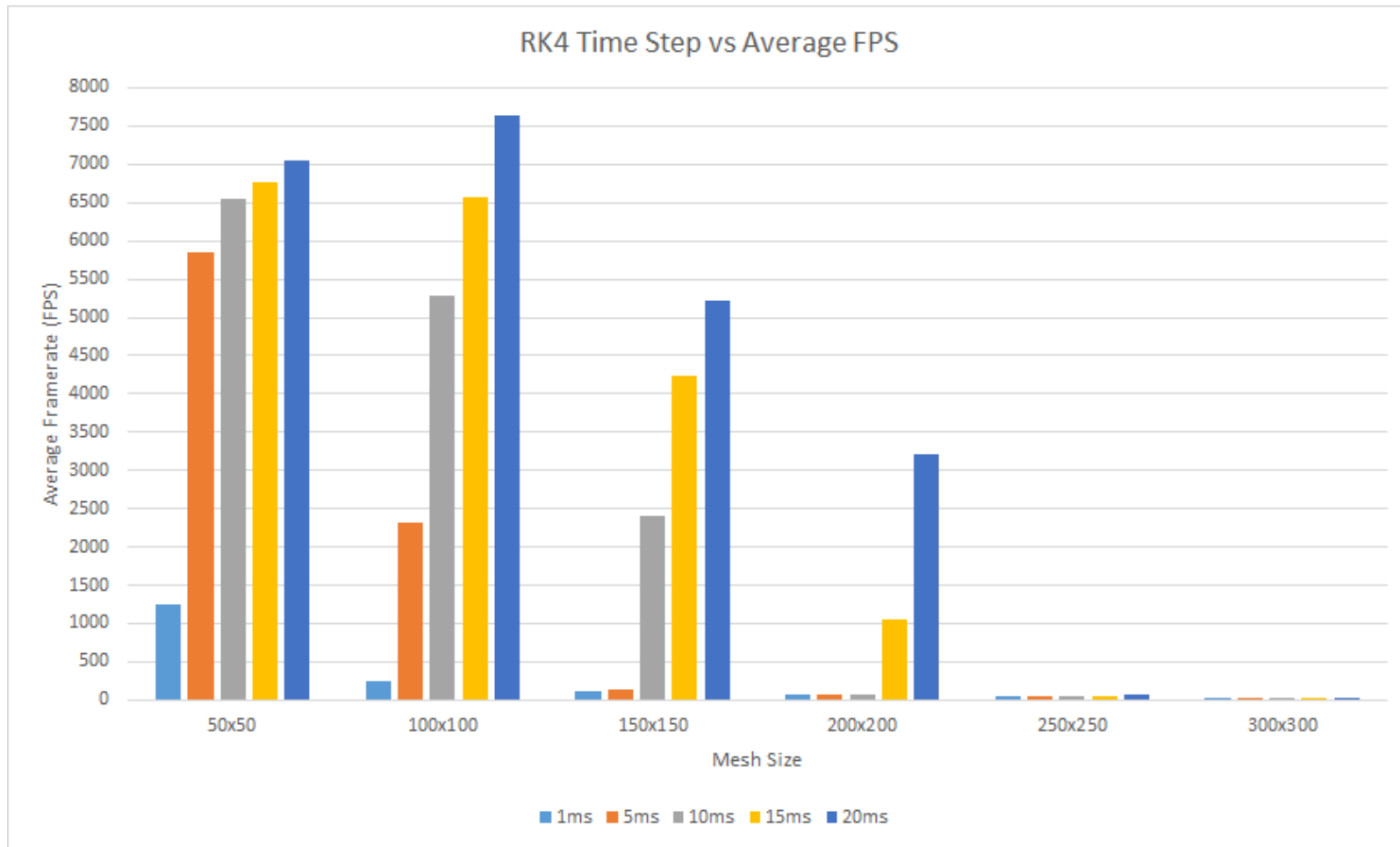
C.4.2 Flag Data

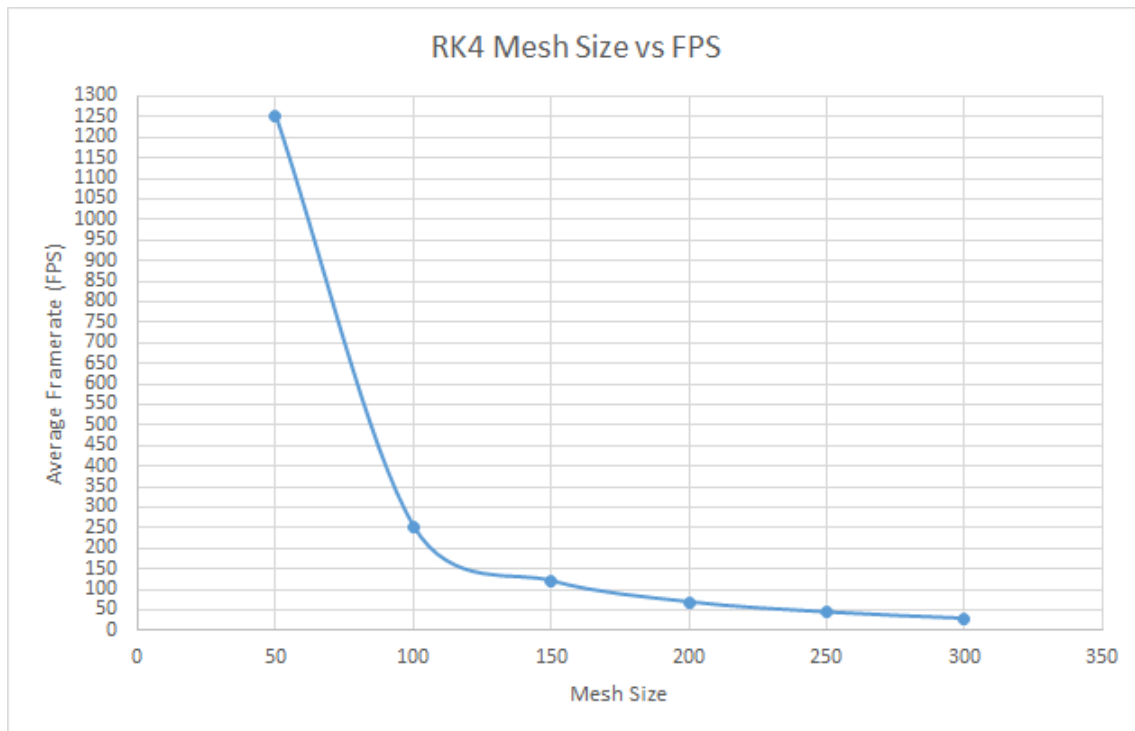Figure C.50: Fourth Order Runge-Kutta mesh size against average FPS (flag)

Figure C.51: Fourth Order Runge-Kutta mesh size against average FPS (flag)
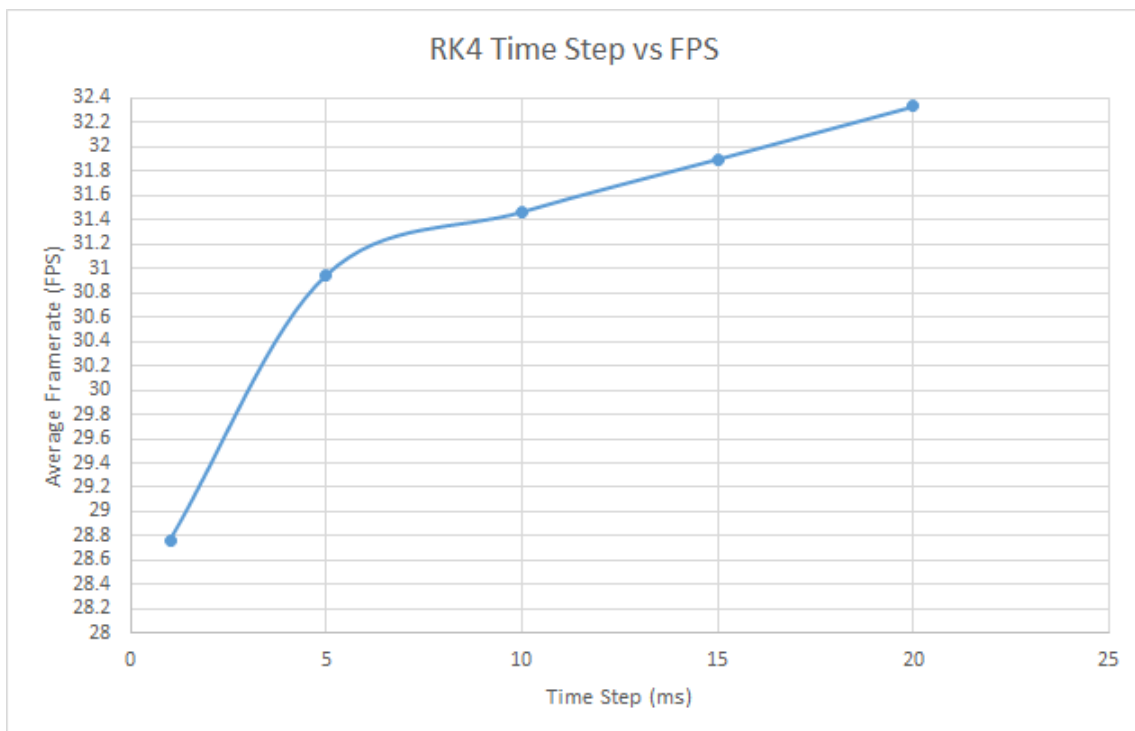

Figure C.52: Fourth Order Runge-Kutta time step against average FPS for a 300 by 300 mesh (flag)
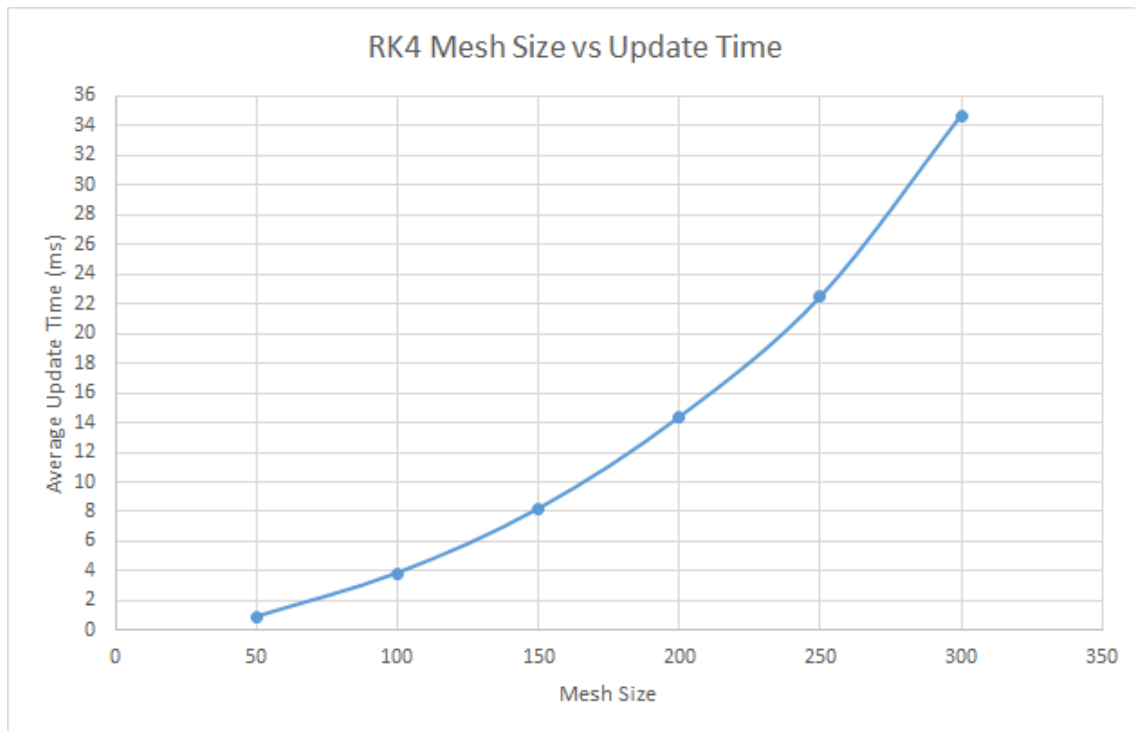
Figure C.53: Fourth Order Runge-Kutta mesh size against average update time (flag)
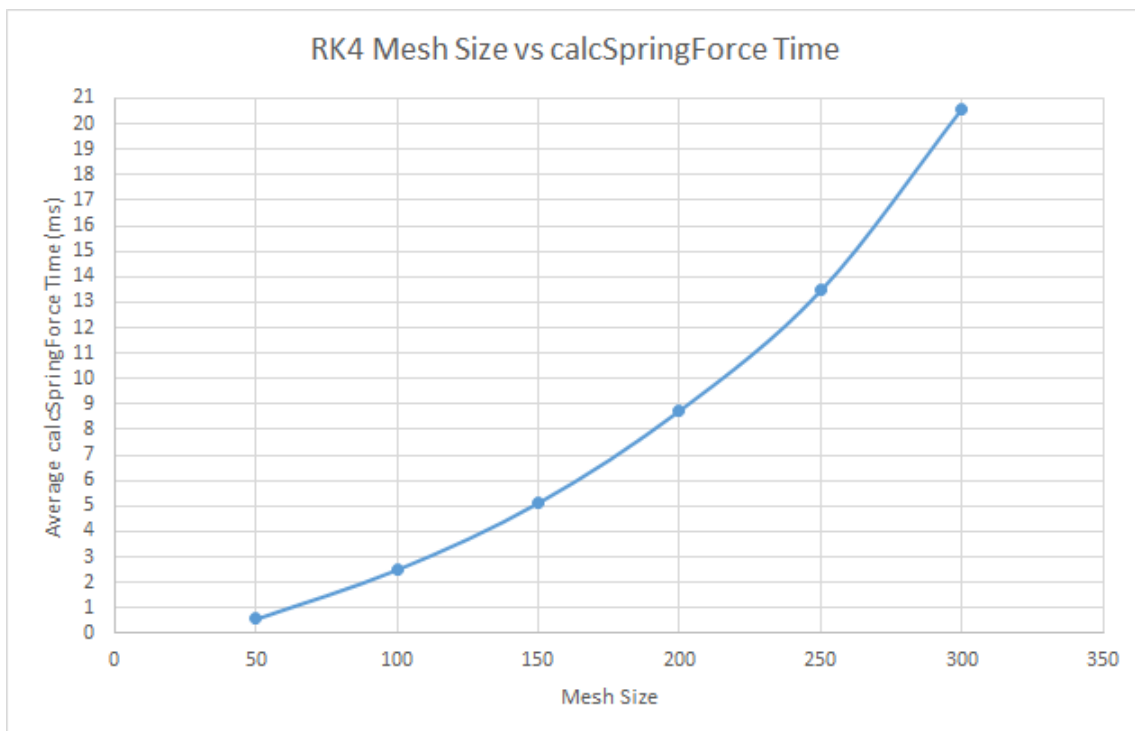
Figure C.54: Fourth Order Runge-Kutta mesh size against average internal force time (flag)
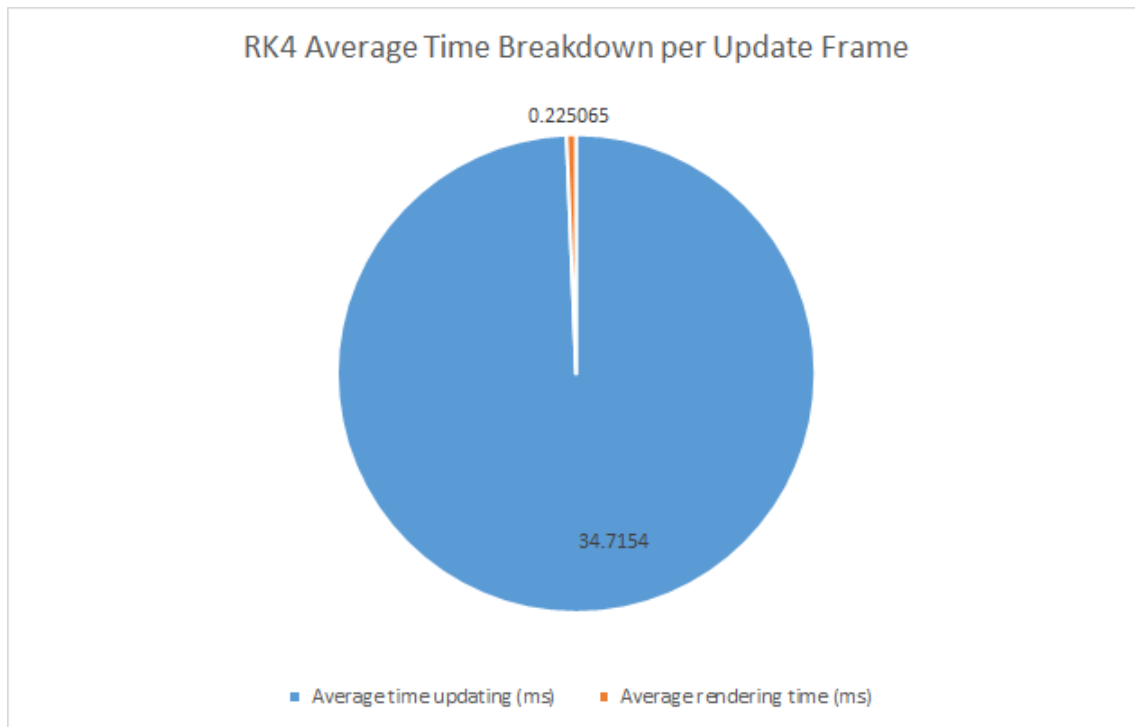
Figure C.55: Fourth Order Runge-Kutta frame time breakdown (flag)
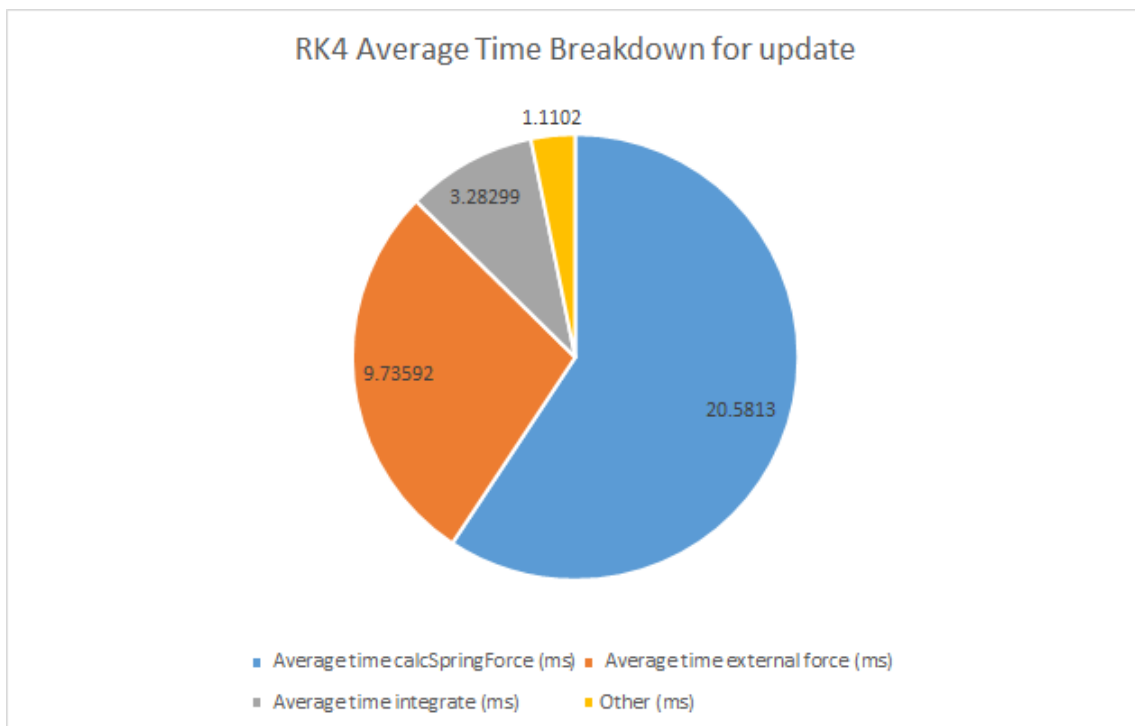
Figure C.56: Fourth Order Runge-Kutta update time breakdown (flag)

C.5 All Integrators

C.5.1 Sheet Data

Figure C.57: Mesh size against average FPS for all integrators with 1ms time step (sheet)

Figure C.58: Mesh size against average FPS for all integrators with 5ms time step (sheet)

Figure C.59: Mesh size against average FPS for all integrators with 10ms time step (sheet)

Figure C.60: Mesh size against average FPS for all integrators with 15ms time step (sheet)

Figure C.61: Mesh size against average FPS for all integrators with 20ms time step (sheet)

Figure C.62: Average update time for each integrator (sheet)

C.5.2   Flag Data

Figure C.63: Mesh size against average FPS for all integrators with 1ms time step (flag)

Figure C.64: Mesh size against average FPS for all integrators with 5ms time step (flag)
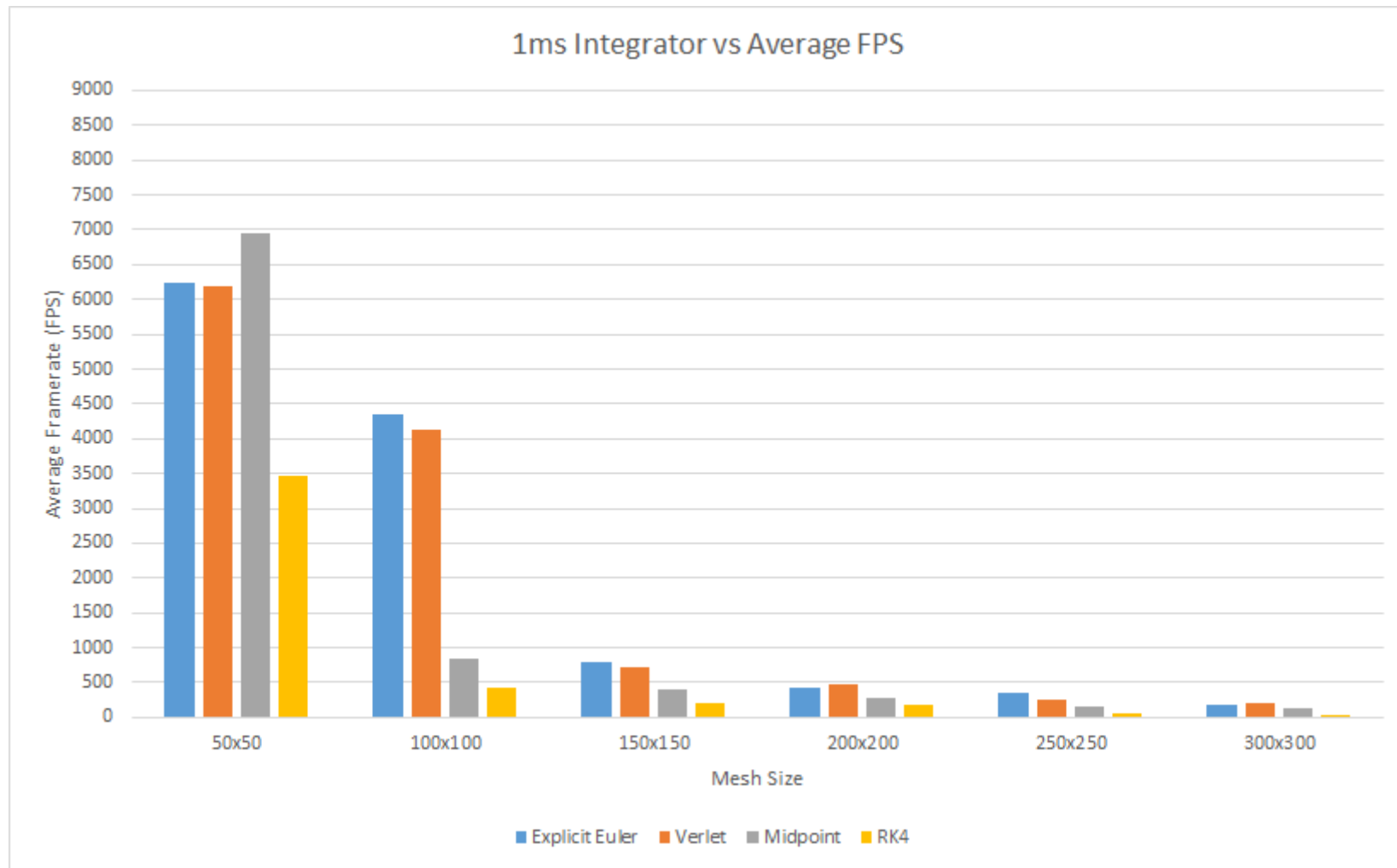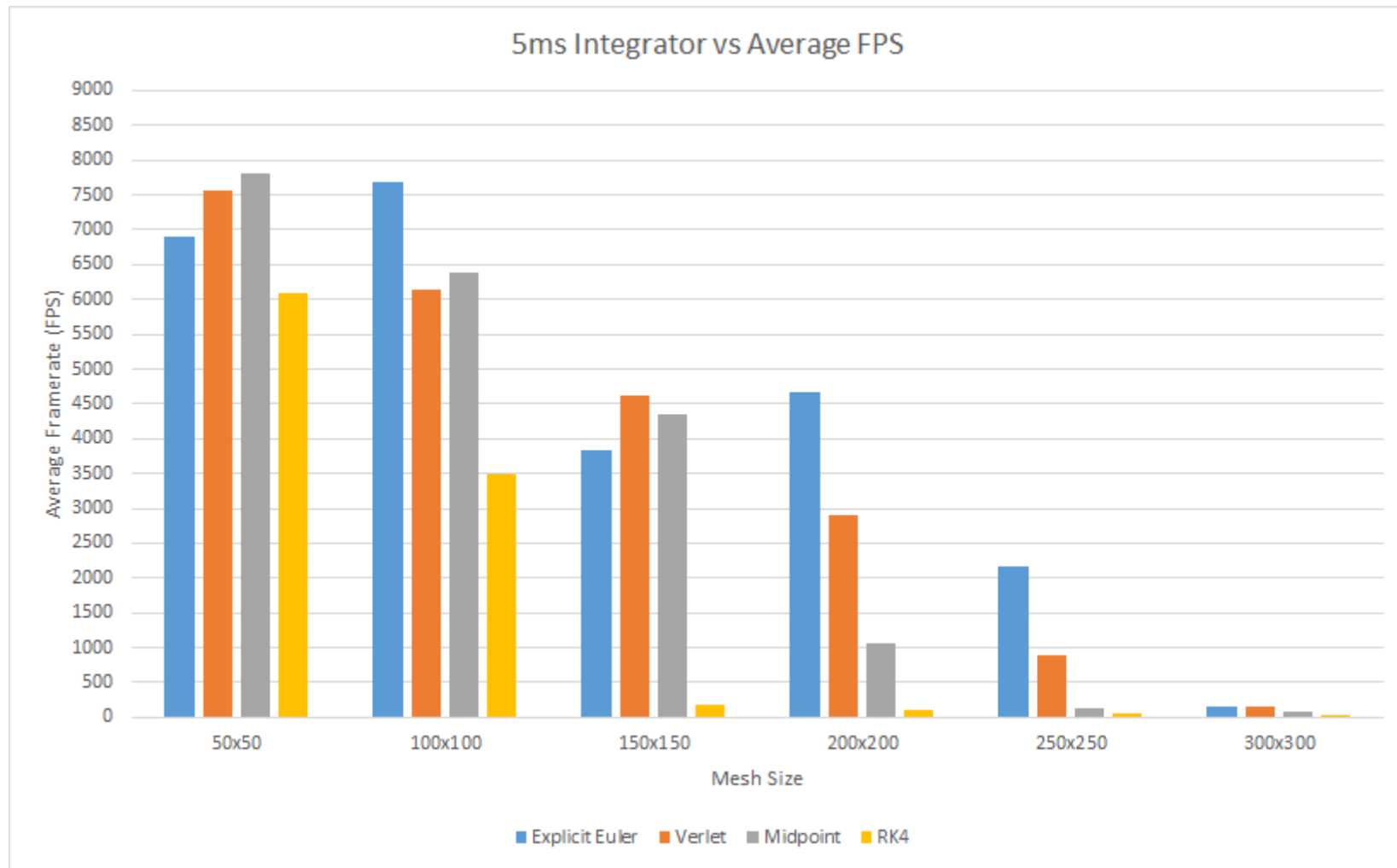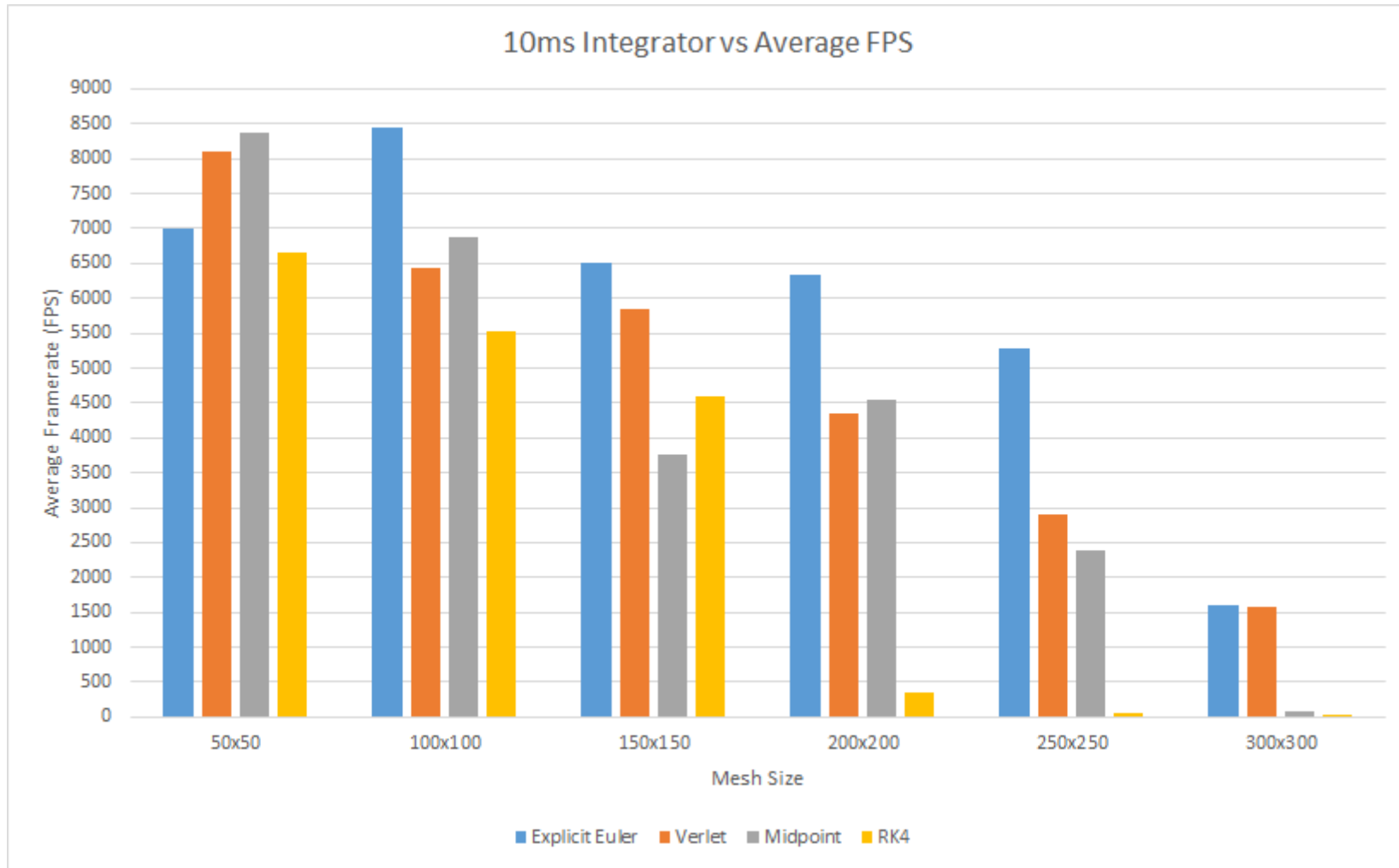
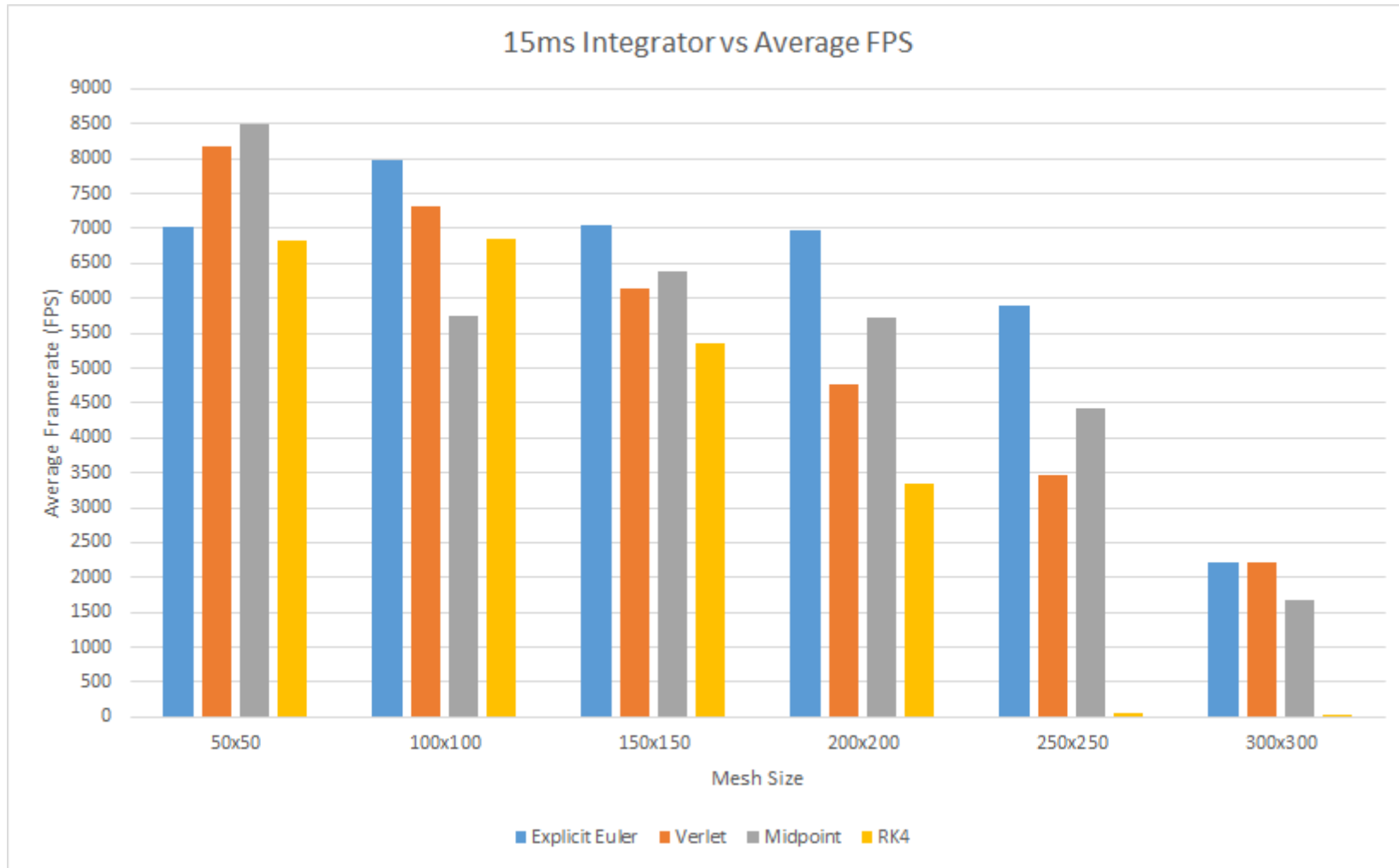Figure C.65: Mesh size against average FPS for all integrators with 10ms time step (flag)

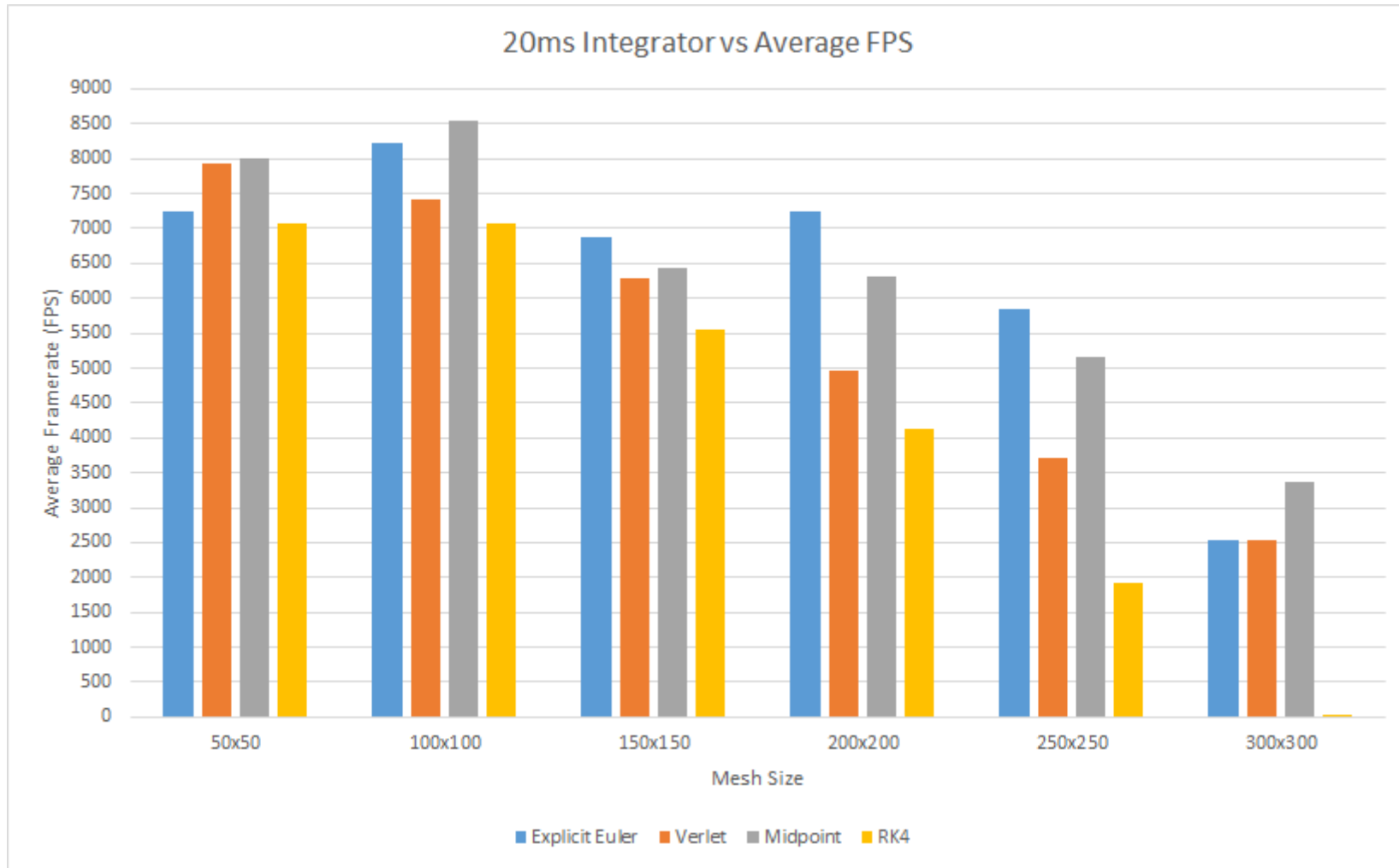Figure C.66: Mesh size against average FPS for all integrators with 15ms time step (flag)

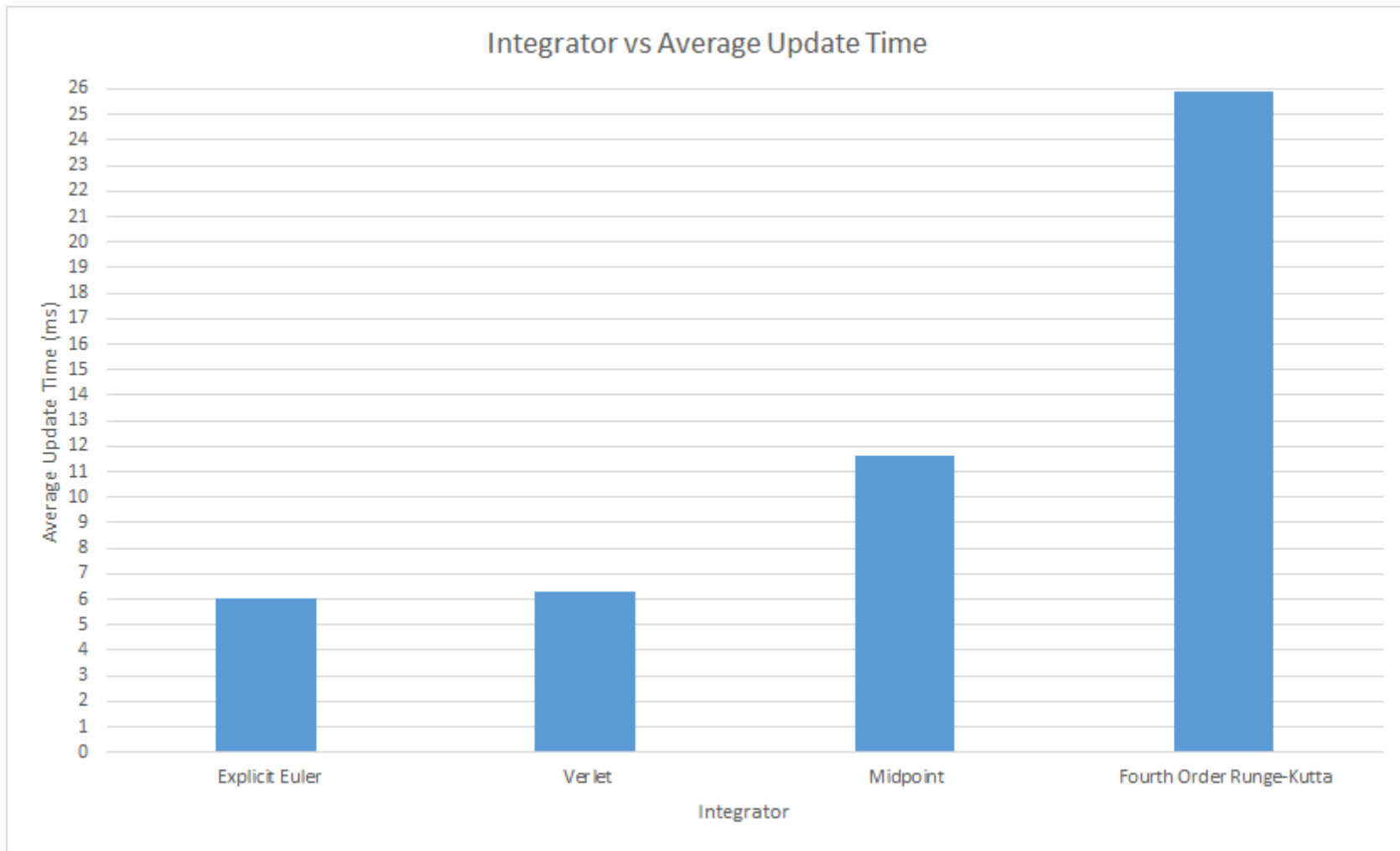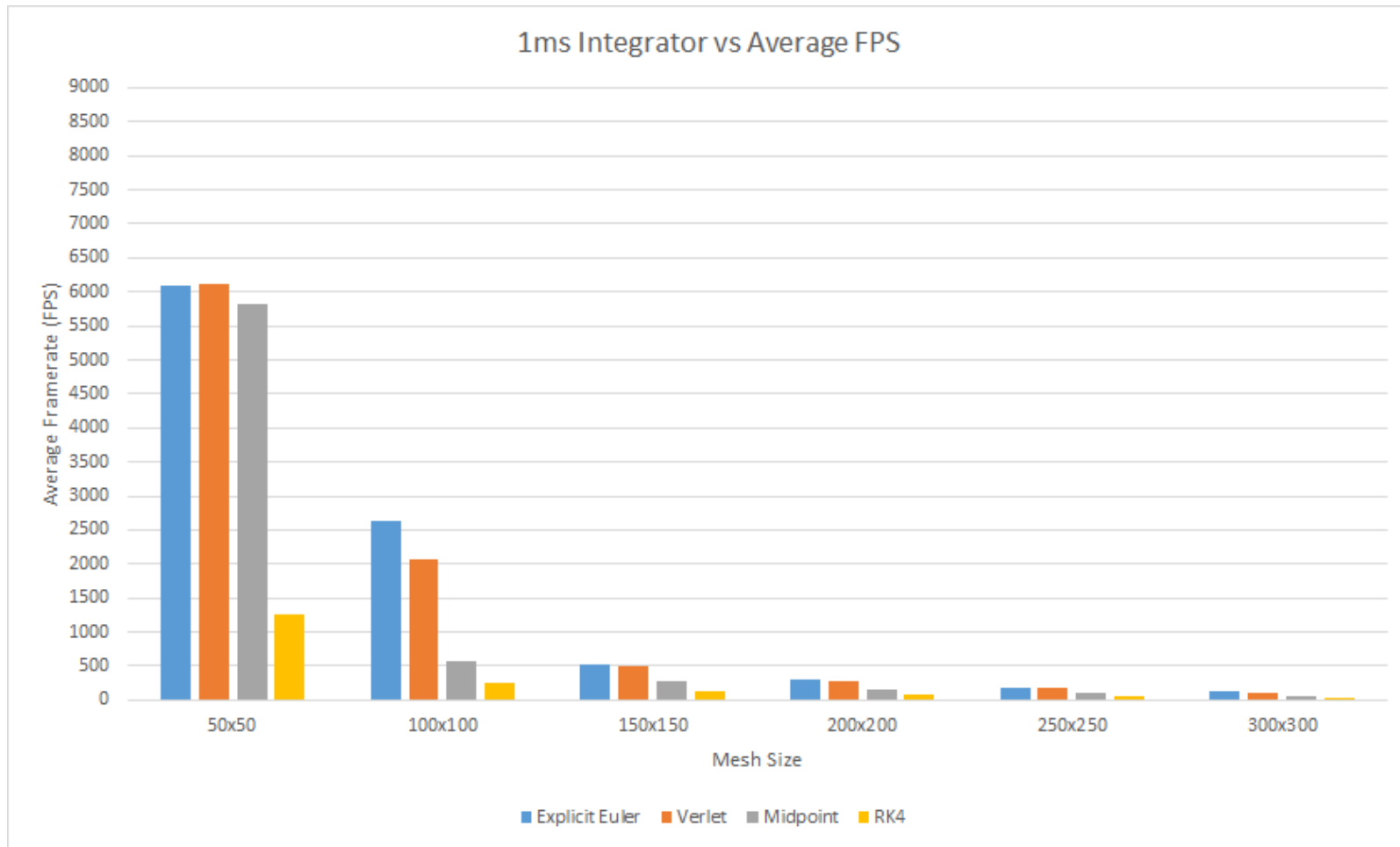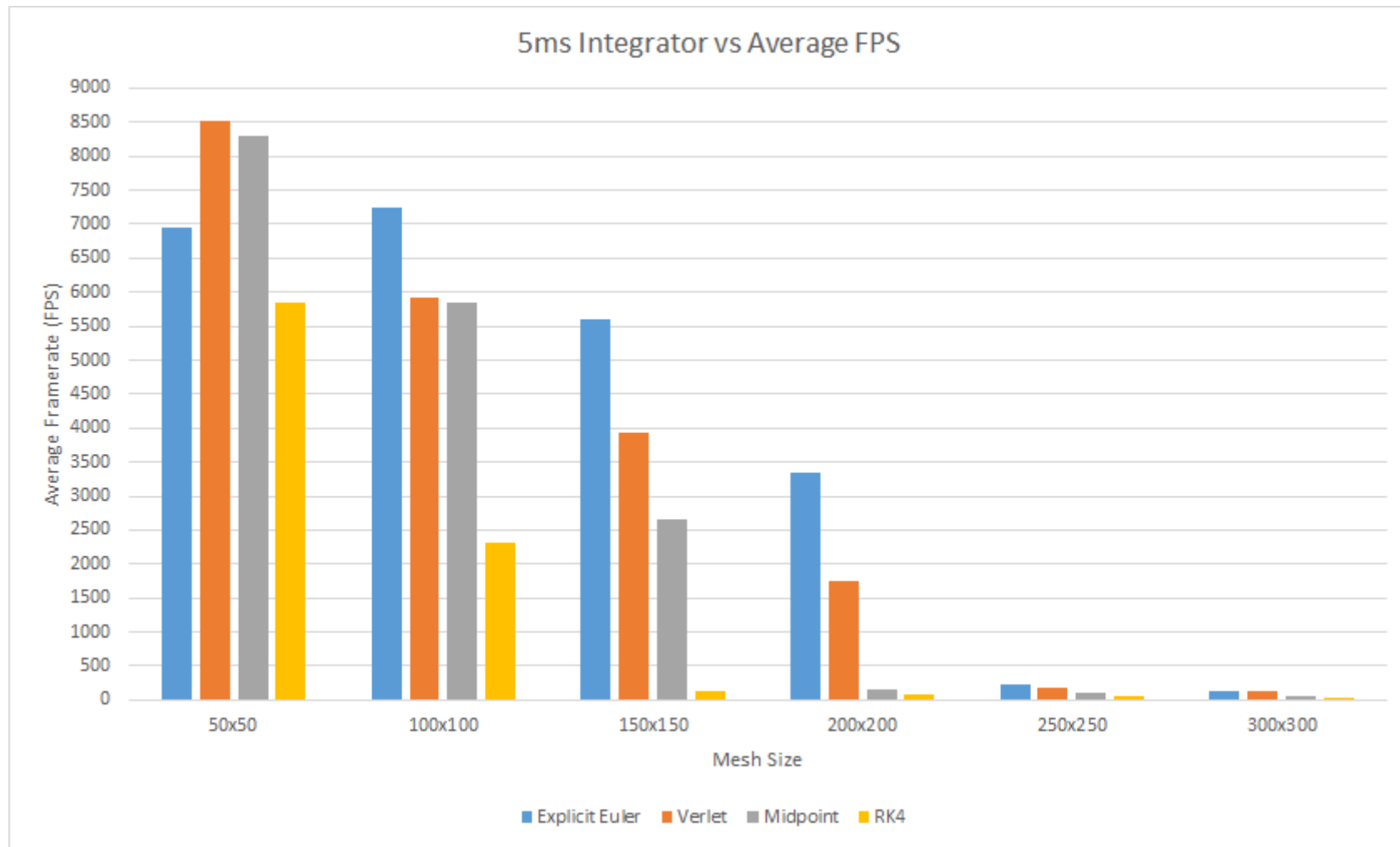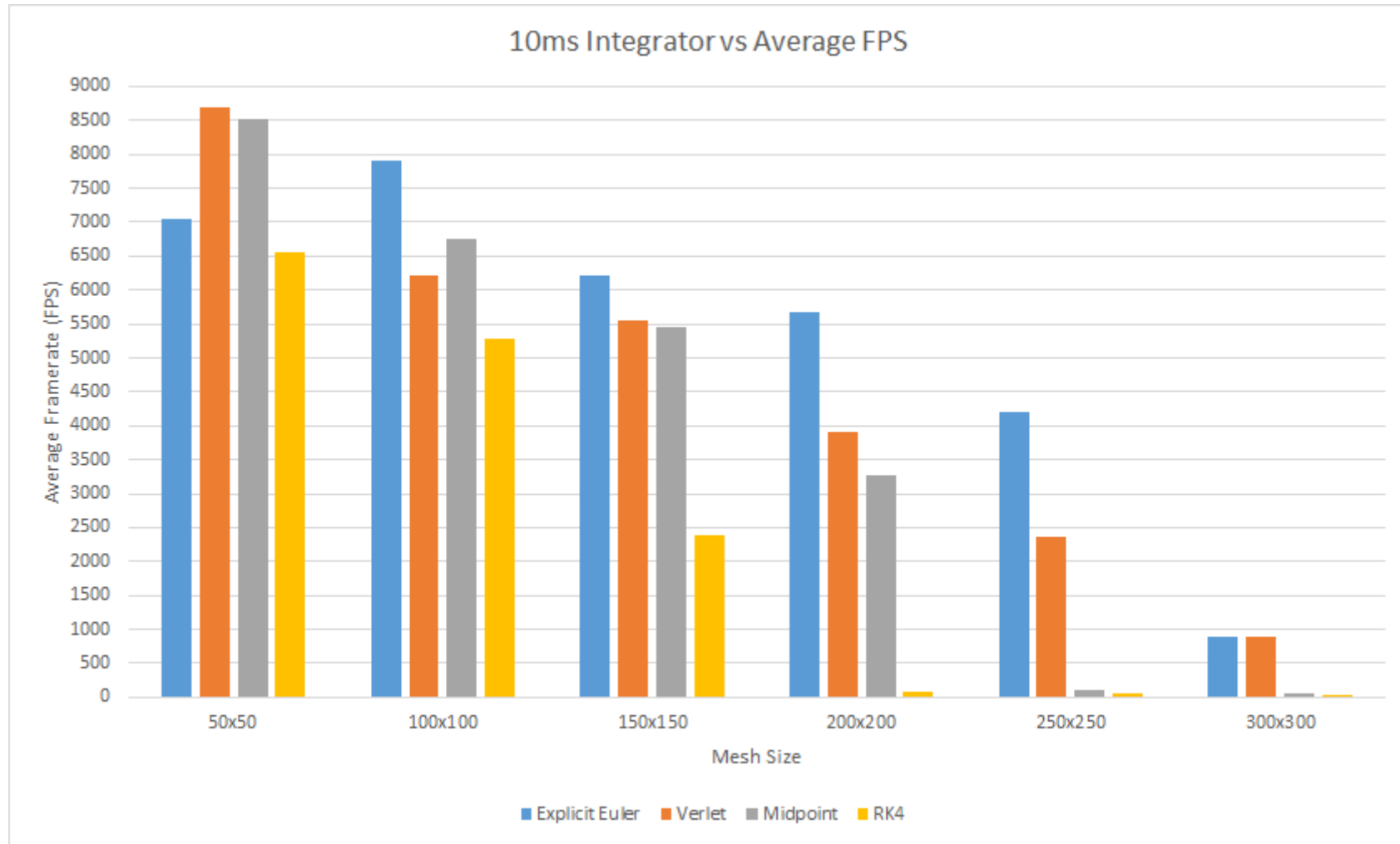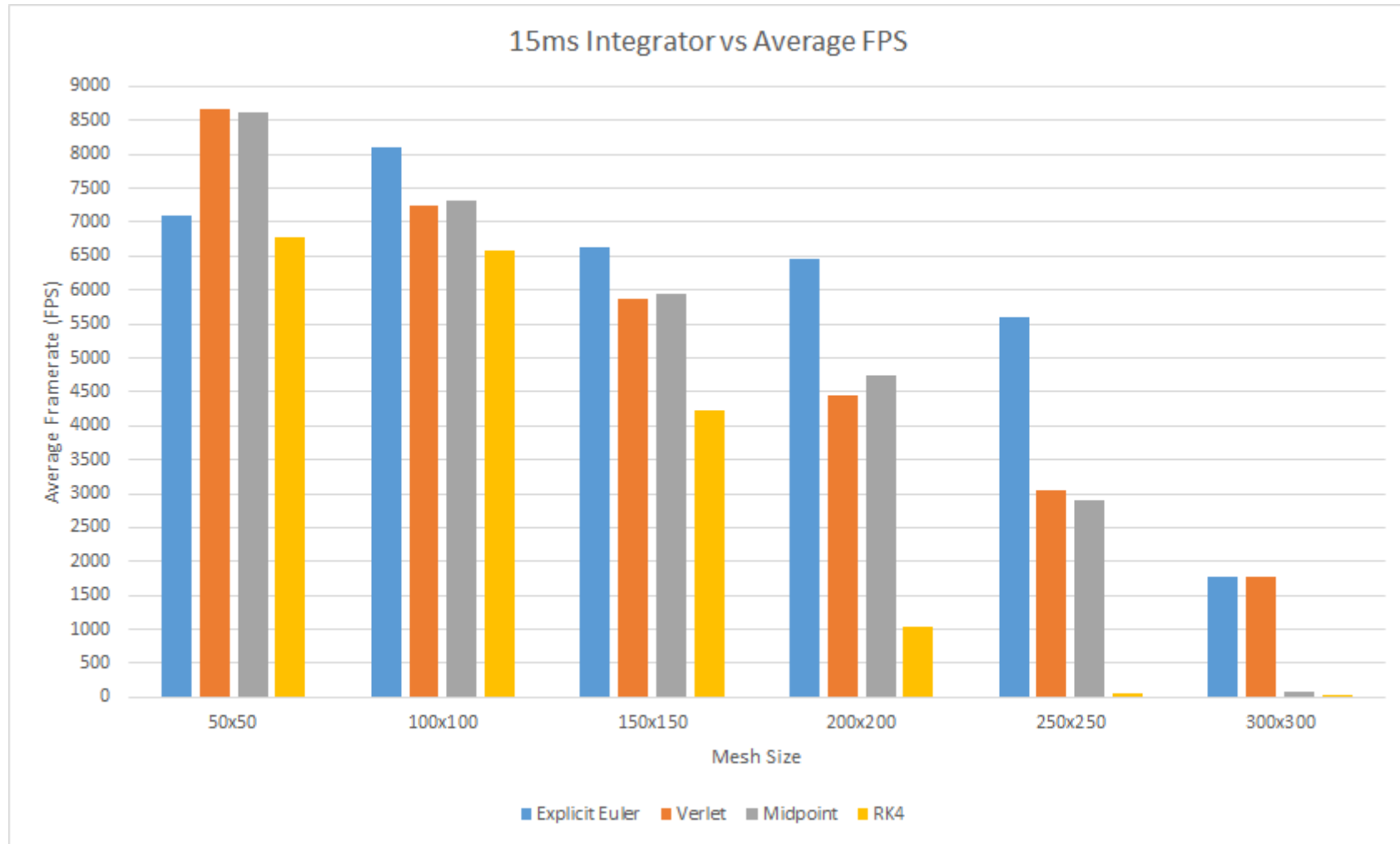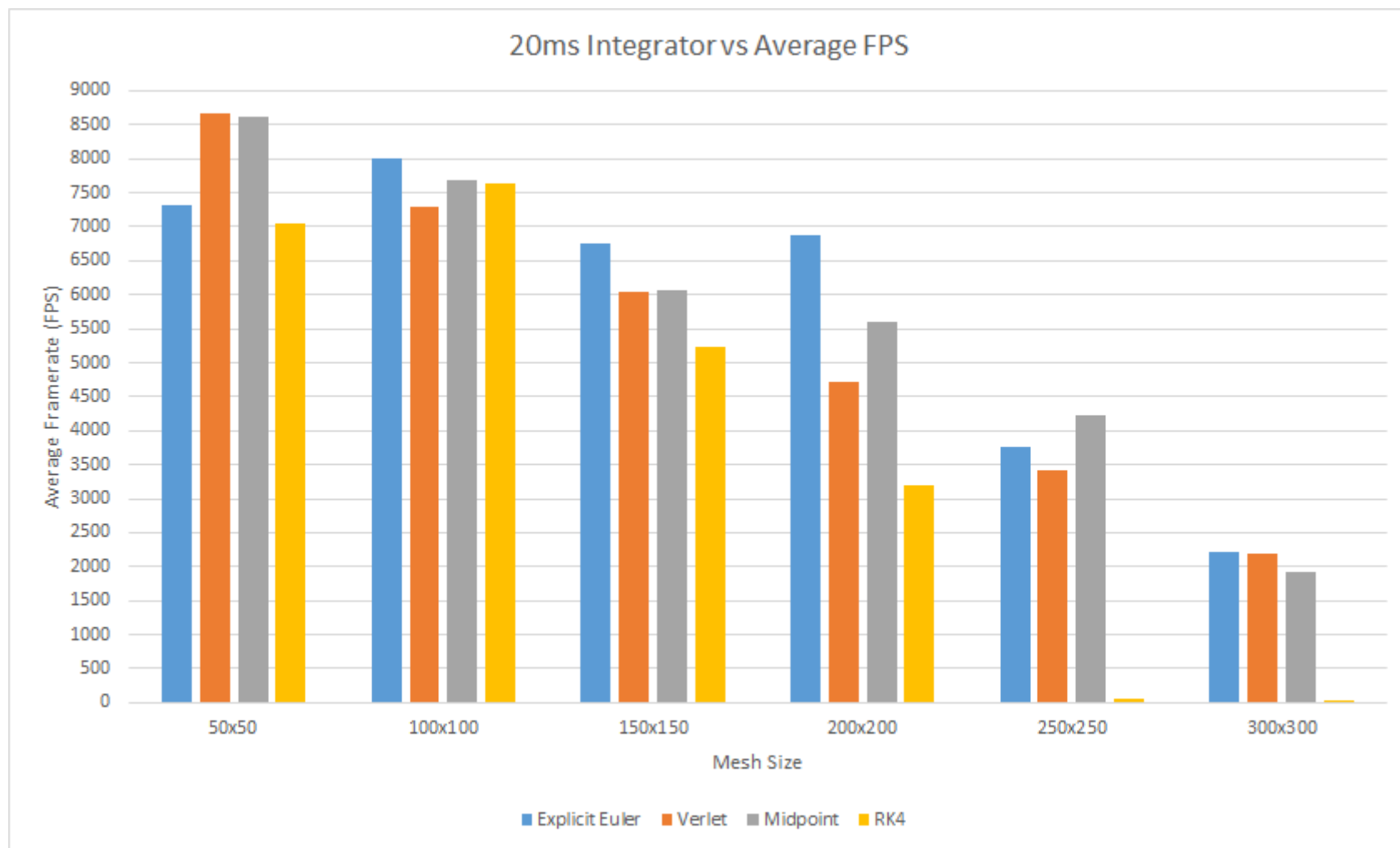Figure C.67: Mesh size against average FPS for all integrators with 20ms time step (flag)
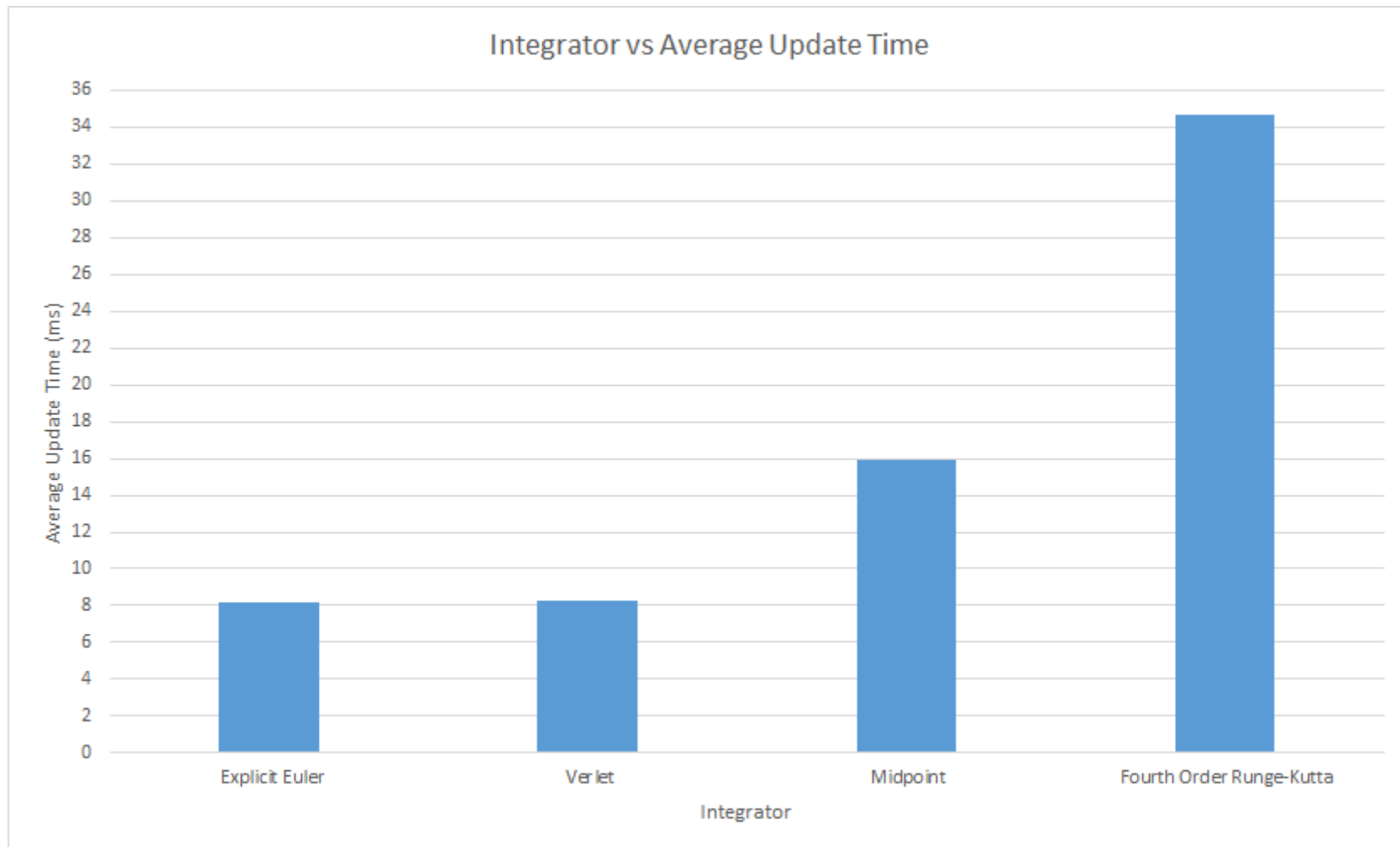
Figure C.68: Average update time for each integrator (flag)

References

Baraff, David and Andrew Witkin (1998). "Large Steps in Cloth Simulation." In: *SIGGRAPH*, pp. 43–54.

Bartels, Pieterjan (2014). *Simulation of Tearable Cloth*. URL: `https://nccastaff.bournemouth.ac.uk/jmacey/CGITech/reports2015/PBartels{\_}PieterjanBartels{\_}CGITECH{\_}final.pdf` (visited on 03/10/2016).

Choi, Kwang-Jin and Hyeong-Seok Ko (2002). "Stable but Responsive Cloth." In: *SIGGRAPH*, pp. 604–611.

Enqvist, Henrik (2010). *The Secrets Of Cloth Simulation In Alan Wake*. URL: `http://www.gamasutra.com/view/feature/132771/the{\_}secrets{\_}of{\_}cloth{\_}simulation{\_}in{\_}.php?page=1` (visited on 03/03/2016).

Jakobsen, Thomas (2005). *Advanced Character Physics*. URL: `http://www.gotoandplay.it/{\_}articles/2005/08/advCharPhysics.php` (visited on 03/03/2016).

Kang, Young-Min, Jeong-Hyeon Choi, and Hwan-Gue Cho (2000). "Fast and Stable Animation of Cloth with an Approximated Implicit Method." In: *Computer Graphics International*. Geneva.

Kim, Tae-Yong (2011). *Character Clothing in PhysX-3*.

Lander, Jeff (2000b). *Devil in the Blue Faceted Dress: Real Time Cloth Animation*. URL: `http://www.gamasutra.com/view/feature/131851/devil{\_}in{\_}the{\_}blue{\_}faceted{\_}dress{\_}.php` (visited on 03/03/2016).

Magnenat-Thalmann, Nadia and D. Thalmann (2004). *Handbook of Virtual Humans*. 1st. Chichester: Wiley.

Mesit, Jaruwan, Ratan Guha, and Shafaq Chaudhry (2007). "3D soft body simulation using mass-spring system with internal pressure force and simplified implicit integration." In: *Journal of Computers*.

Mongus, D. et al. (2012). "A hybrid evolutionary algorithm for tuning a cloth-simulation model." In: *Applied Soft Computing Journal*.

Mosegaard, Jesper (2009). *Mosegaards Cloth Simulation Coding Tutorial*. URL: `http://cg.alexandra.dk/?p=147` (visited on 07/05/2016).

Müller, Matthias et al. (2006). "Position Based Dynamics." In: *VRIPHYS*, pp. 71–80.

Naveen. *What is Waterfall Model in software testing and what are advantages and disadvantages of Waterfall Model*. URL: `http://testingfreak.com/waterfall-model-software-testing-advantages-disadvantages-waterfall-model/` (visited on 06/15/2016).

Ng, Hing N. and Richard L. Grimsdale (1996). "Computer Graphics Techniques for Modeling Cloth." In: *IEEE Computer Graphics & Applications* 16, pp. 28–42.

Parent, Rick (2012). *Computer Animation Algorithms and Techniques*. Third. Waltham: Elsevier. URL: `https://www.dawsonera.com/readonline/9780124159730/startPage/20`.

Provot, Xavier (1995). "Deformation Constraints in a Mass-Spring Model to Describe Rigid Cloth Behaviour." In: *Graphics Interface'95*, pp. 141–155.

Tang, Min et al. (2013). "A GPU-based streaming algorithm for high-resolution cloth simulation." In: *Computer Graphics Forum*.

Vassilev, T, B Spanlang, and Y Chrysanthou (2001). "Fast Cloth Animation on Walking Avatars." In: *Eurographics*.

Volino, Pascal, Frederic Cordier, and Nadia Magnenat-Thalmann (2005). "From early virtual garment simulation to interactive fashion design." In: *Computer-Aided Design* 37.6, pp. 593–608.

Volino, Pascal and Nadia Magnenat-Thalmann (2001). "Comparing Efficiency of Integration Methods." In: *Conference on Computer Graphics International*.

Wacker, Markus, Bernhard Thomaszewski, and Michael Keckeisen (2005). "Physical Models, Numerical Solvers for Cloth Animation and Virtual Cloth Design." In: *Eurographics*.

Wang, Jianchun, Xinrong Hu, and Yi Zhuang (2009). "The dynamic cloth simulation performance analysis based on the improved spring-mass model." In: *International Conference on Wireless Networks and Information Systems, WNIS 2009*, pp. 282 –285.

Xinrong, Hu et al. (2009). "Review of cloth modeling." In: *2009 Second ISECS International Colloquium on Computing, Communication, Control, and Management, CCCM 2009*.

Yalçın, M Adil and Cansın Yıldız. *Techniques for Animating Cloth*. URL: `http://www.cs.bilkent.edu.tr/{~}cansin/projects/cs567-animation/cloth/cloth-paper.pdf` (visited on 05/25/2016).

Zeller, Cyril (2005). "Cloth Simulation On The GPU." In: *SIGGRAPH*.

Zhang, Dongliang and Matthew M F Yuen (2001). "Cloth simulation using multilevel meshes." In: *Computers and Graphics (Pergamon)*.

Zink, Nico and Alexandre Hardy (2007). "Cloth Simulation and Collision Detection using Geometry Images." In: *AFRIGRAPH*. New York: ACM, pp. 187–195.

Bibliography

Akiya, Naoko, Scott Bury, and John M. Wassick (2011). "A General Model for Soft Body Simulation in Motion." In: *Winter Simulation Conference*. 2010, pp. 2194–2205.

Baraff, David and Andrew Witkin (1998). "Large Steps in Cloth Simulation." In: *SIGGRAPH*, pp. 43–54.

Bartels, Pieterjan (2014). *Simulation of Tearable Cloth*. URL: https://nccastaff.bournemouth.ac.uk/jmacey/CGITech/reports2015/PBartels{_}PieterjanBartels{_}CGITECH{_}final.pdf (visited on 03/10/2016).

Bender, Jan, Daniel Weber, and Raphael Diziol (2013). "Fast and stable cloth simulation based on multi-resolution shape matching." In: *Computers and Graphics (Pergamon)*.

Bhardwaj, Manas (2013). *A beginner's guide to various Software development methodologies*. URL: http://manasbhardwaj.net/a-beginners-guide-to-various-software-development-methodologies/ (visited on 06/15/2016).

Bourg, David M. and Bryan Bywalec (2013). *Physics for Game Developers*. Second. Sebastopol: O'Reilly. ISBN: ISBN 9781449361051. URL: https://www.dawsonera.com/abstract/9781449361051.

Boxerman, Eddy (2003). "Speeding Up Cloth Simulation." Master's Thesis. The University of British Columbia.

Bridson, Robert, Ronald Fedkiw, and John Anderson (2002). "Robust Treatment of Collisions, Contact and Friction for Cloth Animation." In: *SIGGRAPH*, pp. 594–603.

Choi, Kwang-Jin and Hyeong-Seok Ko (2002). "Stable but Responsive Cloth." In: *SIGGRAPH*, pp. 604–611.

— (2005). "Research problems in clothing simulation." In: *Computer Aided Design* 37, pp. 585–592.

Conger, David (2004). *Physics Modeling for Game Programmers*. First. Boston: Course Technology / Cengage Learning. URL: http://site.ebrary.com/lib/staffordshire/reader.action?docID=10065752.

De Farias, Thiago S M C et al. (2008). "A high performance massively parallel approach for real time deformable body physics simulation." In: *Proceedings - Symposium on Computer Architecture and High Performance Computing*.

Desbrun, Mathieu, Peter Schröder, and Alan Barr (1999). "Interactive Animation of Structured Deformable Objects." In: *Graphics Interface*. San Francisco: Morgan Kaufmann Publishers Inc., pp. 1–8.

Enqvist, Henrik (2010). *The Secrets Of Cloth Simulation In Alan Wake*. URL: `http://www.gamasutra.com/view/feature/132771/the{\_}secrets{\_}of{\_}cloth{\_}simulation{\_}in{\_}.php?page=1` (visited on 03/03/2016).

Ertekin, Burak (2014). *Cloth Simulation*. URL: `https://nccastaff.bournemouth.ac.uk/jmacey/CGITech/reports2015/BErtekin{\_}burakertekin-cgitech.pdf` (visited on 03/10/2016).

Fielder, Glenn. *Integration Basics*. URL: `http://gafferongames.com/game-physics/integration-basics/` (visited on 06/30/2016).

Garre, Carlos and Alvaro Pérez (2008). *A simple Mass-Spring system for Character Animation*. URL: `http://www.gmrv.es/{~}cgarre/APO{\_}MassSpring{\_}Jun08.pdf` (visited on 05/25/2016).

Gibson, Sarah F. F. and Brian Mirtich (1997). *A Survey of Deformable Modeling in Computer Graphics*. Tech. rep. Cambridge: MERL.

Harada, Takahiro (2006). "Real-time Cloth Simulation Interacting with Deforming High-Resolution Models." In: *SIGGRAPH*.

— (2008). "Real-Time Rigid Body Simulation on GPUs." In: *GPU Gems 3*. Pearson Education Inc. Chap. 29. URL: `http://http.developer.nvidia.com/GPUGems3/gpugems3{\_}ch29.html`.

Jakobsen, Thomas (2005). *Advanced Character Physics*. URL: `http://www.gotoandplay.it/{\_}articles/2005/08/advCharPhysics.php` (visited on 03/03/2016).

Kang, Young-Min, Jeong-Hyeon Choi, and Hwan-Gue Cho (2000). "Fast and Stable Animation of Cloth with an Approximated Implicit Method." In: *Computer Graphics International*. Geneva.

Kim, Tae-Yong (2011). *Character Clothing in PhysX-3*.

Lander, Jeff (2000a). *Collision Response: Bouncy, Trouncy, Fun*. URL: `http://www.gamasutra.com/view/feature/3427/collision{\_}response{\_}bouncy{\_}.php` (visited on 03/24/2016).

— (2000b). *Devil in the Blue Faceted Dress: Real Time Cloth Animation*. URL: `http://www.gamasutra.com/view/feature/131851/devil{\_}in{\_}the{\_}blue{\_}faceted{\_}dress{\_}.php` (visited on 03/03/2016).

Magnenat-Thalmann, Nadia and D. Thalmann (2004). *Handbook of Virtual Humans*. 1st. Chichester: Wiley.

Mesit, Jaruwan, Ratan Guha, and Shafaq Chaudhry (2007). "3D soft body simulation using mass-spring system with internal pressure force and simplified implicit integration." In: *Journal of Computers*.

Mesit, Jaruwan and Ratan K. Guha (2008). "Soft Body Simulation with Leaking Effect." In: *2008 Second Asia International Conference on Modelling & Simulation (AMS)*. IEEE, pp. 390–395.

Miguel, E et al. (2012). "Data-Driven Estimation of Cloth Simulation Models." In: *Computer Graphics Forum* 31.2, pp. 519–528.

Mongus, D. et al. (2012). "A hybrid evolutionary algorithm for tuning a cloth-simulation model." In: *Applied Soft Computing Journal*.

Mosegaard, Jesper (2009). *Mosegaards Cloth Simulation Coding Tutorial*. URL: `http://cg.alexandra.dk/?p=147` (visited on 07/05/2016).

Müller, Matthias et al. (2006). "Position Based Dynamics." In: *VRIPHYS*, pp. 71–80.

Naveen. *What is Waterfall Model in software testing and what are advantages and disadvantages of Waterfall Model*. URL: `http://testingfreak.com/waterfall-model-software-testing-advantages-disadvantages-waterfall-model/` (visited on 06/15/2016).

Ng, Hing N. and Richard L. Grimsdale (1996). "Computer Graphics Techniques for Modeling Cloth." In: *IEEE Computer Graphics & Applications* 16, pp. 28–42.

NVidia (2007). *Cloth Simulation*. URL: `http://developer.download.nvidia.com/SDK/10/direct3d/Source/Cloth/doc/Cloth.pdf` (visited on 05/25/2016).

O 'connor, Corey and Keith Stevens (2003). *Modeling Cloth Using Mass Spring Systems*. (Visited on 03/10/2016).

Ozgen, Oktar et al. (2010). "Underwater Cloth Simulation with Fractional Derivatives." In: *ACM Trans. Graph* 29.23.

Parent, Rick (2012). *Computer Animation Algorithms and Techniques*. Third. Waltham: Elsevier. URL: `https://www.dawsonera.com/readonline/9780124159730/startPage/20`.

Plath, Jan (2000). "Realistic modelling of textiles using interacting particle systems." In: *Computers & Graphics* 24, pp. 897–905.

Provot, Xavier (1995). "Deformation Constraints in a Mass-Spring Model to Describe Rigid Cloth Behaviour." In: *Graphics Interface'95*, pp. 141–155.

Santos Souza, Marco, Aldo Von Wangenheim, and Eros Comunello (2014). "Fast Simulation of Cloth Tearing." In: *SBC Journal on Interactive Systems* 5.1, pp. 44–48.

Schmitt, N et al. (2013). "Multilevel Cloth Simulation using GPU Surface Sampling." In: *Workshop on Virtual Reality Interaction and Physical Simulation VRIPHYS*.

Scrum Alliance. *Learn About Scrum*. URL: `https://www.scrumalliance.org/why-scrum` (visited on 06/15/2016).

Selle, Andrew et al. (2009). "Robust High-Resolution Cloth Using Parallelism, History-Based Collisions and Accurate Friction." In: *IEEE Transactions on Visualization and Computer Graphics* 15, pp. 339–350.

Tang, Min et al. (2013). "A GPU-based streaming algorithm for high-resolution cloth simulation." In: *Computer Graphics Forum*.

Vassilev, T, B Spanlang, and Y Chrysanthou (2001). "Fast Cloth Animation on Walking Avatars." In: *Eurographics*.

Vassilev, Tzvetomir and Bernhard Spanlang (2002). "A Mass-Spring Model For Real Time Deformable Solids." In: *East-West Vision*.

Vassilev, Tzvetomir Ivanov (2010). "Comparison of Several Parallel API for Cloth Modelling On Modern GPUs." In: *CompSysTech*, pp. 131–136.

— (2011). "Comparison of Parallel Algorithms for Modelling Mass-springs Systems with Several APIs on Modern GPUs." In: *CompSysTech*, pp. 204–209.

Volino, Pascal, Frederic Cordier, and Nadia Magnenat-Thalmann (2005). "From early virtual garment simulation to interactive fashion design." In: *Computer-Aided Design* 37.6, pp. 593–608.

Volino, Pascal, Martin Courchesne, and Nadia Magnenat-Thalmann (1995). "Versatile and Efficient Techniques for Simulating Cloth and Other Deformable Objects." In: *SIGGRAPH*, pp. 137–144.

Volino, Pascal and Nadia Magnenat-Thalmann (1997a). "Developing Simulation Techniques for an Interactive Clothing System." In: *International Conference on Virtual Systems and MultiMedia*. IEEE, pp. 109–118.

— (1997b). "Interactive Cloth Simulation: Problems and Solutions." In: *JWS97-B*. Geneva.

— (2001). "Comparing Efficiency of Integration Methods." In: *Conference on Computer Graphics International*.

Wacker, Markus, Bernhard Thomaszewski, and Michael Keckeisen (2005). "Physical Models, Numerical Solvers for Cloth Animation and Virtual Cloth Design." In: *Eurographics*.

Wang, Jianchun, Xinrong Hu, and Yi Zhuang (2009). "The dynamic cloth simulation performance analysis based on the improved spring-mass model." In: *International Conference on Wireless Networks and Information Systems, WNIS 2009*, pp. 282 –285.

Wang, Xiuzhong and Venkat Devarajan (2004). "2D Structured Mass-spring System Parameter Optimization based on Axisymmetric Bending for Rigid Cloth Simulation." In: *SIGGRAPH*, pp. 317–323.

Xinrong, Hu et al. (2009). "Review of cloth modeling." In: *2009 Second ISECS International Colloquium on Computing, Communication, Control, and Management, CCCM 2009*.

Yalçın, M Adil and Cansın Yıldız. *Techniques for Animating Cloth*. URL: `http://www.cs.bilkent.edu.tr/{~}cansin/projects/cs567-animation/cloth/cloth-paper.pdf` (visited on 05/25/2016).

Zeller, Cyril (2005). "Cloth Simulation On The GPU." In: *SIGGRAPH*.

Zhang, Dongliang and Matthew M F Yuen (2001). "Cloth simulation using multilevel meshes." In: *Computers and Graphics (Pergamon)*.

Zhenfang, Cao and He Bing (2012). "Research of Fast Cloth Simulation Based on Mass- Spring Model." In: *National Conference on Information Technology and Computer Science*, pp. 323–327.

Zink, Nico and Alexandre Hardy (2007). "Cloth Simulation and Collision Detection using Geometry Images." In: *AFRIGRAPH*. New York: ACM, pp. 187–195.